TEM WAVE PROPERTIES OF INHOMOGENEOUS TRANSMISSION LINES USING THE EQUIVALENT SOURCE METHOD

A Thesis presented to

The Faculty of Graduate Studies of

University of Manitoba

in

Partial Fulfilment of the Requirements

for the degree of

Master of Science in Electrical Engineering

by

Brij P. Aggarwal

September 1975

"TEM WAVE PROPERTIES OF INHOMOGENEOUS TRANSMISSION LINES USING THE EQUIVALENT SOURCE METHOD"

by

BRIJ R. AGGARWAL

A dissertation submitted to the Faculty of Graduate Studies of the University of Manitoba in partial fulfillment of the requirements of the degree of

MASTER OF SCIENCE

To my parents

with

deepest gratitude.

ABSTRACT

This thesis is mainly concerned with the analysis, using the equivalent source method, of inhomogenious transmission lines to obtain their properties. The quasi-static TEM mode is assumed and numerical results are obtained for the characteristic impedance, the relative effective dielectric constant, relative velocity, attenuation and inductive and capacitive coupling coefficients for a number of microstrip configurations. These include standard microstrip, suspended substrate microstrip, coupled microstrip and suspended substrate coupled microstrip lines.

Microstrip lines with rectangular inner and outer conductor are considered but the method is equally applicable to transmission lines of arbitrary cross-section and any number of conductors provided the TEM mode approximation holds good.

ACKNOWLEDGEMENT

The author wishes to express his sincere appreciation to Professor Ernest Bridges of the department of Electrical Engineering, University of Manitoba, who suggested this problem and gave him guidance throughout this project.

The author owes a debt of gratitude to Miss Nirmala Daulat for without her encouragement this thesis would not have been completed. Mr. and Mrs. Ram Garg deserve considerable credit for their invaluable assistance. Financial help provided by the University of Manitoba is gratefully acknowledged.

LIST OF FIGURES

Fig.(1.1) -	General method - Geometry of the problem.	5
Fig.(2.1) -	Open microstrip.	10
Fig.(2.2) -	Microstrip enclosed in a box.	11
Fig.(2.3) -	Integral contours and sub-regions in the dielectric for attenuation calculation.	18
Fig.(2.4) -	Division of segments on the strip.	20
Fig.(2.5) -	Characteristic impedance versus W/H, T=H/8.	22
Fig.(2.6) -	Characteristic impedance versus W/H,T=H/40.	22
Fig.(2.7) -	Relative wavelength versus W/H, T=H/8.	23
Fig.(2.8) -	Relative wavelength versus W/H, T=H/40.	23
Fig.(2.9) -	Effective dielectric constant versus W/H, T=H/8.	24
Fig.(2.10)-	Effective dielectric constant versus W/H, T=H/40.	24
Fig.(2.11)-	Relative velocity versus W/H, T=H/8.	25
Fig.(2.12)-	Relative velocity versus W/H, T=H/40.	25
Fig.(2.13)-	Conductor attenuation constant versus W/H, T=H/8, ϵ_r =9.35.	26
Fig.(2.14)-	Attenuation constant versus frequency.	29
Fig.(2.15)-	Attenuation constant versus frequency.	30
Fig.(2.16)-	Attenuation constant versus frequency.	31
Fig.(2.17)-	Surface charge density versus strip width.	34
Fig.(3.1) -	Suspended substrate microstrip with three dielectric layers.	36
Fig.(3.2) -	Numbering of contours fir suspended substrate microstrip.	37

Fig.(3.3) - Suspended substrate microstrip with two dielectric layers. 39

Fig.(3.4) - Characteristic impedance versus 2WL/W. 41

Fig.(3.5) - Relative wavelength versus 2WL/W. 41

Fig.(3.6) - Conductor attenuation constant versus 2WL/W. 42

Fig.(3.7) - Effective dielectric constant versus 2WL/W. 42

Fig.(3.8) - Dielectric attenuation constant versus 2WL/W. 43

Fig.(3.9) - Characteristic impedance versus W/H. 43

Fig.(3.10)- Effective dielectric constant versus W/H. 44

Fig.(3.11)- Relative wavelength versus W/H. 44

Fig.(3.12)- Conductor attenuation constant versus W/H. 45

Fig.(3.13)- Dielectric attenuation constant versus W/H. 45

Fig.(4.1) - Open coupled microstrip line. 51

Fig.(4.2) - Coupled microstrips enclosed in a box. 53

Fig.(4.3) - Contour numbering for the coupled microstrips. 54

Fig.(4.4) - Relative velocity versus W/H, D=.2H. 61

Fig.(4.5) - Relative velocity versus W/H, D=.6H. 61

Fig.(4.6) - Relative velocity versus W/H, D=H. 62

Fig.(4.7) - $\sqrt{\epsilon_{eff}}$ Zo versus W/H, D=.2H. 65

Fig.(4.8) - $\sqrt{\epsilon_{eff}}$ Zo versus W/H, D=.6H. 65

Fig.(4.9) - $\sqrt{\epsilon_{eff}}$ Zo versus W/H, D=H. 66

Fig.(4.10)- Even and odd mode effective dielectric constant versus W/H, D=.2H. 67

Fig.(4.11)- Even and odd mode effective dielectric constant versus W/H, D=.6H. 68

Fig.(4.12)- Even and odd mode effective dielectric constant versus W/H, D=H. 68

Fig.(4.13)- Inductive coupling coefficient versu W/H. 69
Fig.(4.14)- Capacitive coupling coefficient versus W/H. 70
Fig.(4.15)- Odd mode characteristic impedance versus W/H. 71
Fig.(4.16)- Even mode characteristic impedance versus W/H. 72
Fig.(4.17)- Even mode attenuation constant versus W/H. 73
Fig.(4.18)- Effective dielectric constant versus W/H. 74
Fig.(5.1) - Coupled suspended substrate microstrip. 77
Fig.(5.2) - Contour numbering for coupled suspended substrate microstrip. 78
Fig.(5.3) - Inductive coupling coefficient versus W/H. 82
Fig.(5.4) - Capacitive coupling coefficient versus W/H. 82
Fig.(5.5) - Effective dielectric constant versus W/H. 83
Fig.(5.6) - Odd mode effective dielectric constant versus W/H. 83
Fig.(5.7) - Even and odd mode characteristic impedance versus W/H. 84
Fig.(5.8) - Relative velocity versus W/H, D=.2H. 85
Fig.(5.9) - Relative velocity versus W/H, D=.5H. 85
Fig.(5.10)- Even mode attenuation constant versus W/H. 86
Fig.(5.11)- Even mode attenuation constant versus H1/H. 87
Fig.(5.12)- Characteristic impedance of the coupled line versus W/H. 87
Fig.(5.13)- Effective dielectric constant versus H1/H, D=.2H. 88
Fig.(5.14)- Effective dielectric constant versus H1/H, D=.5H. 88

Fig.(5.15)- Even and odd mode effective dielectric constant versus H1/H, D=.2H. 89

Fig.(5.16)- Even and odd mode effective dielectric constant versus H1/H, D=.5H. 89

Fig.(5.17)- Relative velocity versus H1/H, D=.2H. 90

Fig.(5.18)- Relative velocity versus H1/H, D=.5H. 90

Fig.(5.19)- Even and odd mode characteristic impedance versus H1/H, D=.2H. 91

Fig.(5.20)- Even and odd mode characteristic impedance versus H1/H, D=.5H. 91

Fig.(5.21)- Characteristic impedance of the coupled line versus H1/H. 92

Fig.(5.22)- Capacitive coupling coefficient versus H1/H. 92

Fig.(A.1) - Region S and the actual sources. 96

Fig.(A.2) - Region S and the equivalent sources. 97

Fig.(A.3) - Magnetic current backed by an electrical conductor. 100

Fig.(A.4) - Circuit theory analogue of equivalence principle - Actual sources. 101

Fig.(A.5) - Circuit theory analogue of equivalence principle - Equivalent sources. 101

Fig.(C.1) - Transverse cross-section of single microstrip enclosed in a box. 107

Fig.(E.1) - Flow chart for the computer program. 117

LIST OF TABLES

Table (2.1) - Number of segments on each contour of standard microstrip 20

Table (2.3) - Relative wavelength calculated on variational basis. 28

Table (2.4) - Effective dielectric constant calculated on variational basis. 28

Table (2.2) - Comparison of attenuation for different shapes of strip corner. 33

Table (3.1) - Number of segments on each contour of suspended substrate microstrip, $h_3=0$. 40

Table (3.4) - Parameters of suspended substrate microstrip, $(h_3=0)$. 46

Table (3.2) - Number of segments on each contour of suspended substrate microstrip, $h_3\neq 0$. 47

Table (3.5) - Suspended substrate microstrip parameters for $h_3\neq 0$, $\epsilon_r=3.78$. 48

Table (3.6) - Suspended substrate microstrip parameters for $h_3\neq 0$, $\epsilon_r=9.35$. 48

Table (3.3) - Comparison of attenuation for different microstrip configurations. 49

Table (4.1) - Number of segments on each contour of coupled microstrip. 60

Table (4.2) - Comparison of results for even and odd mode characteristic impedance values. 75

Table (5.1) - Number of segments on each contour of suspended substrate coupled microstrip. 80

TABLE OF CONTENTS

CHAPTER 1 1

1.1 Introduction 1

1.2 The general method 4

CHAPTER 2 10

2.1 Application of the method to microstrip 10

2.2 Theoretical procedure 12

2.3 Effective dielectric constant 14

2.4 Calculation of microstrip parameters 15

2.5 Attenuation calculation 16

2.6 Results and discussion 20

CHAPTER 3 35

3.1 Microstrip with suspended substrate 35

3.2 Results and discussion 39

CHAPTER 4 COUPLED MICROSTRIPS 51

4.1 The method of analysis 51

4.2 Calculation of coupled-line parameters 55

4.3 Results and discussion 60

CHAPTER 5 76

5.1 Coupled suspended substrate microstrip 76

5.2 Results and discussion 80

CONCLUSION 93

APPENDIX A-The equivalence principle 96

APPENDIX B-The method of moments 103

APPENDIX C-The variational principle 107

APPENDIX D-Green's function and identities 112

APPENDIX E-The computer program 116

BIBLIOGRAPHY 131

Chapter 1

1.1 INTRODUCTION

The analytic method used in this thesis is based on the equivalence principle which is presented in detail in appendix A. According to this principle two source systems producing the same field within a specified region of space are called equivalent. The fields of interest in a given region of space need not be determined from the actual source distribution since the equivalent sources serve equally as well to do this.

The analysis presented applies to all inhomogeneous transmission lines of arbitrary cross-section having any number of conductors which can support a TEM mode. In this thesis the method is applied to microstrip lines enclosed in a rectangular box and includes suspended substrate and coupled microstrip type lines.

Since 1951 various approaches have been used to analyse microstrip lines. The conformal mapping technique [8] was one of the earliest methods used for microstrip analysis. Variational techniques [5] have been found to yield satisfactory results with relatively simple formulae but with the limitation that they do not yield a direct solution to the charge distribution nor do they suggest systematic procedures for improving the approximate solution. An extension of the variational method, using the Rayleigh-Ritz procedure [17], requires inversion of large order matrices with elements that have to be generated by numerical integration and, moreover, the adequacy of the charge distribution on the conductors may not be apparent.

The method of images [16] results in equations which usually become difficult to handle. Relaxation techniques [15] are found to give less accurate results, especially for the calculation of attenuation. The finite difference method [18] usually suffers from the same disadvantage.

The method of moments [2], the technique used in this thesis, solves the two dimensional Laplace equation in terms of equivalent sources on the boundary of the region of interest. Appendix B gives a complete description of the method. Either a step approximation or piecewise linear approximation can be used for the source with point matching to test the boundary conditions which may be Dirichlet, Neumann, impedence or a combination of any of these.

The principal approximations used in the method [1] follow:

(a) The contour is approximated by N straight line segments.

(b) The equivalent source is approximated as either a step function or a piecewise linear function.

(c) Boundary conditions are satisfied at discrete points on the boundary.

No further mathematical approximations are made and those that have been made can be carried out to a higher order by increasing the number of straight line segments approximating the boundary.

The accuracy of the solution depends in general on the shape of the boundary, on the boundary conditions and for any particular problem it depends on N, the number of contour segments. Since the solution involves a matrix inversion, we were restricted to an N of the order of 100 because of computing execution time and memory storage considerations. In all problems attempted no ill-conditioned matrices were ever encountered.

The equivalent source solution can be extended easily to regions which contain two or more homogeneous dielectrics as in the case of microstrip or suspended substrate microstrip. In this situation we need additional surface sources on boundary contours dividing the dielectric regions with an integral over each region.

The method had been successfully employed to find potential distributions [1] in any given region of space. The problem of calculating resistence between two conducting surfaces on or within a homogeneous medium or the two body capacitance [1] can easily be evaluated by this procedure.

The general method for microstrip line analysis is given next in the chapter. Chapter 2 deals with the single layer dielectric supported microstrip line and this analysis is extended in Chapter 3 to the suspended substrate microstrip line. Coupled lines over a single dielectric layer are considered in Chapter 4 and this is followed by a consideration of coupled lines of the suspended substrate type.

Numerical results (computed on an IBM 370 computer) are presented for characteristic impedance, relative velocity, relative effective dielectric constant, attenuation and for inductive and capacitive coupling coefficients for single and coupled microstrip. These results are compared with published results [6], [7], [11] -- [14] using other techniques.

1.2 THE GENERAL METHOD

The problem involves finding the solution to Laplace equation in a region of space subjected to general boundary conditions at the bounding contours. Here, we are concerned only with the two dimensional problem. The general method used [1] involves transforming the boundary value problem into an integral equation which is then solved by the method of moments [2].

Consider a two dimensional region R as shown in Fig. 1.1 that is bounded by contour C and in which the potential $\emptyset$ everywhere satisfied the two dimensional Laplacian equation

$$\frac{\partial^2 \phi}{\partial x^2} + \frac{\partial^2 \phi}{\partial y^2} = 0. \qquad (1.1)$$

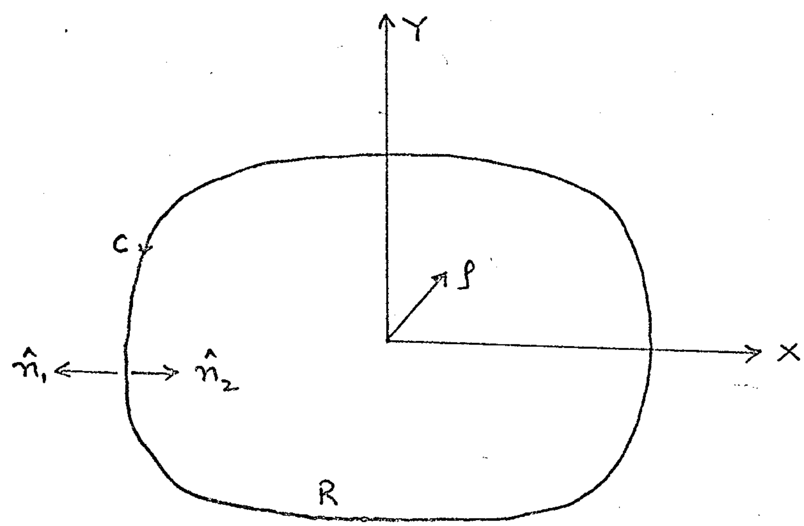

Fig. 1.1

The boundary condition at contour C is specified by

$$\alpha(C)\,\emptyset + \beta_1\,(C)\,\frac{\partial \emptyset}{\partial n_1} + \beta_2(c)\frac{\partial \phi}{\partial n_2} = \gamma(c) \qquad (1.2)$$

where α, β_1, β_2, γ are given functions of C and $\hat{n}1$ and $\hat{n}2$ are respectively outward and inward normals to C.

Dirichlet, Neumann and impedance boundary conditions are special cases of the above general boundary conditions and determine the values of α, β_1, β_2 and γ at a particular point on C.

An arbitrary Laplacian potential distribution in R can be produced by sources on the boundary. If dipole and flux sources are assumed on C then as a consequence of the equivalence principle [3] there are an infinite number of source distributions which can produce the same ϕ in R.

Letting $\sigma(C)$ denote a flux source distribution on C the potential ϕ at any point ρ can be expressed as

$$\phi(\rho) = \oint_C \sigma(C') \ln \frac{k}{|\rho-\rho'|} dc' \qquad (1.3)$$

where k is a constant chosen such that

$$k > |\rho-\rho'|_{max} \qquad (1.4)$$

with ρ and ρ' on C.

The reason for choosing k according to (1.4) is evident if we choose C to be a circle of unit radius. If k = 1 and σ is constant in (1.3) then $\phi = 0$ at the centre of the circle regardless of the magnitude of σ. The problem becomes mathematically indeterminate and requires infinite σ to produce finite ϕ. This cannot occur if we use k according to (1.4). Physically we can think of this restriction as requiring that positive σ produce positive ϕ at every point on C.

Specialising (1.3) to C and applying the boundary condition of (1.2) we get

$$\left[\alpha \phi + \beta_1 \frac{\partial \phi}{\partial n_1} + \beta_2 \frac{\partial \phi}{\partial n_2}\right]_{\rho \text{ on } C} = \gamma(C). \qquad (1.5)$$

Equation (1.5) is an integral equation for determining σ on C and once σ is found $\emptyset$ in R is given by (1.3).

To solve (1.5) the general method of moments [2] is used with pulse functions for expansion and point matching to test the boundary conditions. This gives a step approximation to the equivalent sources $\sigma(C)$.

The analysis which follows is essentially the same as that described in [1].

If we define N points on C approximating the boundary by N straight line segments ΔCi and a pulse function:

$$P_i(C) = 1 \text{ on } \Delta Ci, \quad = 0 \text{ elsewhere.} \tag{1.6}$$

Then σ is given by

$$\sigma = \sum_{i=1}^{N} \sigma_i \quad P_i(C) \tag{1.7}$$

from which we can rewrite (1.3) as

$$\emptyset(\rho) = \sum_{i=1}^{N} \sigma_i \psi_i(\rho) \tag{1.8}$$

where $\psi_i(\rho)$ is Green's function given by

$$\psi i(\rho) = \int_{\Delta C_i} \ln \frac{k}{|\rho - \rho'|} \, dc' \tag{1.9}$$

For a point j on the boundary we have

$$\emptyset(\rho_j) = \emptyset_j = \sum_{i=1}^{N} \sigma_i \; \psi_i \, (\rho_j). \tag{1.10}$$

The boundary equation (1.2) for a specific contour point j becomes

$$\alpha_j \phi_j + \beta_{1j} \frac{\partial \phi_j}{\partial n_1} + \beta_{2j} \frac{\partial \phi_j}{\partial n_2} = \gamma_j . \qquad (1.11)$$

with N such equations generated, j = 1, 2, ... N, defining N segment mid-points.

In terms of equivalent sources and Green's function (1.11) can be rewritten as

$$\alpha_j \left(\sum_{i=1}^{N} \sigma_i \psi_{ji}\right) + \beta_{1j} \frac{\partial}{\partial n_1}\left(\sum_{i=1}^{N} \sigma_i \psi_{ji}\right) + \beta_{2j} \frac{\partial}{\partial n_2}\left(\sum_{i=1}^{N} \sigma_i \psi_{ji}\right) = \gamma_j \qquad (1.12)$$

where $\psi_{ji} = \psi_i(\rho_j)$ is Green's function at the jth element with the ith element at the source point.

Write (1.12) in the form

$$\sum_{i=1}^{N} \left(\alpha_j \psi_{ji} + \beta_{1j} \frac{\partial \psi_{ji}}{\partial n_1} + \beta_{2j} \frac{\partial \psi_{ji}}{\partial n_2}\right) \sigma_i = \gamma_j \qquad (1.13)$$

and define

$$\ell_{ji} = \alpha_j \psi_{ji} + \beta_{1j} \frac{\partial \psi_{ji}}{\partial n_1} + \beta_{2j} \frac{\partial \psi_{ji}}{\partial n_2} \qquad (1.14)$$

Let $[\ell]$ represent the square matrix of elements ℓ_{ji}, then equation (1.13), in matrix form, can now be written as

$$[\ell][\sigma] = [\gamma] \qquad (1.15)$$

where $[\sigma]$ is the column matrix of σ_i and $[\gamma]$ is the column matrix of γ_j.

The equivalent sources are then given by

$$[\sigma] = [\ell]^{-1}[\gamma]. \tag{1.16}$$

Matrix $[\ell]$ is usually well conditioned and can be inverted by any convenient algorithm.

If $[P]$ denotes the row matrix of pulse function Pi, then the functional expression for equivalent sources is

$$\sigma = [P][\sigma] \tag{1.17}$$

$$= [P]\,[\ell]^{-1}[\gamma]. \tag{1.18}$$

Finally, letting $[\psi]$ denote the row matrix of ψ_i then the potential at any point ρ in R is given by

$$\phi = [\psi][\sigma] \tag{1.19}$$

$$= [\psi]\,[\ell]^{-1}[\sigma]. \tag{1.20}$$

Chapter 2

2.1 APPLICATION OF THE METHOD TO MICROSTRIP

The method described in Chapter 1 is now used to analyse the simplest of microstrip configurations as shown in Fig.(2.1). It consists of a single strip resting on a

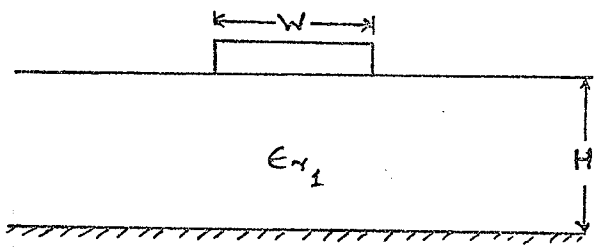

Fig. (2.1)

single dielectric layer of relative permittivity ϵr_1 on a conducting ground plane.

Increasing the number of dielectric layers and enclosing the microstrip in a box are extensions of the above model. Microstrip enclosed in a box is shown in Fig. (2.2).

When a transmission line contains a uniform loss-less medium for wave propagation, the TEM mode of trans-mission can be completely described by the electrostatic field [4] . Even when a non-uniform medium is used, the electrostatic field is an approximation to the dominant

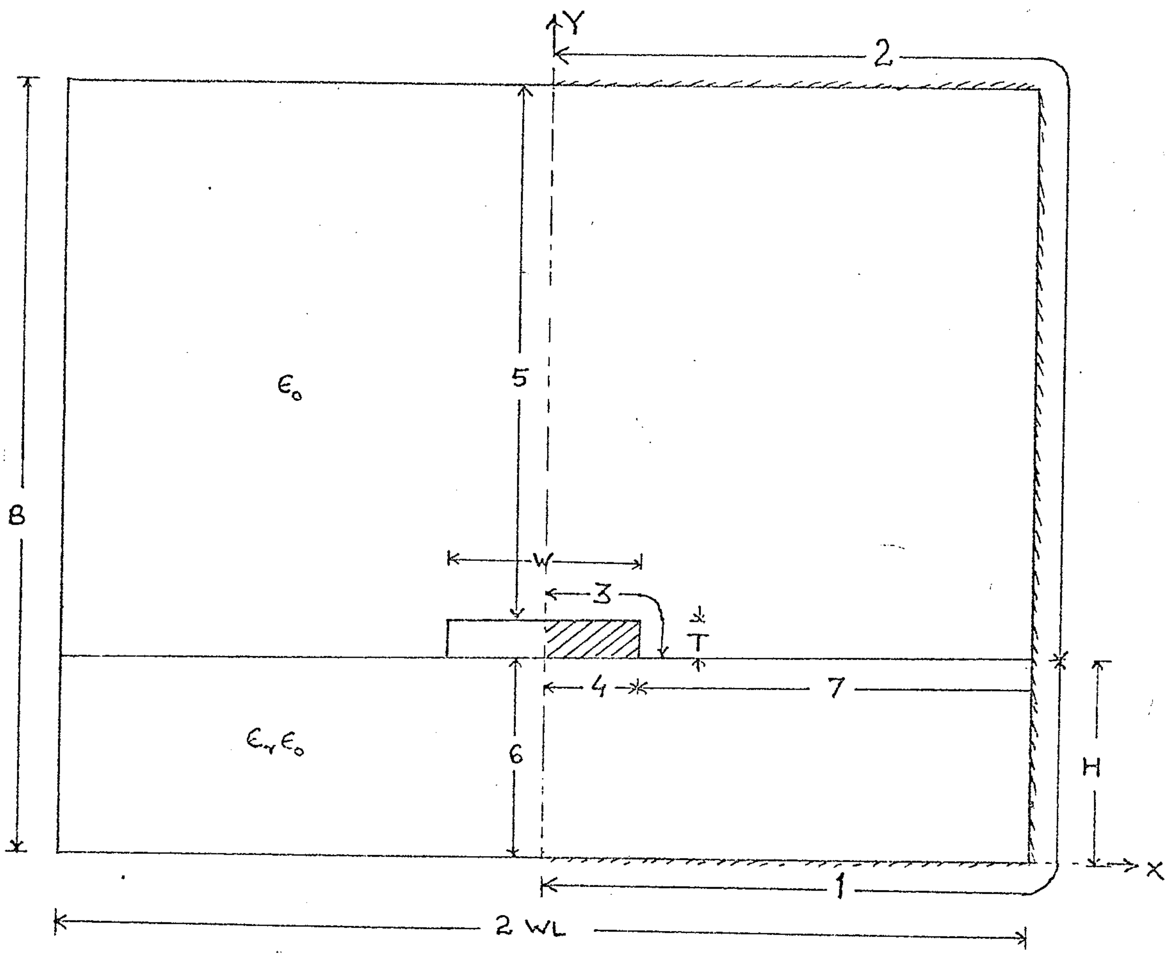

Fig.(2.2)

mode of the field in the line. This approximation holds good provided the cross-sectional dimensions of the line are much smaller than the wavelength used.

The present analysis for the microstrip parameters is based on the theory of distributed parameter transmission lines [5] . It depends on a capacitance calculation from field values obtainable from the potential distribution. Some results are also presented using the variational approach [6] , which necessitates the calculation of the magnetostatic field, a problem similar to that of determining the electrostatic field, but this time the magnetic boundary conditions must be satisfied. The variational method is presented in appendix C.

2.2 THEORETICAL PROCEDURE

The quasistatic potential distribution Ø for every homogeneous sub-region of the microstrip structure shown in Fig. (2.2) must satisfy the two dimensional Laplace equation

$$\nabla^2 \phi(x, y) = 0. \qquad (2.1)$$

Equation (2.1) is solved numerically satisfying the boundary conditions for the potential distribution along every contour of interest.

As the microstrip structure shown is symmetrical about the y-axis, we consider only the right half portion for analysis purposes. If the boundary contours are numbered as indicated in Fig. (2.2), the boundary conditions to be satisfied are:

$$\phi = V1 \text{ on contour (1) and (2),} \tag{2.2}$$

$$\phi = V2 \text{ on contour (3) and (4),} \tag{2.3}$$

$$\frac{\partial \phi}{\partial n_1} = 0 \text{ on contour (5) and (6),} \tag{2.4}$$

$$\epsilon_{r_2}\frac{\partial \phi}{\partial n_1} + \epsilon_{r_1}\frac{\partial \phi}{\partial n_2} = 0 \text{ on contour (7),} \tag{2.5}$$

where V1 and V2, respectively, are the potentials given to the shield and the strip; n_1 and n_2 are the normals on appropriate sides of the contour separating dielectric regions; ϵ_{r_1} is the relative permittivity of the dielectric supporting the strip and $\epsilon_{r_2} = \epsilon_{r_0} = 1$ for the air region.

From the electrostatic potential distribution so calculated, the electric field values are then evaluated and from which we are able to determine the surface charge distribution and hence the capacitance of the line on a per unit length basis.

As pointed out earlier the magnetostatic field is needed to be able to apply the variational approach [6]. The problem of obtaining the magnetostatic field is similar to that for the electrostatic field but the boundary conditions to be satisfied in this situation are:

$$\frac{\partial \psi}{\partial n_1} = 0 \quad \text{on contour (1), (2), (3) and (4)} \tag{2.6}$$

$$\psi = V1 \quad \text{on contour (6),} \tag{2.7}$$

$$\psi = V2 \quad \text{on contour (5)} \tag{2.8}$$

$$\frac{\partial \psi}{\partial n_1} + \frac{\partial \psi}{\partial n_2} = 0 \quad \text{on contour (7)} \tag{2.9}$$

where V1, V2, n_1, n_2 have their usual meaning and ψ represents the magnetostatic scaler potential.

The magnetostatic problem is homogeneous as suggested by boundary condition (2.9). This is due to the fact that even though the material supporting the strip has a relative dielectric constant ϵ_{r_1} differing from that of free space, it has relative permeability μ_{r_1} the same as that of free space so that $\mu_1 = \mu_2$

2.3 EFFECTIVE DIELECTRIC CONSTANT

In microstrip the electric field extends into the air region outside the dielectric substrate and therefore has to be considered as a capacitor with a mixed dielectric. In situations of this type the concept of an effective dielectric constant is useful and is taken to be the weighted mean of the dielectric constants of the two materials. If the two dielectric materials in the capacitor are replaced by a material with a dielectric constant equal to the effective dielectric constant, the value of the capacitance remains unchanged.

Another definition that is useful, especially for capacitors that are partially filled with a dielectric and the remaining portion air, is that of an effective filling fraction defined by Wheeler [8] , which is

$$\epsilon_{reff} = (1-q) + q\,\epsilon_r \qquad (2.10)$$

where ϵ_r is the relative dielectric constant of the dielectric material and q is the effective filling fraction which depends on the fraction of the total volume filled with dielectric material.

2.4 CALCULATION OF MICROSTRIP PARAMETERS

The capacitance approach as described by Yamishta [5] is used to calculate the microstrip parameters. The microstrip capacitance is required for two situations, first, when the line is homogeneous, that is with no dielectric present and, secondly, for the actual line with its dielectric present.

To evaluate these capacitance values we let $\epsilon_{r_1} = \epsilon_{r_0} = 1$ for the homogeneous line and then $\epsilon_{r_1} = \epsilon_{r_1}$ for the inhomogeneous line in boundary condition equation (2.5).

If Co is the capacitance per unit length of line for the unloaded case and C that for the loaded case, then its characteristic impedance, Z, is given by

$$Z = \frac{1}{\sqrt{CCo}\, Vo} \qquad (2.11)$$

where Vo is the velocity of propagation of light in free space.

If V represents the velocity of wave propagation in microstrip then

$$V = Vo\sqrt{\frac{Co}{C}} \; . \qquad (2.12)$$

The relative velocity is

$$V_R = \sqrt{\frac{Co}{C}} \, . \tag{2.13}$$

With a wavelength, λ , in terms of the free space wavelength, λ_o , given by

$$\lambda = \lambda_o \sqrt{\frac{Co}{C}} \, . \tag{2.14}$$

The relative effective dielectric constant is

$$\epsilon_{r\,eff} = \frac{C}{Co} = \frac{1}{V_R^{\,2}} \, . \tag{2.15}$$

2.5 ATTENUATION CALCULATION

In microstrip, signal attenuation results mainly from two sources:

(i) Conductor losses in the shield and strip.

(ii) Dielectric losses.

To calculate the conductor losses the actual surface charge density, ρ_s, on the strip and the shield are determined, using Gauss's theorem, from the calculated potential distribution. The conductor surface current density, i_s, is the product of the surface charge density, ρ_s, and the velocity of propagation [4]

$$i_s = \rho_s V \, . \tag{2.16}$$

The attenuation loss for the conductors, α_c is evaluated using

$$\alpha_C = \frac{\text{Power loss in the conductors}}{2 \times \text{power transmitted}} . \qquad (2.17)$$

The power loss in each conductor is then

$$P_{LC} = \oint_C R_s \; i_s{}^2 \; dl \qquad (2.18)$$

where the path of integration is around the conductor surface. R_s is the surface resistence of the conductor and is given by

$$R_s = \frac{1}{\text{skin depth} \times \text{conductivity}} \qquad (2.19)$$

$$= \sqrt{\frac{w \; \mu_0}{2 \sigma}} . \qquad (2.20)$$

Where w is the frequency in radians per second, μ_0 is the free space permeability and σ is the conductor conductivity. Referring to Fig.(2.3) for the integration contours, the total conductor losses from (2.18) are then

$$P_{LC} = 2 \int_{C_1} R_S i_S{}^2 dl + 2 \int_{C_2} R_S i_S{}^2 dl . \qquad (2.21)$$

The integrals were evaluated numerically by dividing each contour into segments. The current density is

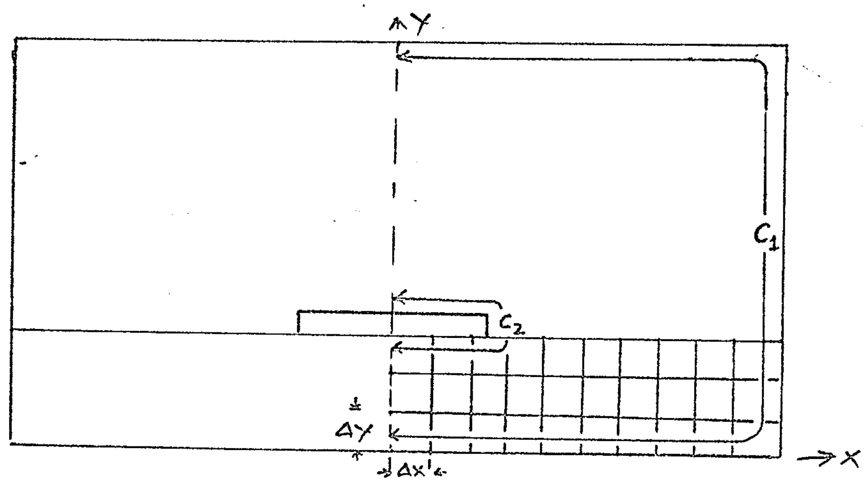

Fig. (2.3)

calculated at the centre of each segment and is assumed to be constant on the length of the segment. Thus (2.21) becomes

$$P_{LC} = 2 \sum_{N} R_S\, i_{SN}{}^2\, \Delta l + 2 \sum_{M} R_S i_{SM}{}^2\, \Delta l \,. \qquad (2.22)$$

The total current through each conductor is found by summing the current through each conductor segment. The power transmitted is given by the product of the total current and the potential difference applied between conductors. The transmitted power can also be obtained from

$$P_T = \frac{(V2-V1)^2}{Z} \,. \qquad (2.23)$$

Hence the conductor attenuation may be calculated using (2.17).

The dielectric power loss, P_{LD}, as given by [4] is

$$P_{LD} = \iint_S \sigma_d E^2 \, dx \, dy \tag{2.24}$$

where the surface integral is defined as the cross-sectional area of the dielectric region, E is the total electric field for a point in the dielectric, σ_d is the conductivity of the dielectric. σ_d is determined from the loss tangent for the dielectric, $\tan\delta$, and is given by

$$\sigma_d = w \epsilon \tan\delta \tag{2.25}$$

where ϵ is the dielectric constant of the material used. It should be noted that σ_d is frequency dependent.

To evaluate (2.24) numerically the dielectric region is divided into N subregions and the total electric field calculated at the centre of each subregion. The electric field is assumed to be constant throughout each subregion.

Referring to Fig. (2.3), (2.24) can be rewritten as

$$P_{LD} = \sum_N \sigma_d E_N^2 \, \Delta x \, \Delta y \, . \tag{2.26}$$

The attenuation constant, α_d, for the dielectric is given by

$$\alpha_d = \frac{P_{LD}}{2P_T} \tag{2.27}$$

with P_T given by (2.23).

2.6 RESULTS AND DISCUSSION

A numerical analysis of the microstrip configuration of Fig. (2.2) is carried out using a computer program written for the equivalent source method. A description and listing of this program is given in Appendix E.

The conductor and dielectric boundary contours were numbered as shown in Fig. (2.2) with the number of segments assigned to each contour as given in Table (2.1).

Table (2.1)

Contour number	1	2	3	4	5	6	7
Number of segments	12	8	12	10	11	6	11

A total of 70 segments were taken and the appropor-tioning to contours depended upon the field variation along the contour. For example more segments were taken around the strip corner to accomodate the large field variation existing there. A typical division of segments on the strip is shown in Fig. (2.4).

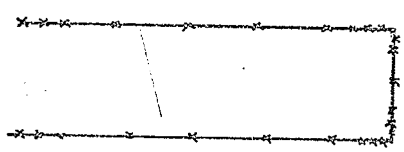

Fig. (2.4)

Computer execution time in seconds/accuracy for 50, 70 and 100 segments was found to be 9/.95, 12/.99, 32/.995. So 70 segments were considered to be economical and accurate enough. The accuracy of results was tested by taking the ratio of the characteristic impedance of the microstrip line as calculated using the charge on the shield with that obtained by using the charge on the strip. This testing method was developed since it was noticed that the characteristic impedance values as calculated from the shield and strip charge converged with increasing number of segements used and also with adjustment of segment size to the field variation along the contour. It was noted that the characteristic impedance as calculated on the basis of shield charge always gave a lower bound value while the characteristic impedance as calculated using the charge on the strip always gave an upper bound value.

The effect on the characteristic impedance, Figs. (2.5) --- (2.6), relative wavelength, Figs. (2.7) --- (2.8), effective dielectric constant, Figs. (2.9) --- (2.10), relative velocity, Figs. (2.11) --- (2.12), and attenuation, Fig. (2.13), (at a frequency of 1GHZ) of the microstrip line of varying the strip width W in the range $.5 \leq W/H \leq 7$ was examined. The dielectric substrate thickness H and enclosing box dimensions (B = 15 H and WL = 12.5 H) were kept constant. The dielectric material had a relative dielectric constant of 8.875, selected to allow comparison with the results of Stinehelfer [15] . The

Characteristic impedance versus W/H.

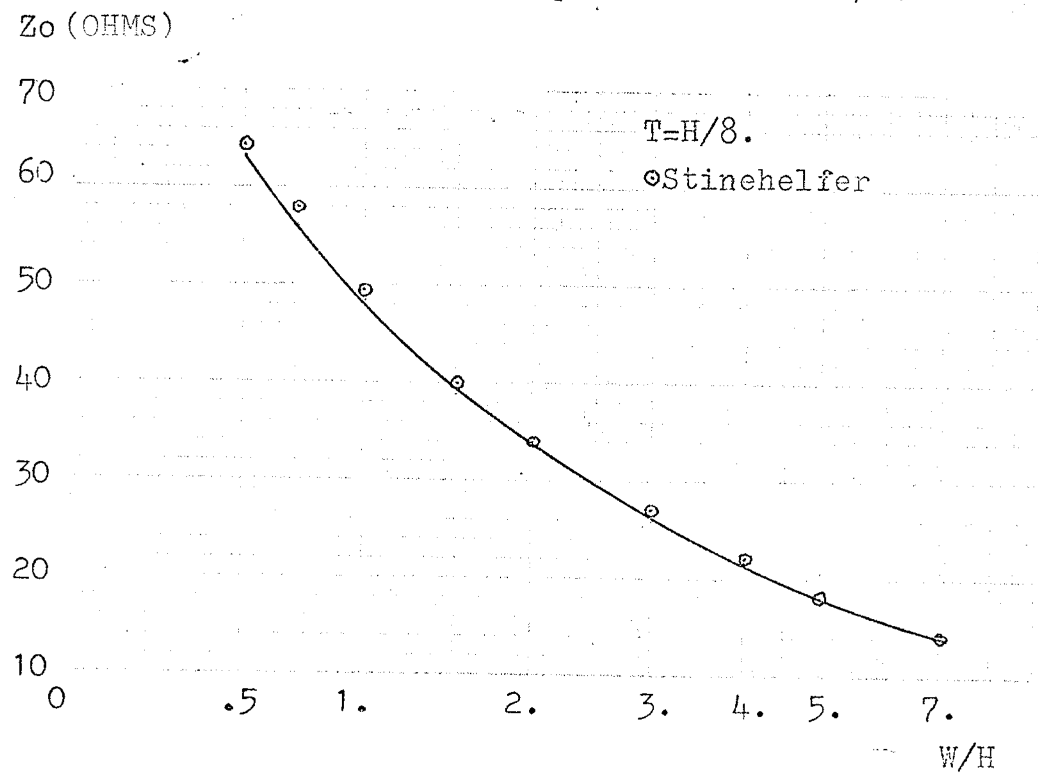

Fig.(2.5)

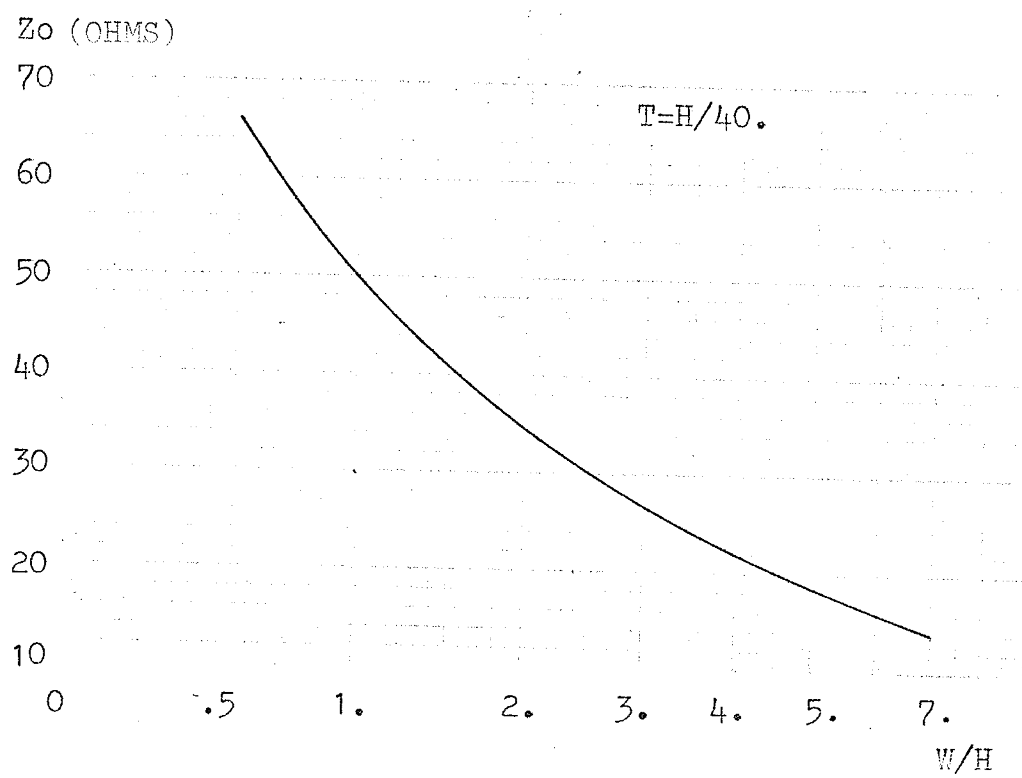

Fig.(2.6)

Relative wavelength versus W/H.

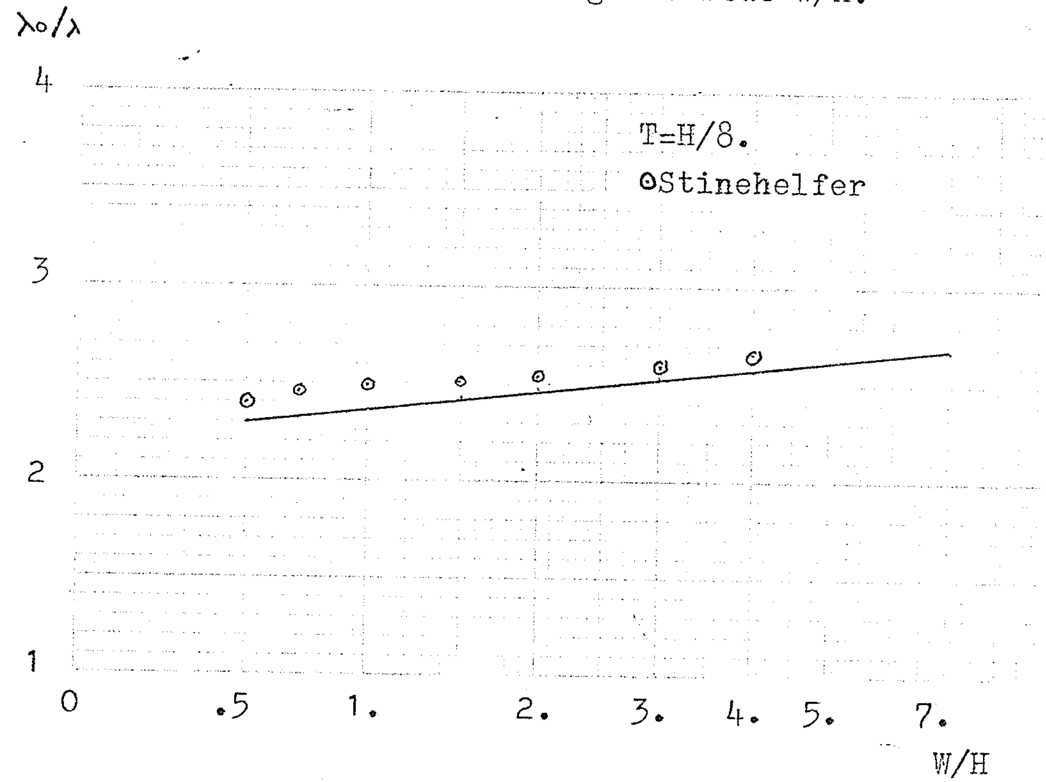

Fig.(2.7)

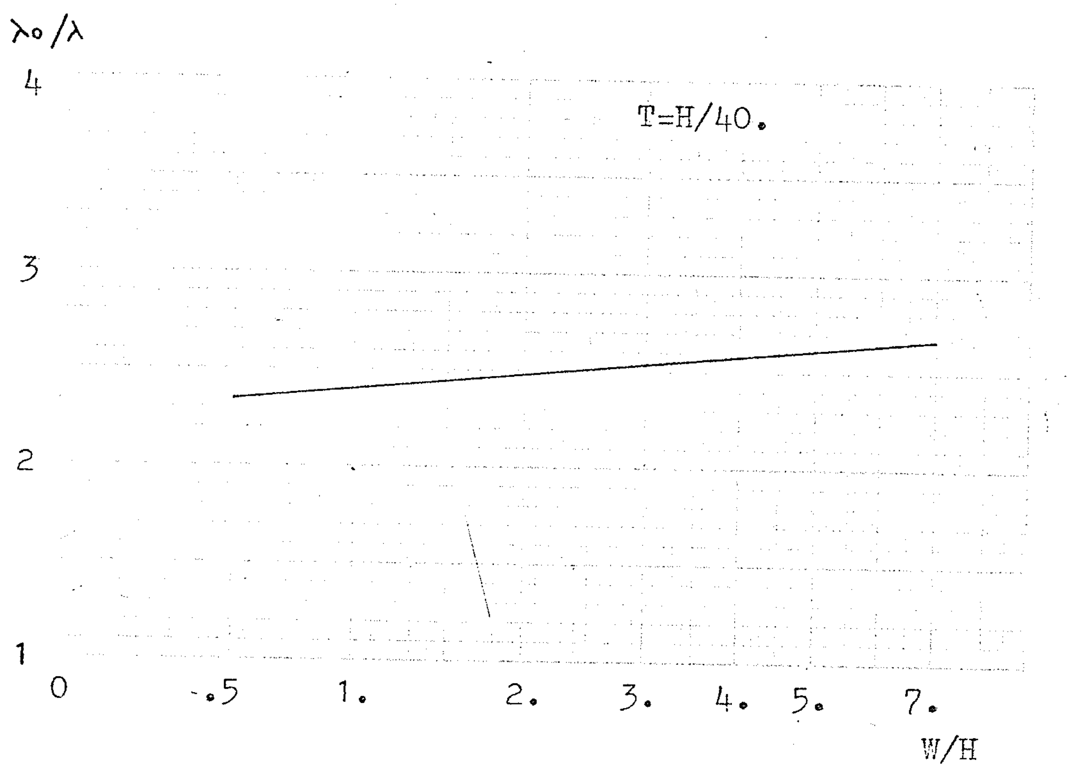

Fig.(2.8)

Effective dielectric constant versus W/H.

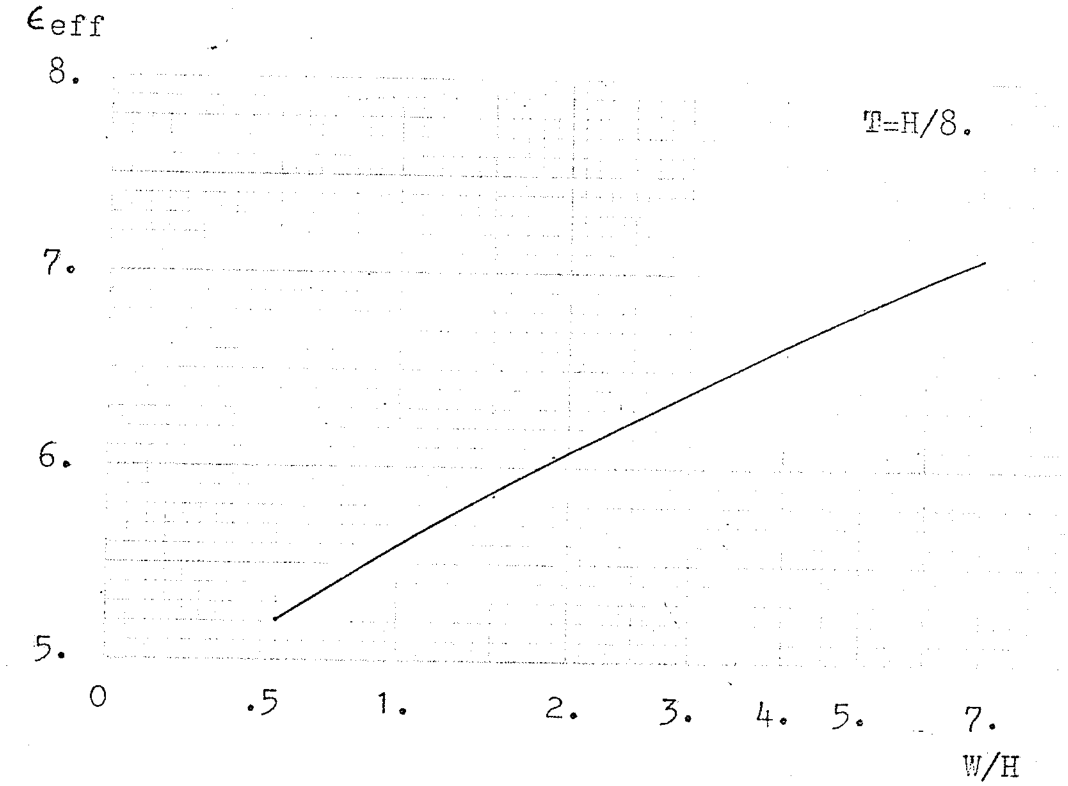

Fig.(2.9)

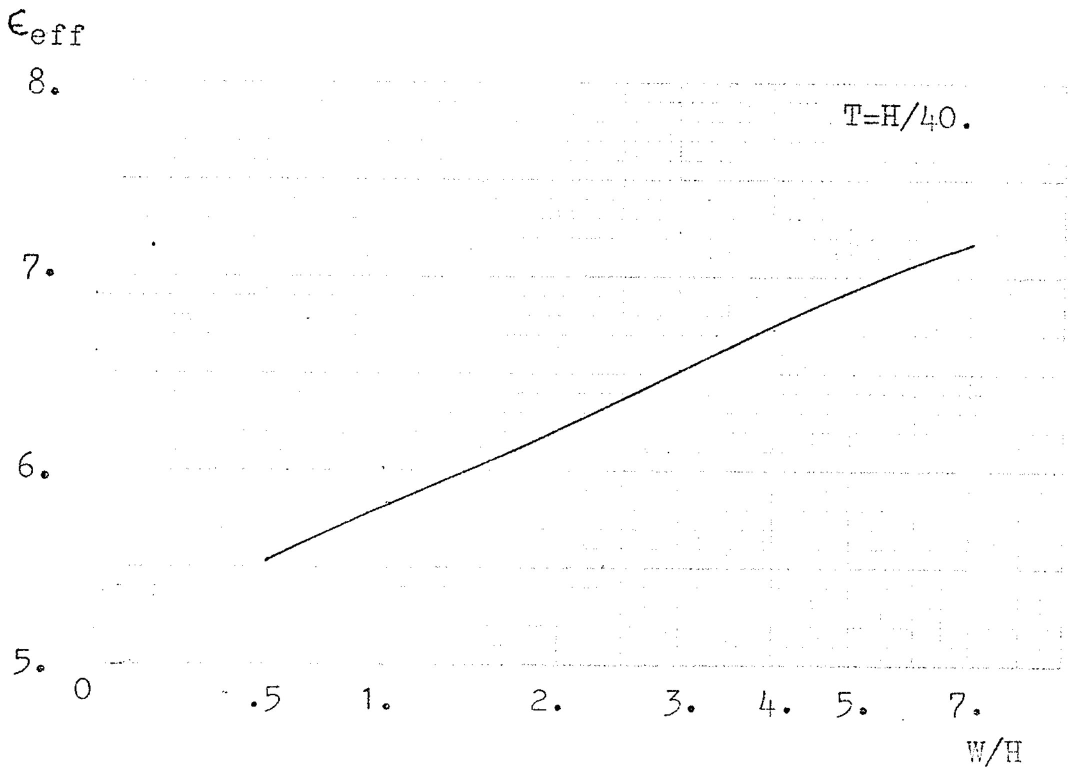

Fig.(2.10)

Relative velocity versus W/H.

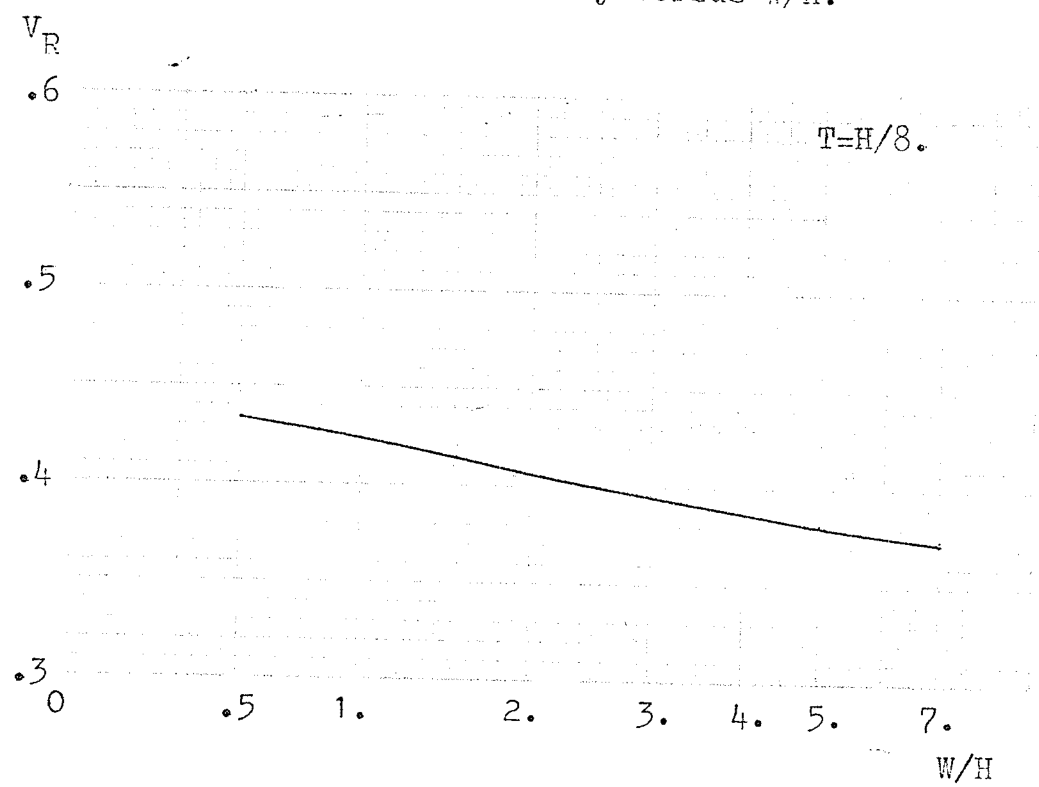

Fig.(2.11)

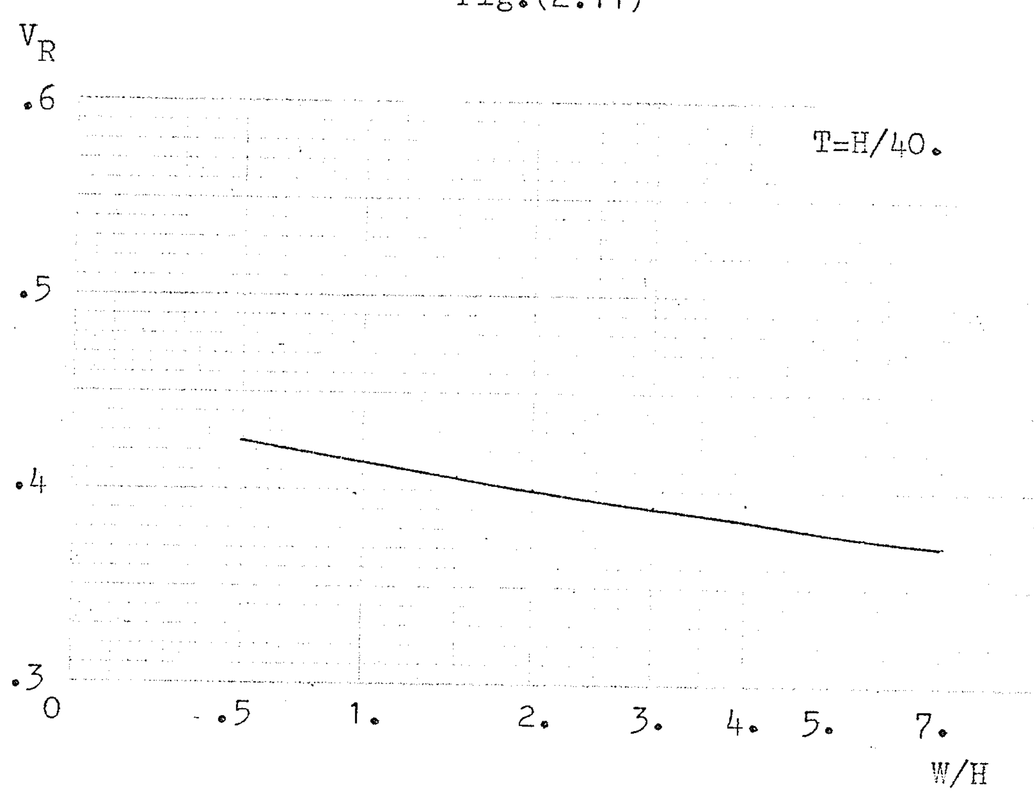

Fig.(2.12)

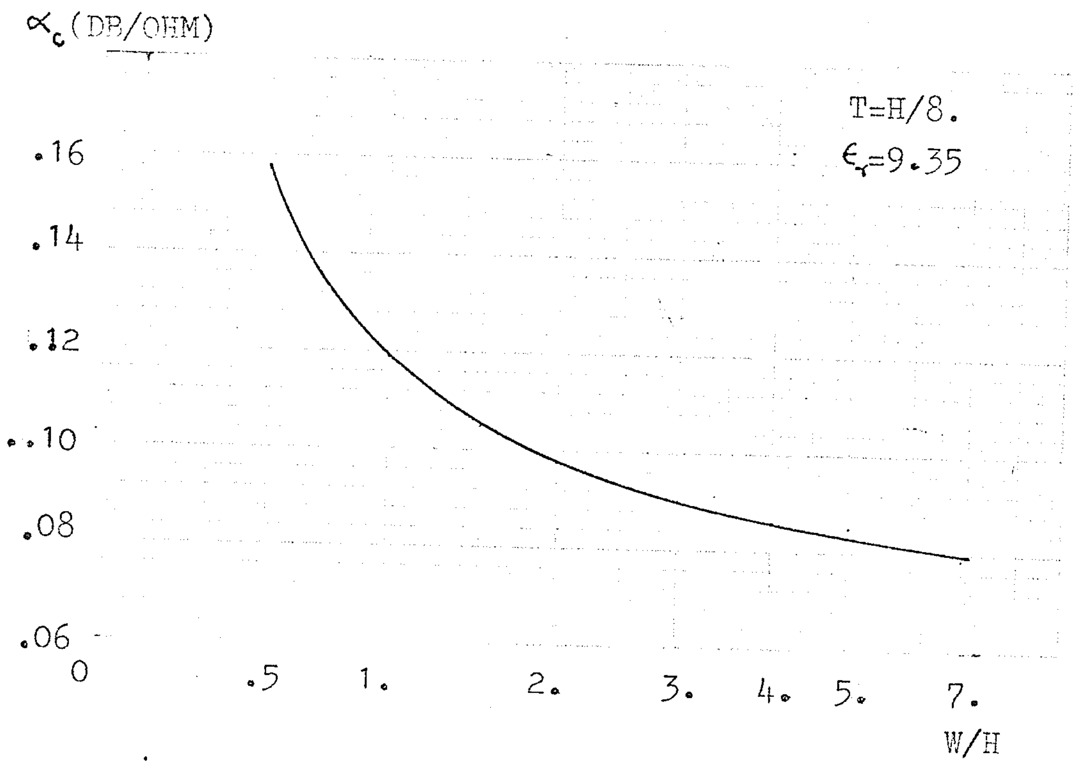

Fig.(2.13). Conductor attenuation constant versus W/H.

thickness of the strip T was taken as H/8 and this was changed to H/40 for a second set of results.

Calculated values of characteristic impedance (Fig. (2.5)) and relative wavelength (Fig. (2.7)) as determined on a capacitance basis compare well with the results of Stinehelfer [15]. Table (2.3) compares results for the relative wavelength calculated on the capacitance and variational basis to those of Stinehelfer [15]. A better comparison is seen for the variational calculation than from the capacitance calculation. Table (2.4) presents results for the effective dielectric constant as calculated using the variational approach.

The attenuation of the microstrip over the frequency range 1-5 GHZ is calculated next. Three different sets of microstrip dimensions, selected to correspond with those used in the reference publications, for the configuration of Fig. (2.2), are considered. The dimensions are shown on each graph, i.e., Fig. (2.14) -- Fig. (2.16). The dielectric is taken to be alumina ($\epsilon_r = 9.35$) which is that used mostly in practice.

Fig. (2.14) -- Fig. (2.16) show attenuation data which are in good agreement with experimental values as given by Pucel et al [7], except for those in Fig. (2.16). In fact our results show better agreement with experimental results than the Pucel et al [7] theory. A possible explanation for the disagreement in Fig. (2.16) is that these

TABLE (2.3)

COMPARISON OF RELATIVE WAVELENGTH FOR MICROSTRIP OF FIG.(2.2) CONFIGURATION, T=H/8, ϵ_r=8.875.

W/H	Variational calculation	Stinehelfer	Capacitance calculation
0.5	2.48	2.45	2.30
0.7	2.53	2.48	2.33
1.0	2.59	2.52	2.38
1.5	2.68	2.55	2.43

TABLE (2.4)

VARIATIONAL EFFECTIVE DIELECTRIC CONSTANT FOR MICROSTRIP FIG.(2.2) CONFIGURATION, T=H/8.

W/H	ϵ_r=8.875	ϵ_r=9.35
0.5	6.16	6.45
0.7	6.39	6.69
1.0	6.71	7.02
1.5	7.19	7.53

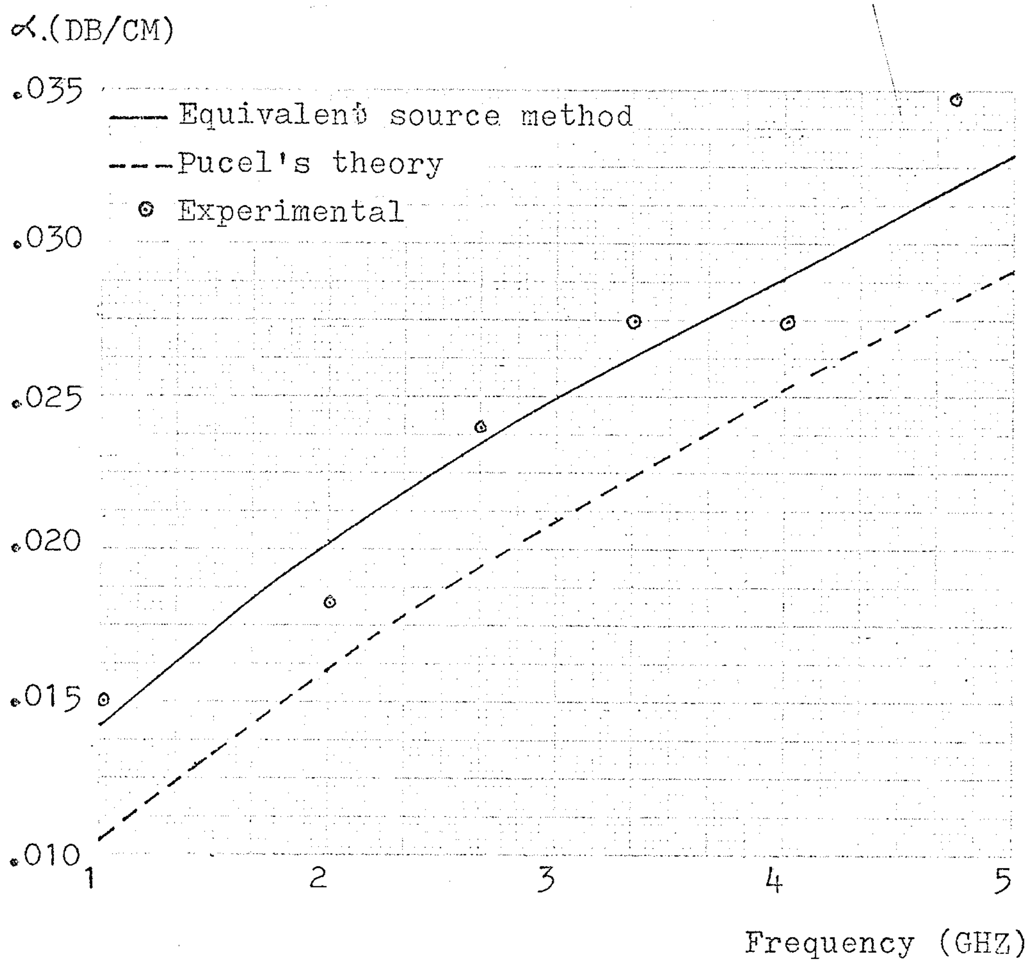

Fig.(2.14). Attenuation constant versus frequency for the microstrip on alumina substrate.
(H=.05",W=.02",T=.00031",WL=5H,B=5H,Zo=70Ω)

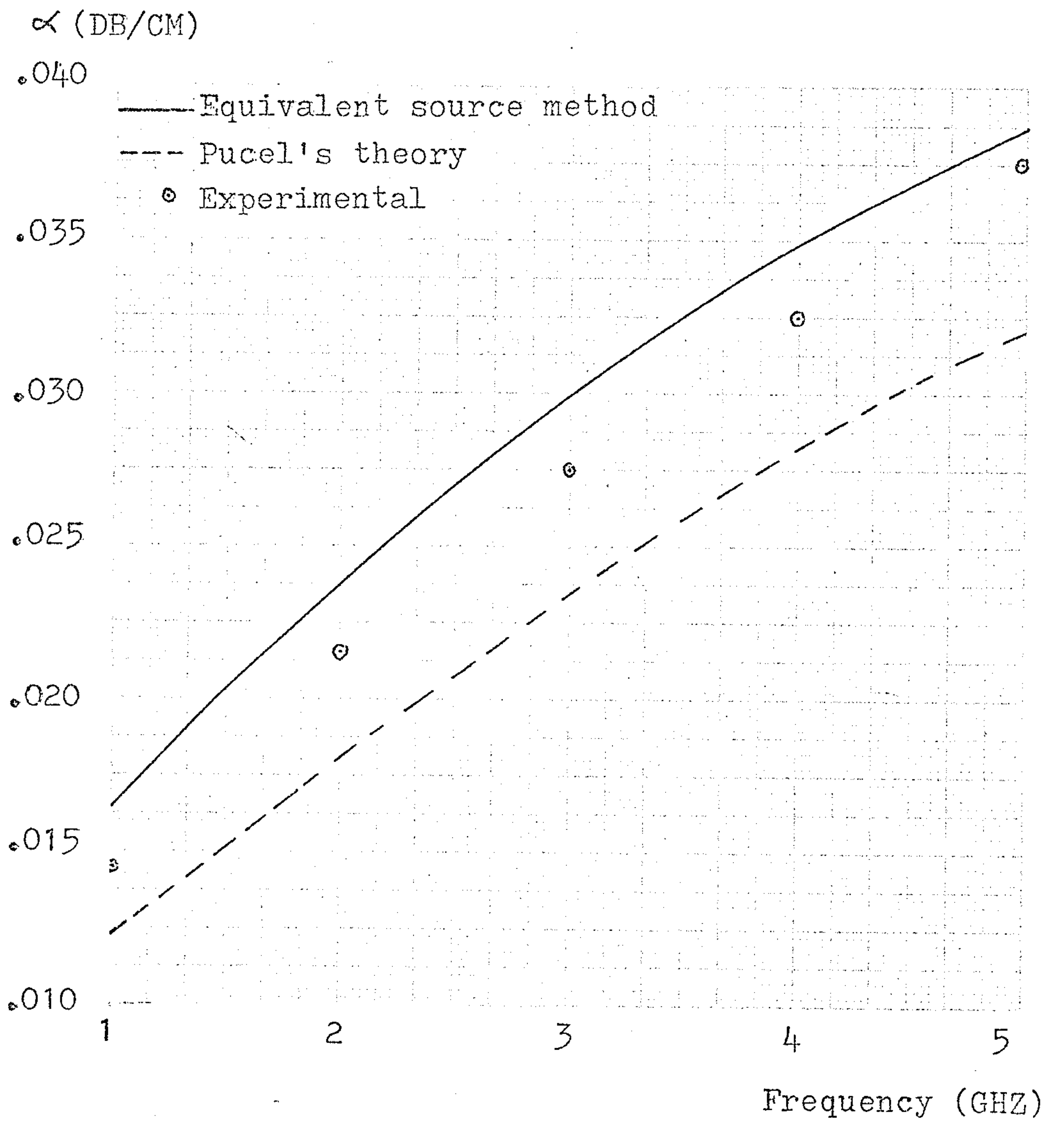

Fig.(2.15). Attenuation constant versus frequency for the microstrip on alumina substrate.

(H=.02",W=.049",T=.00046",WL=10H,B=5H,Zo=30Ω)

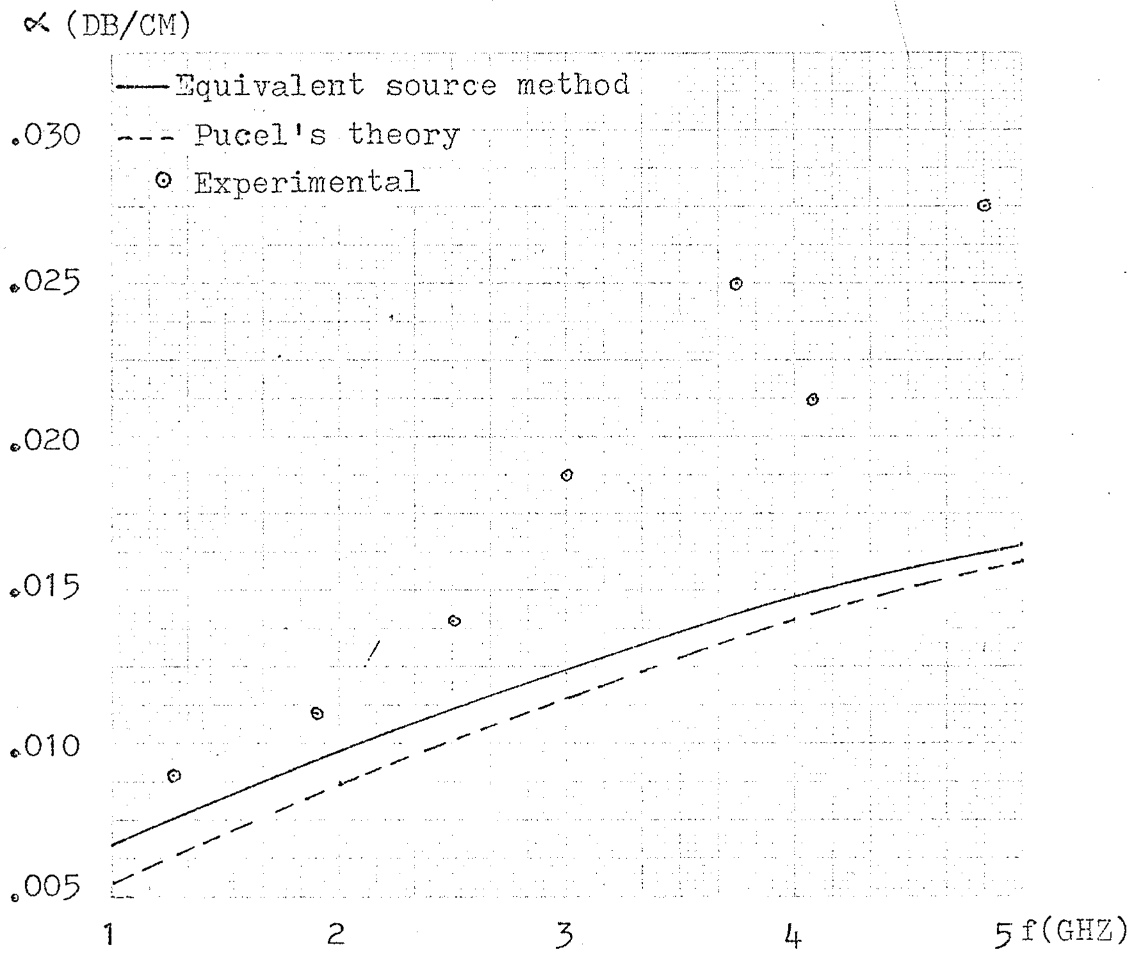

Fig.(2.16). Attenuation constant versus frequency for the microstrip on alumina substrate.

(H=.05",W=.12",T=.00039",WL=10H,B=5H,Zo=30Ω)

results correspond to a microstrip configuration with thicker substrate and higher W/H ratio compared to the other two configurations considered. It is possible that a surface mode or higher microstrip mode is responsible for this discrepency. The TE_1 surface mode must be ruled out because it has too high a cut-off frequency. However, the TM_0 surface mode has a zero cut-off frequency and a transverse field distribution similar to that for the dominant strip mode and therefore it might be launched rather easily with a wide strip configuration. One other possible explanation is that the loss tangent for the frequency range 1-5 GHZ might have a considerably higher value than the value used.

The reason why the presented attenuation results are higher in each case from Pucel's [7] theory is partially due to the fact that we are considering microstrip enclosed in a box while Pucel et al [7] analyse an open microstrip and partially due to the singularity of field at the strip corner. The charge density tends towards being singular at sharp corner contours. An attempt to round the contour corners resulted in a considerable reduction in losses (db /wavelength calculated at a frequency of 1 GHZ) as is evident by an inspection of Table (2.2)

An attempt to compare the attenuation results with those of Gunn [9] was made but proved futile as insufficient information was available on his microstrip dimensions.

Table (2.2)

Corner Shape	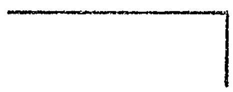		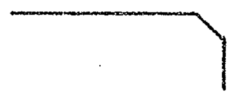		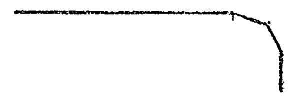	
	Shield	Strip	Shield	Strip	Shield	Strip
db/λ	.0578276	.1378121	.0578227	.1214095	.0578143	.1179450

However, his assumption of a cubic function representation for charge distribution on the strip is far out from the charge distribution as determined by the equivalent source method, Fig. (2.17) . The functional representation considered by Yamishta [4] is a better approximation to the numerically determined ones, as is seen in the next chapter where our attenuation results compare favourably with the Yamishta results. Our calculated charge distribution compares well with that calculated by Mittra and Itoh [19].

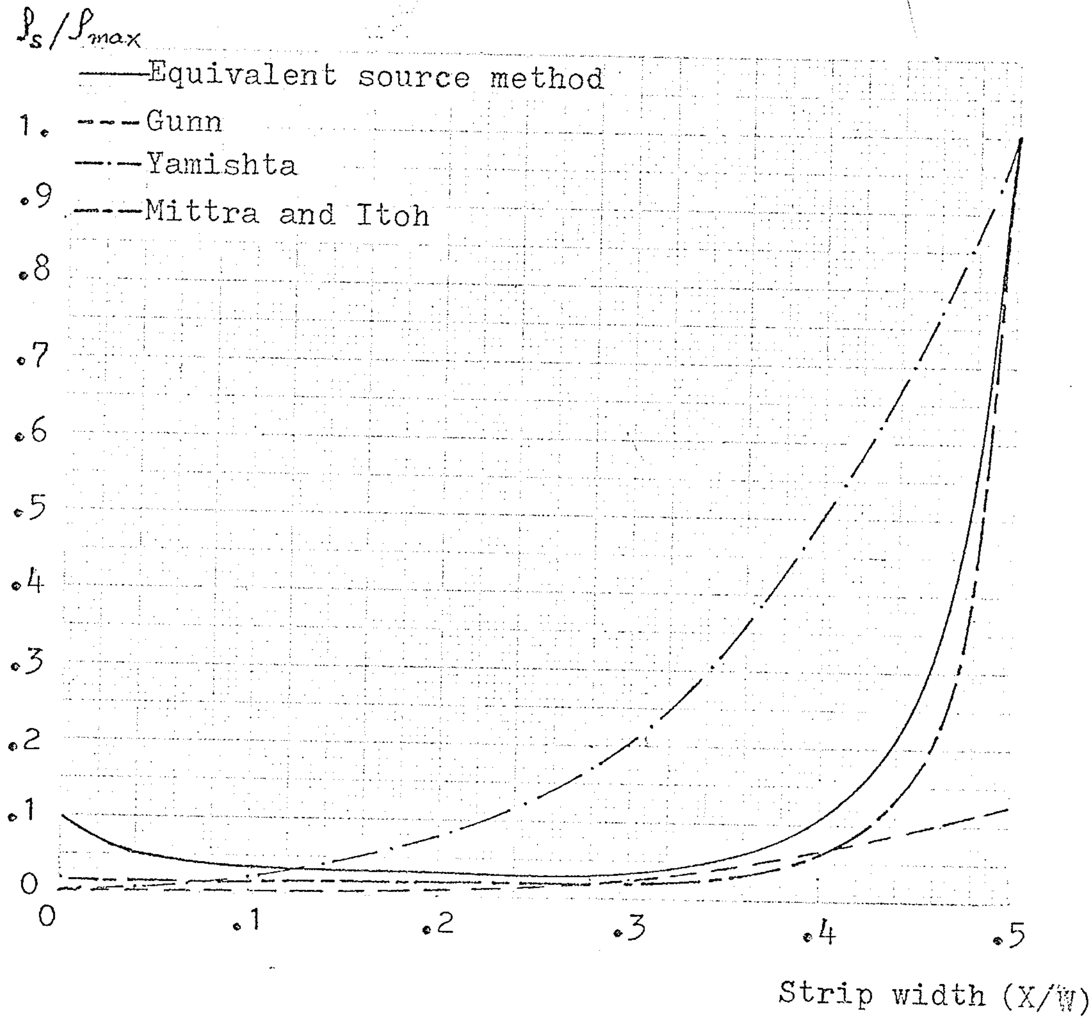

Fig.(2.17). Surface charge density versus strip width.

Chapter 3

3.1 MICROSTRIP WITH SUSPENDED SUBSTRATE

The method described in Chapter 1 is next applied to microstrip configurations consisting of any number of dielectric layers. The analysis is exactly the same as that for single substrate microstrip examined in Chapter 2 except for the consideration of additional surface sources on the boundary contours which separate the dielectric layers.

Suspended substrate microstrip line which is enclosed in a box is shown in Fig. (3.1). Single layer microstrip is a special case of this configuration when $h_1 = h_3 = 0$. The analysis, still based on the assumption of quasistatic TEM mode of propagation, requires the potential distribution ϕ for every homogeneous sub-region. As the microstrip structure is symmetrical about the y-axis, we will consider only the right half region and this is reproduced in Fig. (3.2).

Equation (2.1) is numerically solved satisfying the boundary conditions for the potential distribution along every contour of interest. For the boundary contours as numbered in Fig. (3.2), the boundary conditions to be satisfied are:

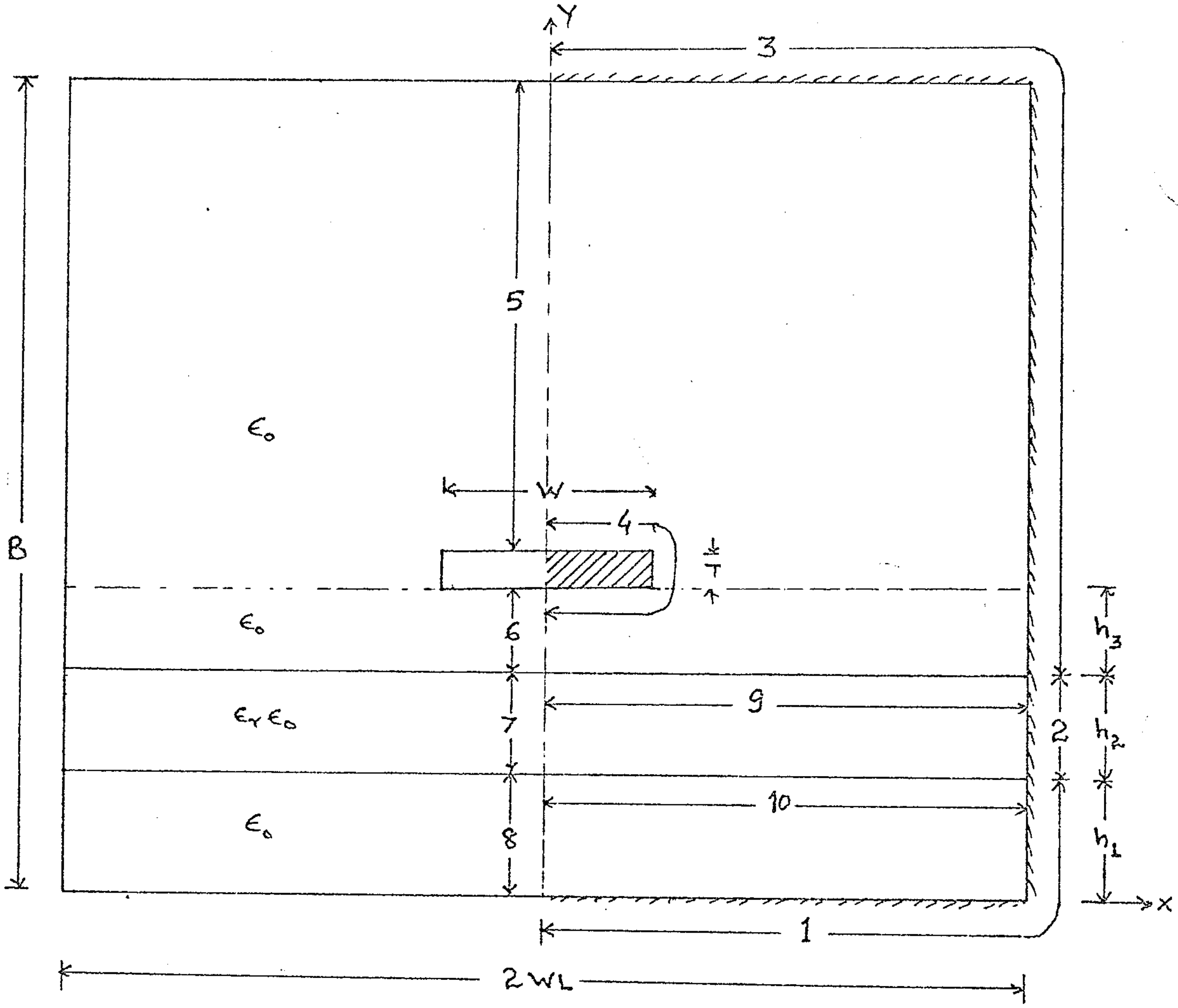

Fig.(3.1)

$$\emptyset = V1 \qquad \text{on contours 1, 2, 3 and 4,} \tag{3.1}$$

$$\emptyset = V2 \qquad \text{on contours 5 and 6,} \tag{3.2}$$

$$\frac{\partial \emptyset}{\partial n_1} = 0 \qquad \text{on contours 7, 8, 9 and 10,} \tag{3.3}$$

$$\epsilon_{r_2}\frac{\partial \phi}{\partial n_1} + \epsilon_{r_3}\frac{\partial \phi}{\partial n_2} = 0 \quad \text{on contour 11,} \tag{3.4}$$

$$\epsilon_{r_1}\frac{\partial \phi}{\partial n_1} + \epsilon_{r_2}\frac{\partial \phi}{\partial n_2} = 0 \qquad \text{on contour 12} \tag{3.5}$$

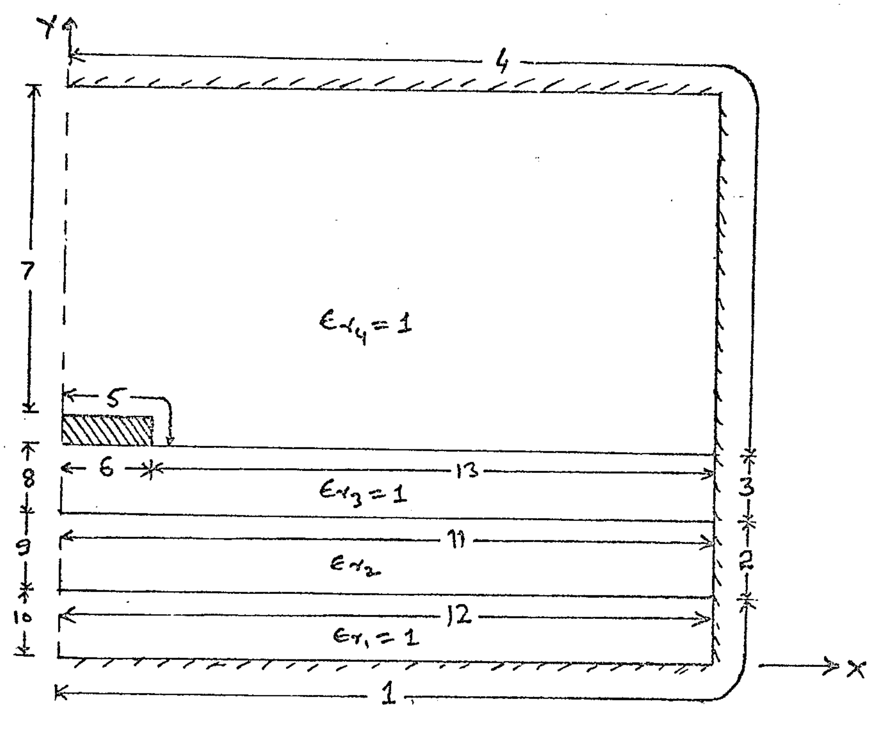

Fig. (3.2)

where V1 and V2 are respectively the potentials on the shield and strip, n_1 and n_2 are normals to the two sides of contours,

ϵ_{r_2} is the relative permittivity of the dielectric substrate and $\epsilon_{r_1} = \epsilon_{r_3} = 1$ if the region is assumed to be free space. However, in practice, to provide support to the strip, some low dielectric constant material like polystyrene foam ($\epsilon_r = 1.03$) is used.

The characteristic impedance, the propagation velocity, the wave length and the relative effective dielectric constant for the configuration of Fig. (3.1) were obtained using equations (2.11), (2.12), (2.14), (2.15), respectively.

3.2 RESULTS AND DISCUSSION

The suspended substrate microstrip configuration of Fig. (3.1) was considered first for the special case when $h_3 = 0$. The contours were numbered as shown in Fig. (3.3) with the number of segments selected for each contour listed in Table (3.1).

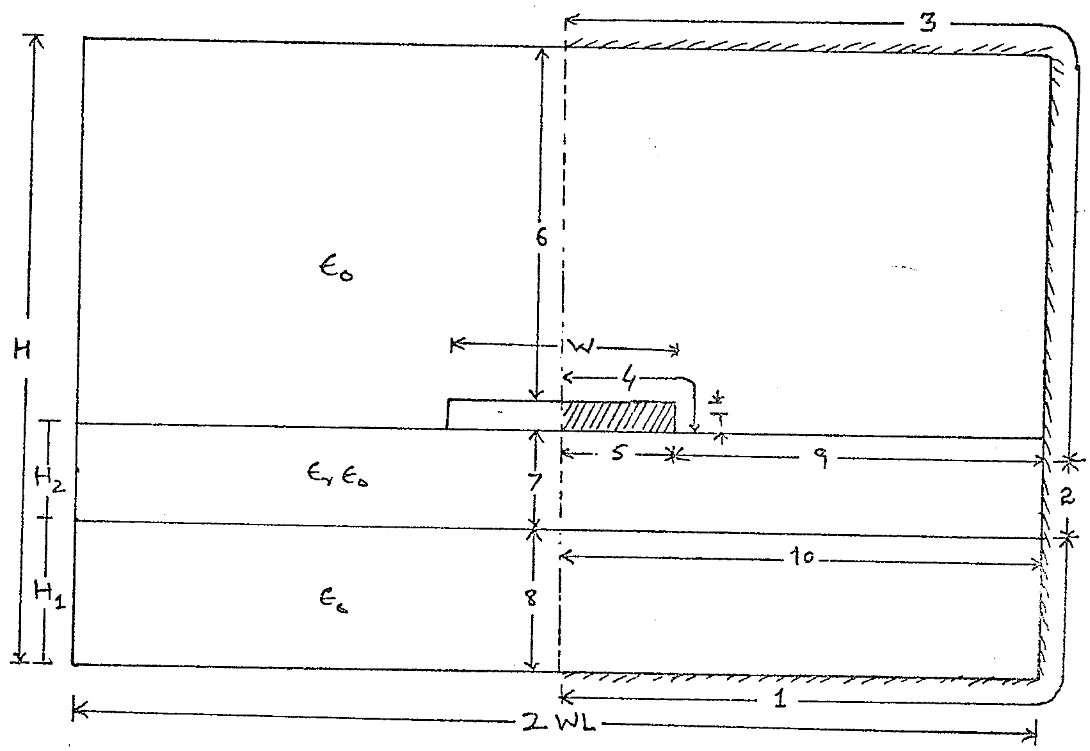

Fig. (3.3)

A total of 100 segments was used with segment lengths small where there was considerable variation of the field along the contour.

Table (3.1)

Contour number	1	2	3	4	5	6	7	8	9	10
Number of segments	15	3	12	17	13	10	6	4	10	10

The microstrip characteristic impedance, Fig. (3.4), relative wavelength, Fig. (3.5), effective dielectric constant, Fig. (3.7), conductor attenuation constant ($\alpha_c W/R_s$), Fig. (3.6) and dielectric attenuation constant (α_d / σ_d), Fig. (3.8) was calculated for a fixed strip width but varying width dimension of the enclosing box in the range $1.5 \leq 2\ WL/W \leq 10$. The height of enclosing box H, thickness of dielectric substrate ($H_2 = .2H$), suspension height ($H_1 = .4H$) and thickness of strip ($T = H/50$) were kept fixed. The dielectric considered was quartz ($\epsilon_r = 3.78$) and this is changed to alumina ($\epsilon_r = 9.35$) for the second set of results. The width of the strip was then varied ($.5 \leq W/H \leq 10$), keeping the size of the enclosing box fixed ($WL = 5H$) and its effect on the basic parameters determined, Figs.(3.9) -- (3.13). Here the substrate was taken to be alumina ($\epsilon_r = 9.35$). The substrate thickness was next varied on the range $.1 \leq H_2/H \leq .5$, while keeping the strip width constant at $W = H$. Results for alumina ($\epsilon_r = 9.35$) are presented in Table (3.4).

Curves of characteristic impedance, Fig. (3.4), relative wavelength, Fig. (3.5), conductor attenuation constant, Fig. (3.6), and dielectric attenuation constant, Fig. (3.8), compare well with those of Yamishta [4] .

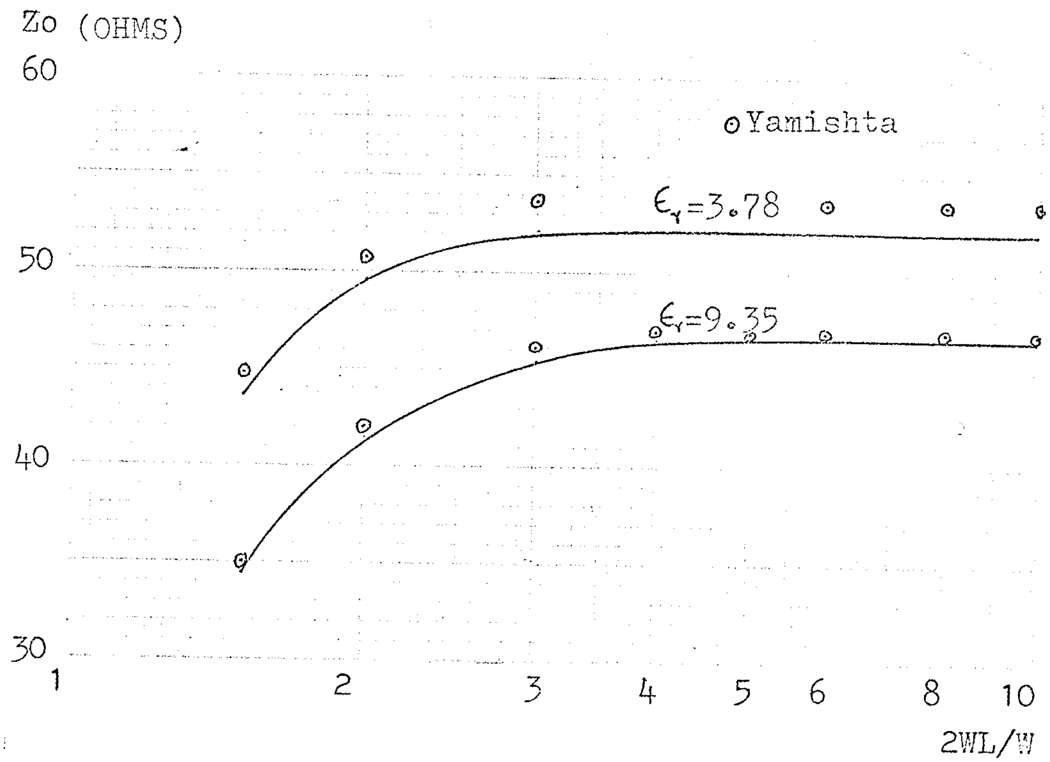

Fig.(3.4). Characteristic impedance versus 2WL/W.

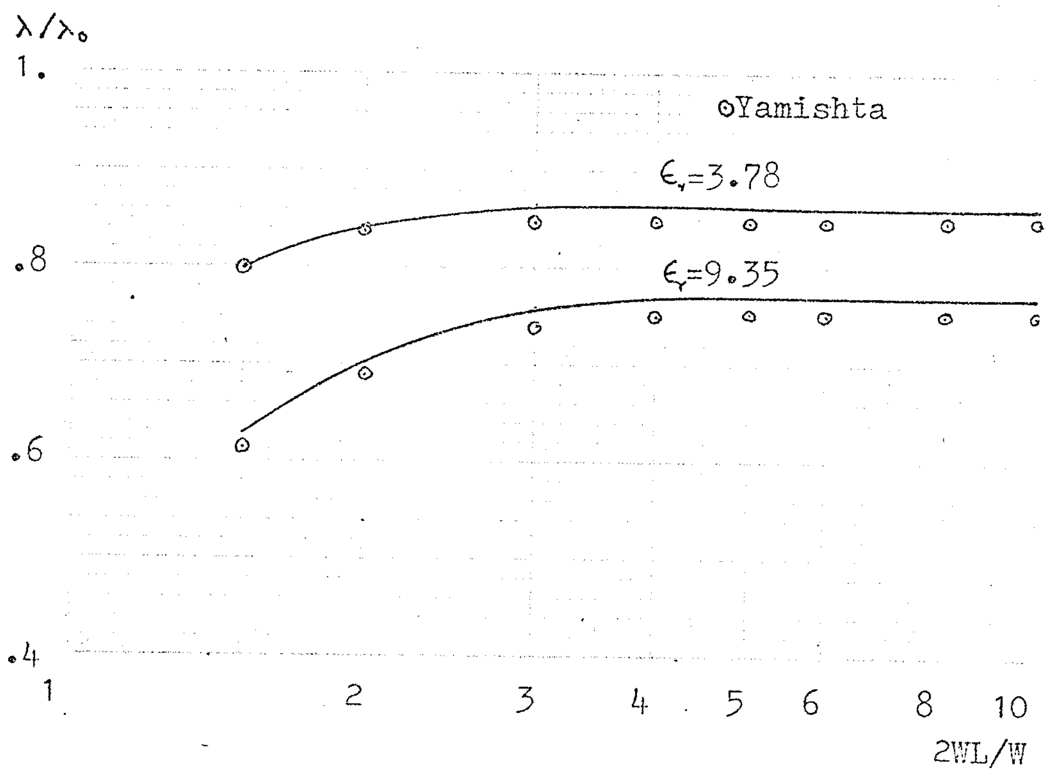

Fig.(3.5). Relative wavelength versus 2WL/W.

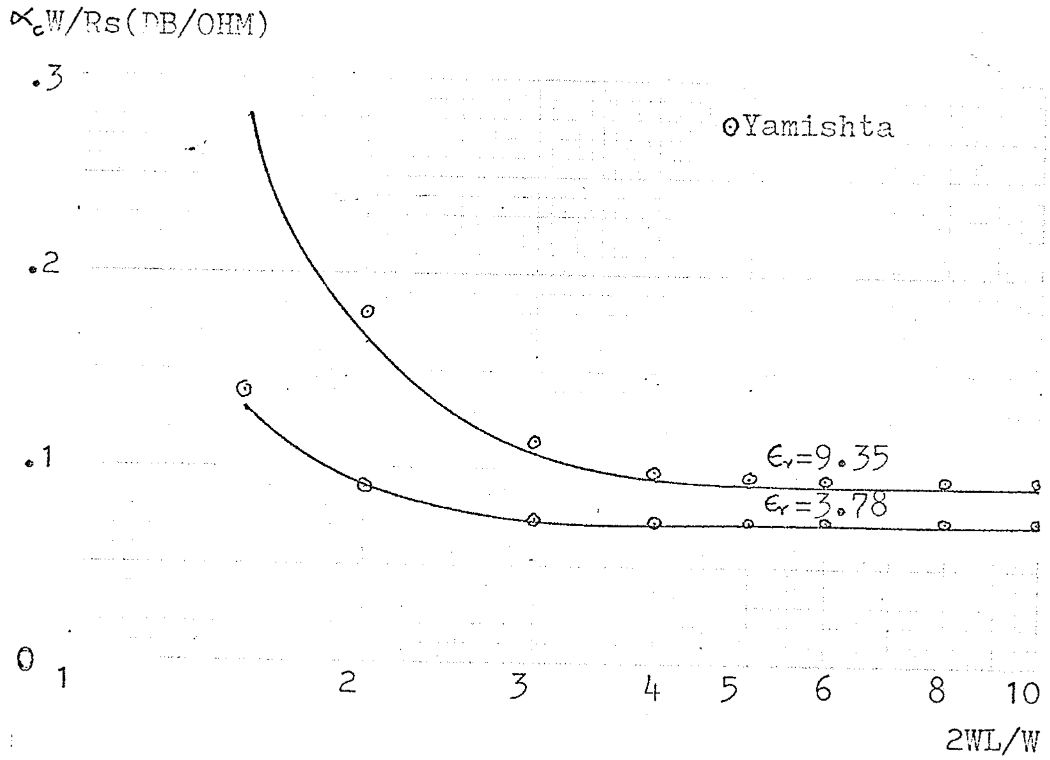

Fig.(3.6). Conductor attenuation constant versus 2WL/W.

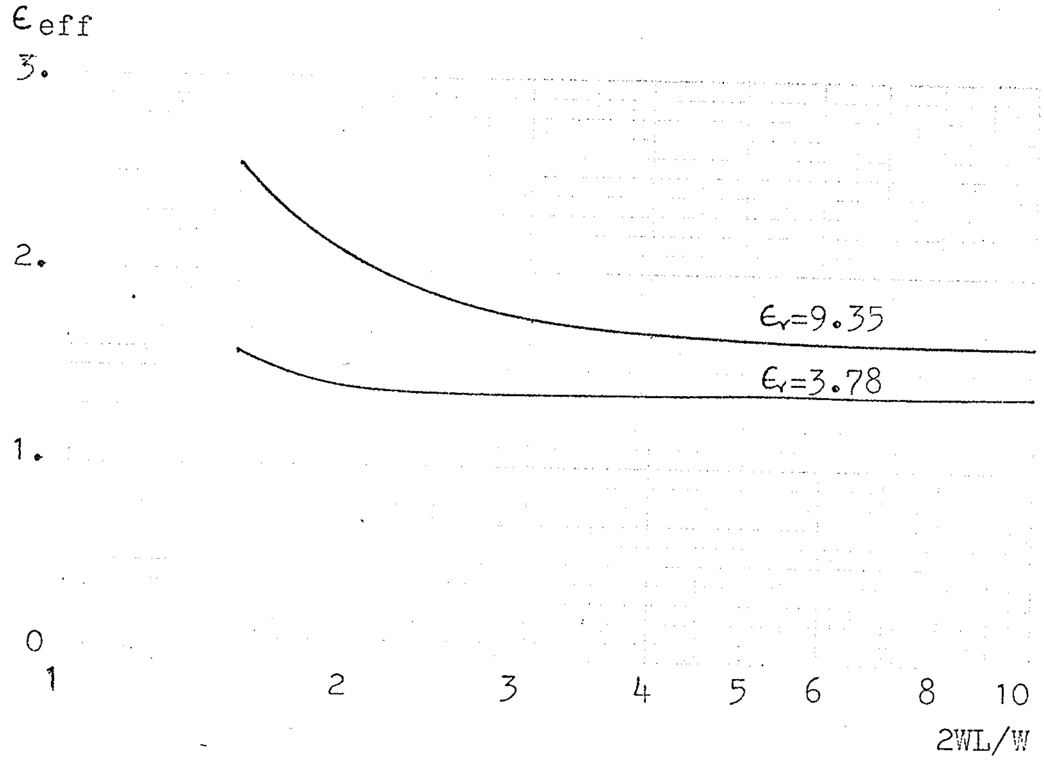

Fig.(3.7). Effective dielectric constant versus 2WL/W.

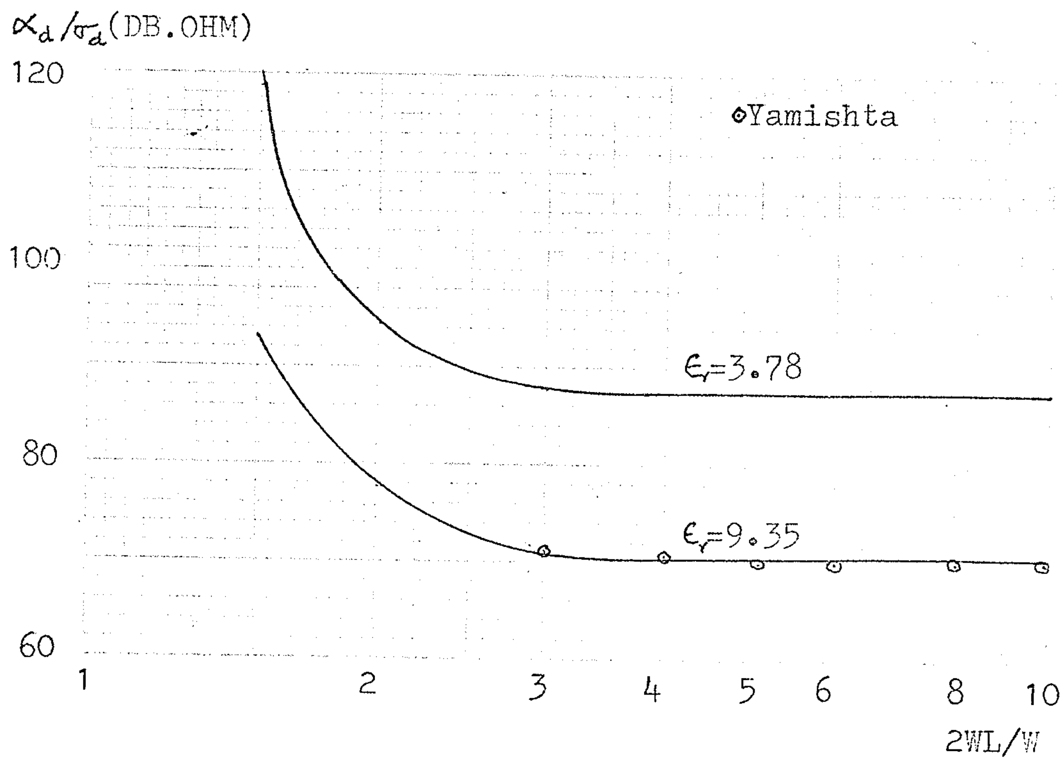

Fig.(3.8). Dielectric attenuation constant versus 2WL/W.

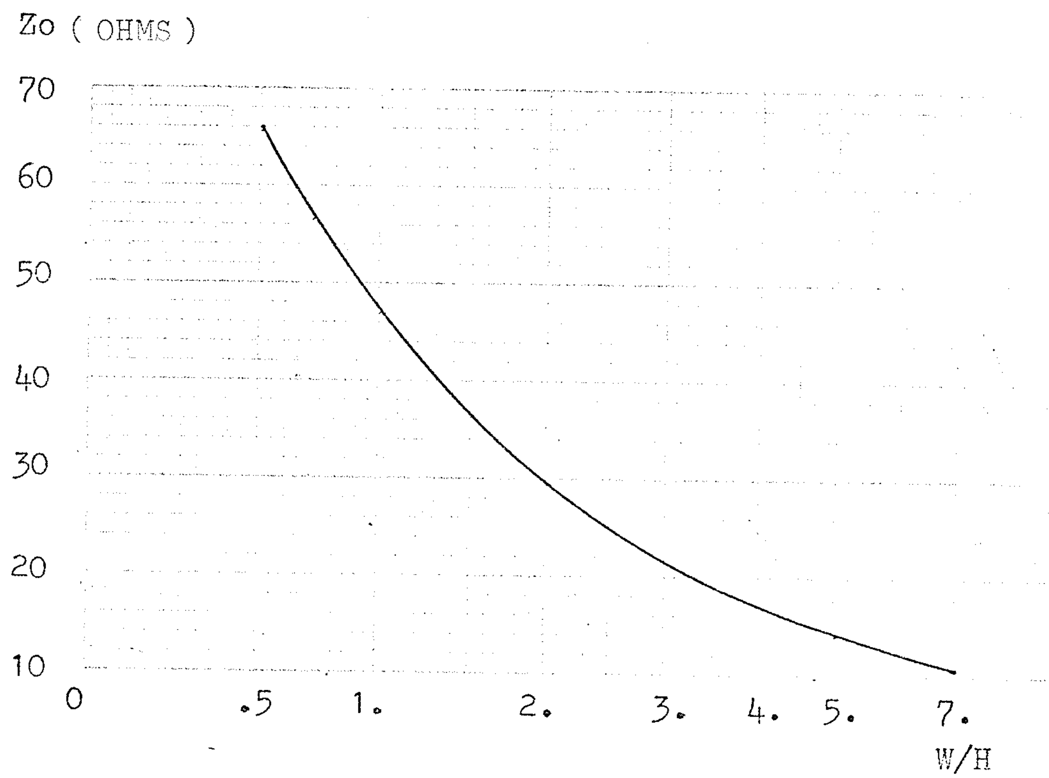

Fig.(3.9). Characteristic impedance versus W/H.

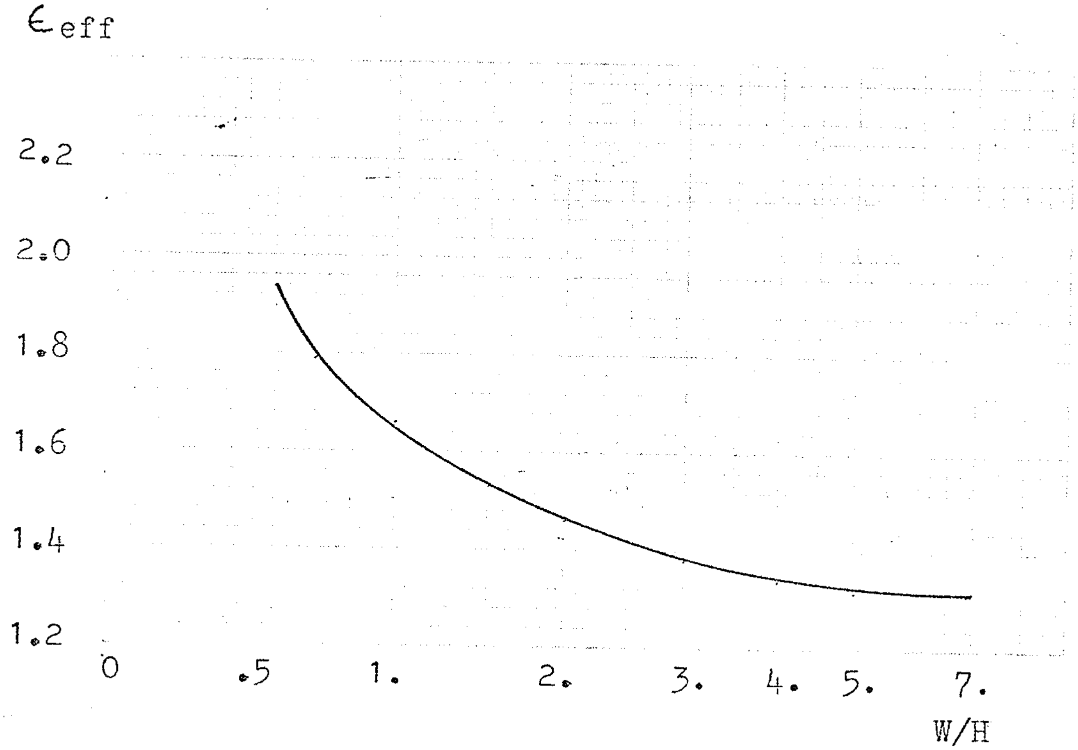

Fig.(3.10). Effective dielectric constant versus W/H.

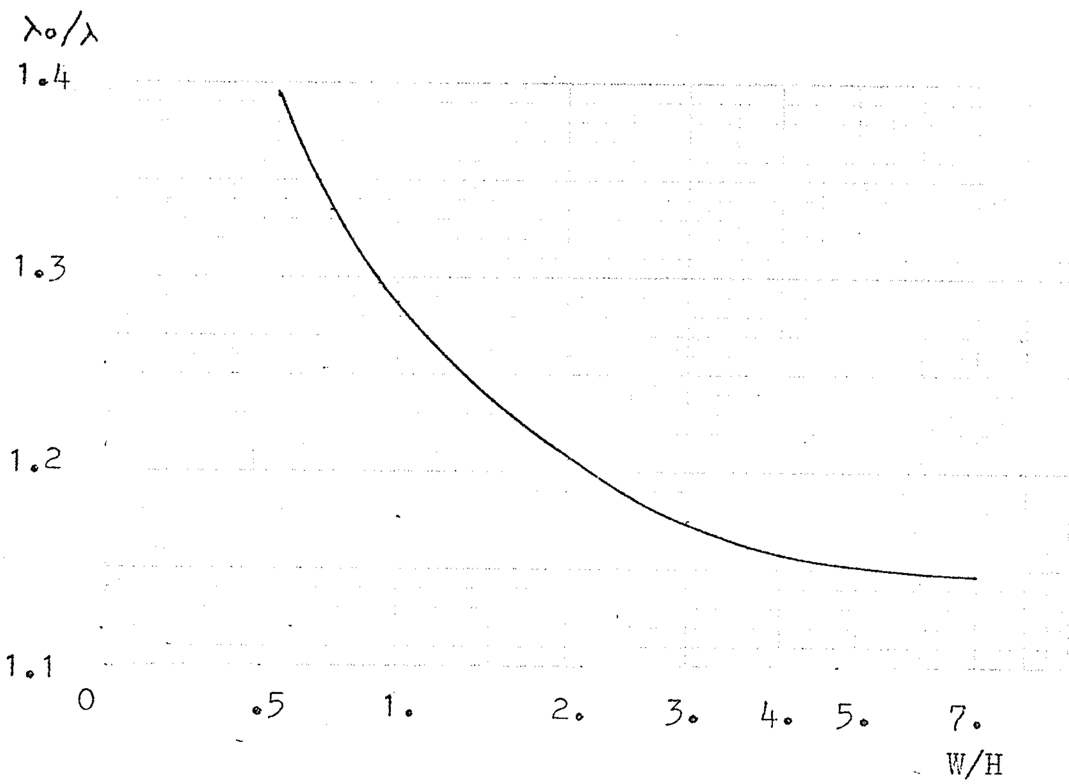

Fig.(3.11). Relative wavelength versus W/H.

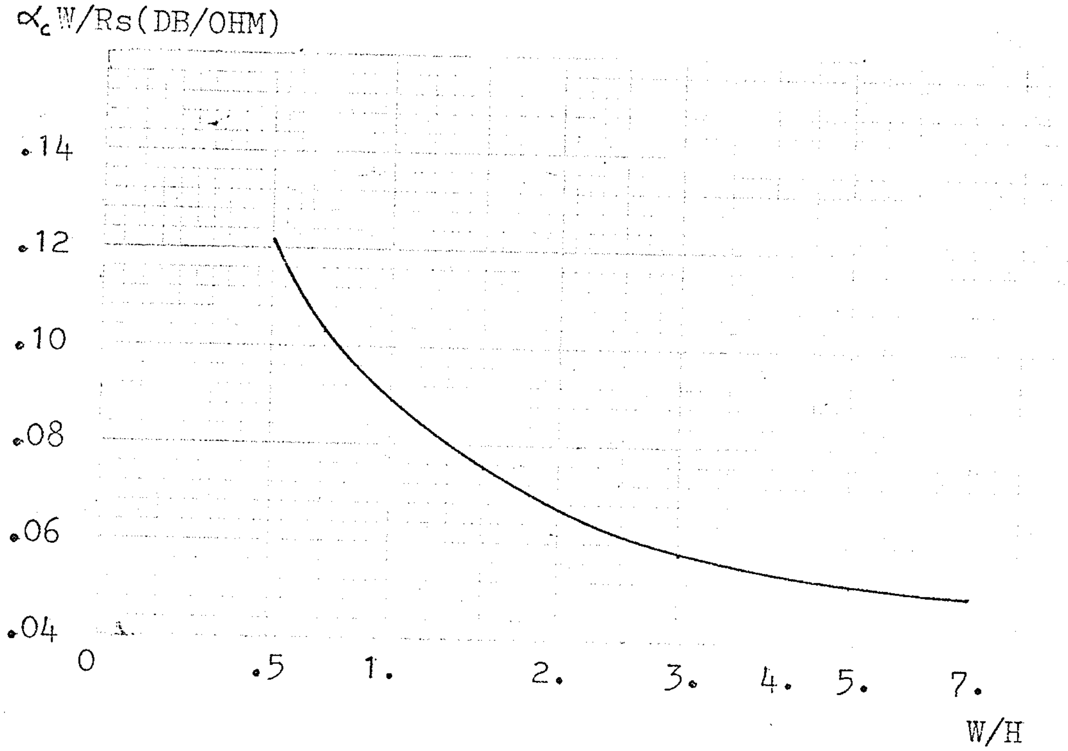

Fig.(3.12). Conductor attenuation constant versus W/H.

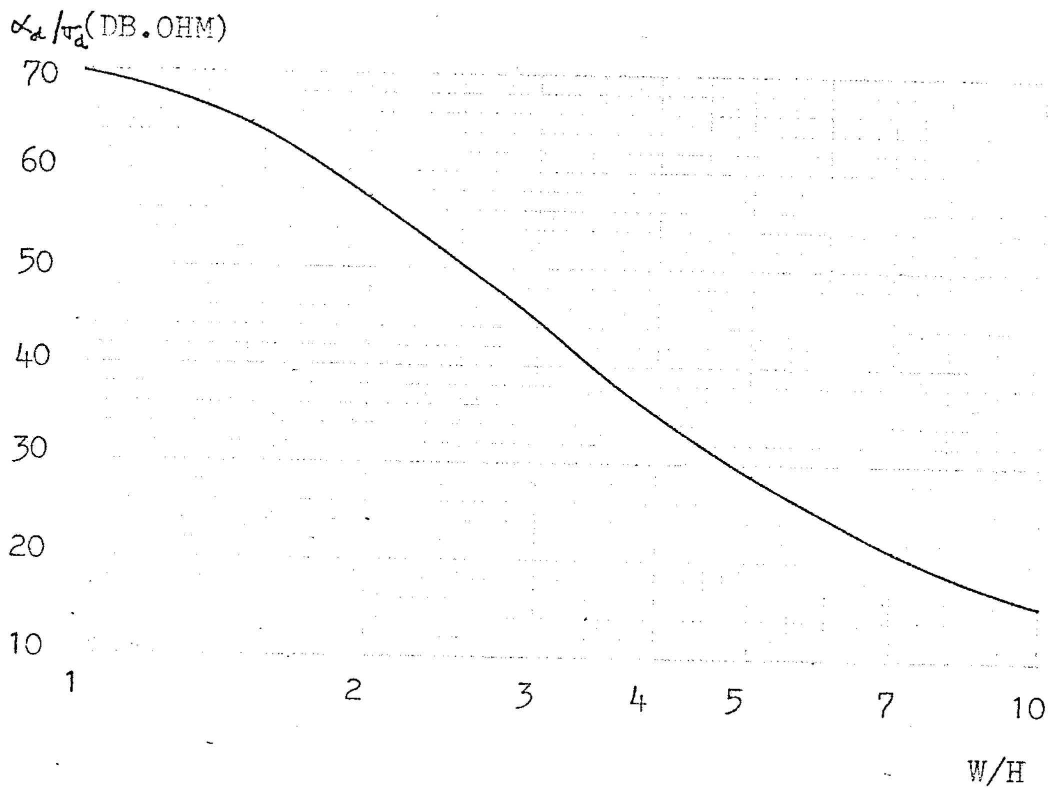

Fig.(3.13). Dielectric attenuation constant versus W/H.

TABLE (3.4)

SUSPENDED SUBSTRATE MICROSTRIP PARAMETERS FOR FIG.(3.3) CONFIGURATION, $\epsilon_r=9.35$

H2/H	Zo (OHMS)	$\epsilon_{effective}$	Relative velocity	$\alpha_c W/Rs$ (DB/OHM)	α_d/σ_d (DB.OHM)
0.1	49.6	1.473	.824	.091	47.80
0.2	46.5	1.679	.772	.093	71.07
0.3	43.2	1.938	.718	.095	82.03
0.4	39.9	2.267	.664	.104	86.77
0.5	36.1	2.780	.601	.122	90.67

The suspended substrate microstrip general configuration of Fig. (3.1) was considered next. The contour numbering is given in Fig. (3.1) and the number of segments selected for each contour is listed in Table (3.2).

Table (3.2)

Contour number	1	2	3	4	5	6	7	8	9	10
Number of segments	7	2	8	50	7	6	3	2	8	7

Again a total of 100 segments was used with the majority of segments placed on the strip contour (contour number 4) so as to accomodate the large field variation at the strip edge.

Dimensions which were kept constant in the analysis are $h_1 = .37W$, $h_2 = .1W$, $h_3 = .1W$, $B = W$, $T = W/100$.

Results are presented in Tables (3.5) and (3.6) for, respectively, a quartz substrate ($\epsilon_r = 3.78$) and alumina substrate ($\epsilon_r = 9.35$). No theoretical or experimental values are available for comparison purposes.

Suspended substrate microstrip overcomes some of the problems encountered with standard microstrip such as its narrow strip width for higher characteristic impedence and high attenuation. Our results indicate that strip widths for single layered microstrip and for suspended substrate microstrip for a characteristic impedence of 50 Ω and for a fixed substrate thickness H are in the ratio 1/4.5.

TABLE (3.5)

SUSPENDED SUBSTRATE MICROSTRIP PARAMETERS FOR FIG.(3.1) CONFIGURATION, $\epsilon_r = 3.78$.

2WL/W	Zo (OHMS)	$\epsilon_{effective}$	Relative velocity	$\alpha_c W/Rs$ (DB/OHM)	α_d/σ_d (DB.OHM)
1.5	52.35	1.15	.9321	.0095	24.39
2.0	57.21	1.13	.9418	.0076	16.64
3.0	58.75	1.11	.9483	.0072	14.94

TABLE (3.6)

SUSPENDED SUBSTRATE MICROSTRIP PARAMETERS FOR FIG.(3.1) CONFIGURATION, $\epsilon_r = 9.35$.

2WL/W	Zo (OHMS)	$\epsilon_{effective}$	Relative velocity	$\alpha_c W/Rs$ (DB/OHM)	α_d/σ_d (DB.OHM)
1.5	49.04	1.311	.8735	.01245	14.13
2.0	54.10	1.261	.8906	.00898	12.64
3.0	56.31	1.212	.9090	.00750	11.61

The attenuation results presented in Fig. (3.6) show that a significant reduction in attenuation is obtained by suspending the substrate. It is further decreased by placing a low dielectric constant substrate in the immediate vicinity of the centre conductor ($h_3 \neq 0$) as seen from Table (3.3).

It should be pointed out that in order to compare the attenuation results for the different microstrip configurations it is necessary that total power transmitted be the same in all cases. This can be done by keeping the characteristic impedance the same for each case.

Table (3.3) compares the attenuation loss for three different microstrip configurations each having a characteristic impedence of 46.5Ω. Losses are calculated in db/ohm ($\alpha_c W/R_s$) for a substrate dielectric constant of 9.35.

Table (3.3)

Type of Configuration	Single Layered Microstrip	Suspended Substrate $h_3 = 0$	Suspended Substrate $h_3 \neq 0$
loss db/ohm ($\alpha_c W/R_s$)	.118	.095	.015

A major reduction in losses occurs when the substrate is moved away from the centre conductor, i.e., when $h_3 \neq 0$. It follows that a major region of loss is the interface region between the centre conductor and the dielectric. A small movement of substrate away from the conductor causes the attenuation to decrease by a large amount. Losses can be further reduced by reducing the thickness of the substrate. It has been shown [9] that losses of the order of that for the air filled line are obtainable with this type of suspended substrate structure.

Chapter 4

COUPLED MICROSTRIPS

Many microwave components use the coupling between paralleled lines as a basic parameter in their design. Examples of such components include directional couplers, filters, delay lines and single to balanced strip line transformers. There are two types of direction coupler which can readily be designed using the microstrip configuration, the coupled type and the branch line type. In the former case, use is made of the natural coupling that exists between two microstrips placed side by side.

4.1 THE METHOD OF ANALYSIS

The basic coupled microstrip configuration is shown in Fig. (4.1). It contains a ground plane, a dielectric stab and two conducting strips placed side by side on top of the dielectric.

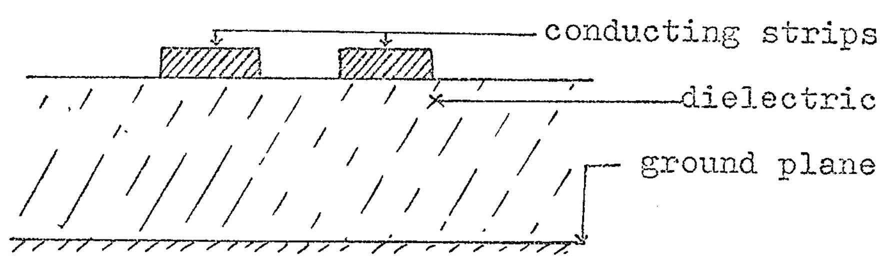

Fig. (4.1)

The numerical solution obtained to the coupled-microstrip problem is good only in the quasi static limit, i.e., when propagation is taken to be TEM. This approximation holds good only for microstrip dimensions which are small compared to the wavelength. This is generally the case with microstrip dimensions and substrate materials frequently used in integrated microwave circuit technology. In the region where this approximation does not hold good, that is when microstrip dimensions are comparable to the wavelength considered, the solution still provides a basis for solving the full propagation problem and serves as a guidence to design.

We will consider the coupled strips as being enclosed in a box as shown in Fig. (4.2). When the two strips are excited by voltage sources of equal amplitude and phase, equal currents flow in the same direction in the two strips. Because of the even symmetry of the electric field about the vertical axis, this mode is called the even coupled-strip mode. An open circuit or magnetic wall could be placed at the symmetry plane without affecting the field distribution.

Similarly, when the two strips are excited by sources of equal amplitude but opposite phase, they carry equal currents but in opposite directions. Due to the odd symmetry of the electric field, this mode is called the odd

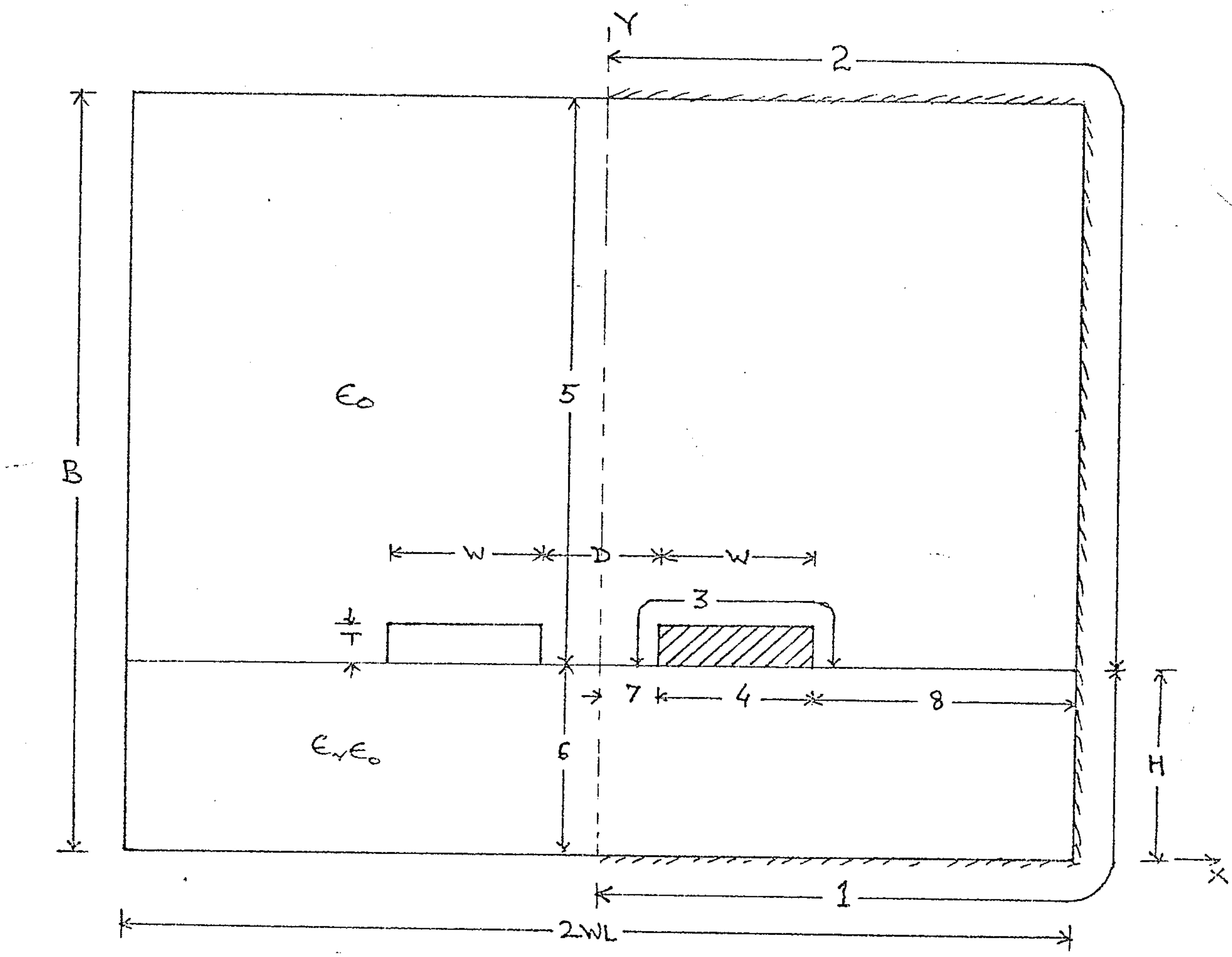

Fig.(4.2)

coupled-strip mode. As the voltage at the line of symmetry is zero, a short circuit or an electric wall may be located at the symmetry plane without affecting the field distribution.

The two dimensional Laplacian equation (2.1) is solved for the potential distribution in each homogeneous subregion of the microstrip. Due to the geometric symmetry about the y-axis, only the half portion shown in Fig. (4.3) is considered.

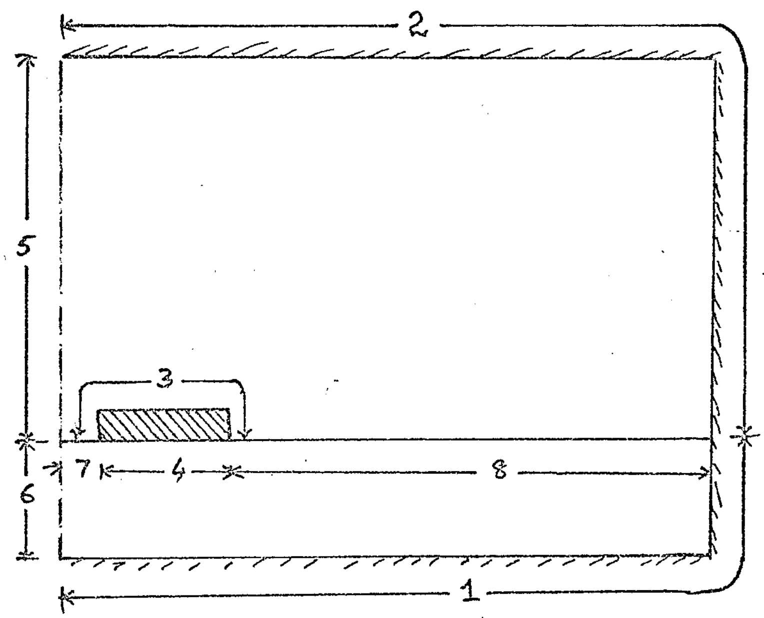

Fig. (4.3)

If the boundary contours are numbered as shown, the boundary conditions to be satisfied are:

(i) For both modes

$$\emptyset = V1 \quad \text{for contours 1 and 2,} \qquad (4.1)$$

$$\emptyset = V2 \quad \text{for contours 3 and 4,} \qquad (4.2)$$

$$\epsilon_{r_2}\frac{\partial\phi}{\partial n_1}+\epsilon_{r_1}\frac{\partial\phi}{\partial n_2} = 0 \quad \text{for contours 7 and 8.} \qquad (4.3)$$

(ii) For the even mode

$$\frac{\partial \phi}{\partial n_1} = 0 \qquad \text{for contours 5 and 6} \qquad (4.4)$$

(iii) For the odd mode

$$\phi = 0 \qquad \text{for contours 5 and 6} \qquad (4.5)$$

The parameters are calculated from evaluated capacitance values as presented in [11] and discussed in Chapter 2.

4.2 CALCULATION OF COUPLED-LINE PARAMETERS

The potential solutions are obtained, using the equivalent source method, for the empty coupled line, i.e., without dielectric (putting $\epsilon_{r_2} = 1$ in boundary condition specified by (4.3)) and for the actual coupled line.

If Co represents the capacitance per unit length of each coupled line for the unloaded case and Cr represents the capacitance per unit length for the loaded case, then using subscript 'e' to represent even mode values we get a relative effective dielectric constant of

$$\epsilon_{e_{eff}} = \frac{Cr_e}{Co_e} \qquad (4.6)$$

The even mode characteristic impedance is then

$$Zo_e = \frac{1}{\sqrt{Co_e Cr_e}\, Vo}$$

$$= \frac{1}{Vo Co_e \sqrt{\epsilon_{e_{eff}}}} \qquad (4.7)$$

This gives an even mode velocity of propagation, Vp_e, of

$$Vp_e = \frac{Vo}{\sqrt{\epsilon e_{eff}}}$$

$$= Vo \sqrt{\frac{Co_e}{Cr_e}} \qquad (4.8)$$

Equation (4.7) can then be rewritten as

$$Zo_e = \frac{1}{Vp_e \; Cr_e} \qquad (4.9)$$

The even-mode wavelength, λe, is

$$\lambda_e = \sqrt{\frac{Co_e}{Cr_e}} \; \lambda_o$$

$$= \frac{\lambda_o}{\sqrt{\epsilon e_{eff}}} \qquad (4.10)$$

If we use the subscript 'o' for odd mode values, the corresponding odd-mode parameter values for the coupled-line are

$$\epsilon o_{eff} = \frac{Cr_o}{Co_o}, \qquad (4.11)$$

$$Vp_o = \frac{Vo}{\sqrt{\epsilon o_{eff}}}$$

$$= Vo \sqrt{\frac{Co_o}{Cr_o}}, \qquad (4.12)$$

$$Zo_o = \frac{1}{\sqrt{Co_o Cr_o} Vo}$$

$$= \frac{1}{Vo\ Co_o \sqrt{\epsilon_{o\ eff}}}$$

$$= \frac{1}{Vp_o\ Cr_o} \qquad (4.13)$$

$$\lambda odd = \sqrt{\frac{Co_o}{Cr_o}}\ \lambda_o$$

$$= \frac{\lambda o}{\sqrt{\epsilon_{o\ eff}}} \qquad (4.14)$$

Here Co_o represents the capacitance per unit length of line for the odd mode for the empty dielectric case and Cr_o is the corresponding value for the loaded case.

Even and odd mode parameter values are related to the coupled line values by the following relations as given in [11] :

(i) The characteristic impedance is

$$Zo = \sqrt{\frac{Co_e + Co_o}{Cr_e + Cr_o}} \cdot \frac{1}{Vo\sqrt{Co_o\ Co_e}}$$

$$= \frac{1}{Vo\sqrt{Co_o Co_e}} \cdot \frac{1}{\sqrt{\epsilon_{eff}}} \qquad (4.15)$$

where the effective dielectric constant ϵ_{eff} is given by

$$\epsilon_{eff} = \frac{Cr_e + Cr_o}{Co_o + Co_e} . \tag{4.16}$$

(2) Two coupled mode inductance parameters, L_1 and L_m, are now defined. In terms of the even and odd mode inductances they are

$$L_1 \equiv \frac{\mu_o \epsilon_o}{2} \left[\frac{1}{Co_e} + \frac{1}{Co_o} \right] ,$$

$$L_m \equiv \frac{\mu_o \epsilon_o}{2} \left[\frac{1}{Co_e} - \frac{1}{Co_o} \right] .$$

As well, an inductive coupling coefficient, K_L, is defined as

$$K_L \equiv \frac{L_m}{L_1}$$

$$= \frac{Co_o - Co_e}{Co_o + Co_e} \tag{4.17}$$

Equation (4.17) may also be written in the form

$$K_L = \frac{1 - \frac{Zo_o}{Zo_e}\sqrt{\frac{\epsilon_{o_{eff}}}{\epsilon_{e_{eff}}}}}{1 + \frac{Zo_o}{Zo_e}\sqrt{\frac{\epsilon_{o_{eff}}}{\epsilon_{e_{eff}}}}} \tag{4.18}$$

(3) Similarly, we can define two coupled mode capacitance parameters, C_1 and C_m, and a capacitive coupling coefficient, K_C, in terms of the even and odd mode capacitances. Thus,

$$C_1 \equiv \frac{1}{2} \left[Cr_e + Cr_o \right] ,$$

$$C_m \equiv \frac{1}{2} \left[Cr_o - Cr_e \right] ,$$

$$K_C \equiv \frac{C_m}{C_1}$$

$$= \frac{Cr_o - Cr_e}{Cr_o + Cr_e} \tag{4.19}$$

Equation (4.19) can be written as

$$K_C = \frac{1 - \frac{Zo_o}{Zo_e}\sqrt{\frac{\epsilon e_{eff}}{\epsilon o_{eff}}}}{1 + \frac{Zo_o}{Zo_e}\sqrt{\frac{\epsilon e_{eff}}{\epsilon o_{eff}}}} . \tag{4.20}$$

(4) The effective propagation constant, β, expressed in terms of coupling coefficients, is then

$$\beta = \frac{W}{Vo} \sqrt{\epsilon_{eff}} \quad \frac{1 - K_L K_C}{1 - K_L^{\,2}} \tag{4.21}$$

where W is the angular frequency in radians per second.

For high directivity and wide bandwidth at tight coupling K_L is usually made approximately equal to K_C. In this special situation (4.21) becomes

$$\beta \approx \frac{W}{Vo} \sqrt{\epsilon_{eff}} . \tag{4.22}$$

4.3 RESULTS AND DISCUSSION

The coupled microstrip configuration, shown in Fig. (4.2), was analysed using the computer program for the equivalent source method. Table (4.1) lists the number and shows the distribution of segments for each contour.

Table (4.1)

Contour number	1	2	3	4	5	6	7	8	Total
Number of segments	16	10	21	15	12	8	6	12	= 100

The effect of varying the strip width on the coupled line characteristic impedance, inductive and capacitive coupling coefficients, relative velocity and effective dielectric constant was determined. The height of the substrate H, dimensions of the enclosing box (WL = 8H, B = 5H) and strip thickness (T = H/50) was kept constant. The strip width was varied on the range $.2 \leq W/H \leq 2$. The dielectric was assumed to be alumina ($\epsilon_r = 9.6$). Sets of results Figures (4.4) — (4.18) were obtained for different strip separations (D = .2H, D = .6H, D = H).

Quasi-TEM theory predicts, and this is as well obvious from the relative velocity curves of Figs. (4.4) — (4.6), that the coupled line must support two waves of unequal phase velocity. The phase velocity is greater

Relative velocity versus W/H.

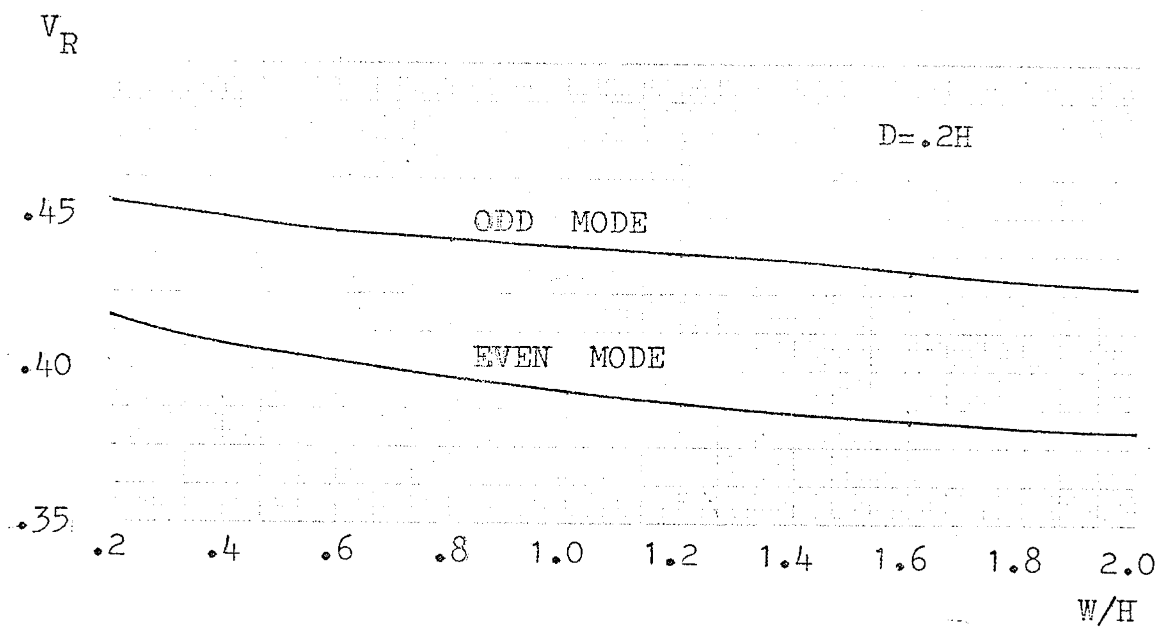

Fig.(4.4)

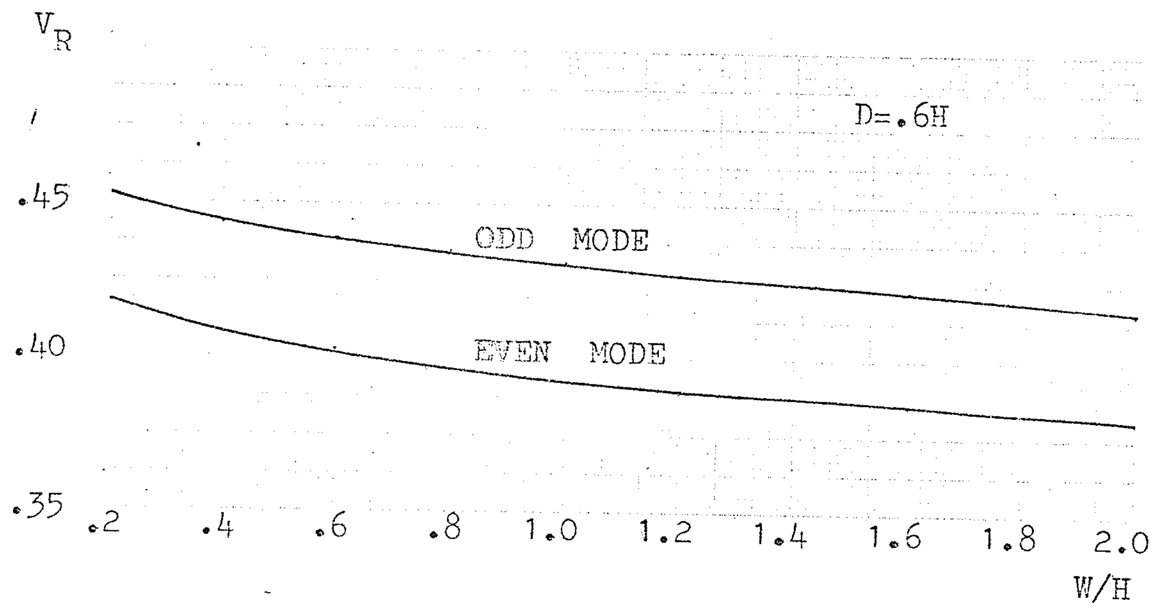

Fig.(4.5)

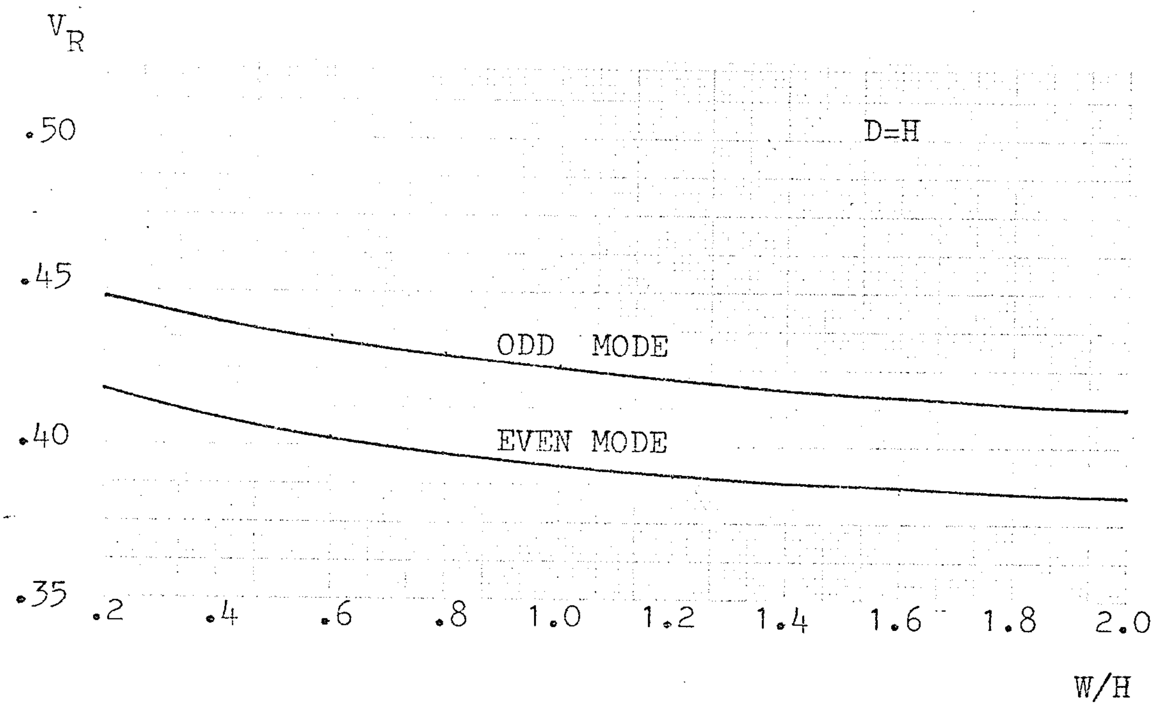

Fig.(4.6). Relative velocity versus W/H.

for the odd mode wave and lesser for the even mode wave. This is due to the fact that the strip capacitance to ground is lower for the even mode case than that for the odd mode case. The difference in velocities decreases as the separation between the strips is increased. As seen from Figs. (4.4) -- (4.6), for a W/H ratio of 1, the difference between even and odd mode relative velocities is .0475 for a separation of D = .2H while this difference is .0313 for a separation of D = H. Correspondingly, the characteristic impedance of the two modes are unequal, being greater for the even mode case than for the odd mode as is seen from Fig. (4.15) and (4.16). Also, this impedance difference increases when the spacing between strips is reduced. This means that tight coupling between strips over a large bandwidth is not obtainable.

From the results presented in Figs. (4.13) and (4.14) it can be seen that in general the inductive coupling coefficient, K_L, is greater than the corresponding capacitive coupling coefficient, K_C, which means that the even mode effective dielectric constant is larger than the odd mode effective dielectric constant and this agrees with the results in Figs. (4.10) -- (4.12). Equations (4.18) and (4.20) predict this as well. In addition inspection of Figs. (4.10) and (4.11) shows that the difference between even and odd mode effective dielectric constant decreases as the separation between the strips is increased but the coupled mode effective dielectric constant increases, Fig. (4.18).

Table (4.2) shows good agreement between the calculated even and odd-mode characteristic impedance values and that of Bryant and Weiss [12] , Judd et al [14] and P.B. Johns et al [13] . The results for the inductive and capacitive coupling coefficient Figs. (4.13) and (4.14), and for $\sqrt{\epsilon_{eff}}$ Zo, Figs. (4.7 — (4.9) are in good agreement with the corresponding results of Krage and Haddad [11] . Some non-agreement may be accounted for by the fact that the results calculated were for coupled microstrips enclosed in a box while other results were determined for an open structure with the strip thickness assumed to be zero.

In the calculation of attenuation the alumina substrate was assumed to be .025" thick. Attenuation data for the even mode is presented in Fig. (4.17). No experimental or theoretical attenuation results are available for comparison purposes.

$\sqrt{\epsilon_{eff}}$ Zo versus W/H.

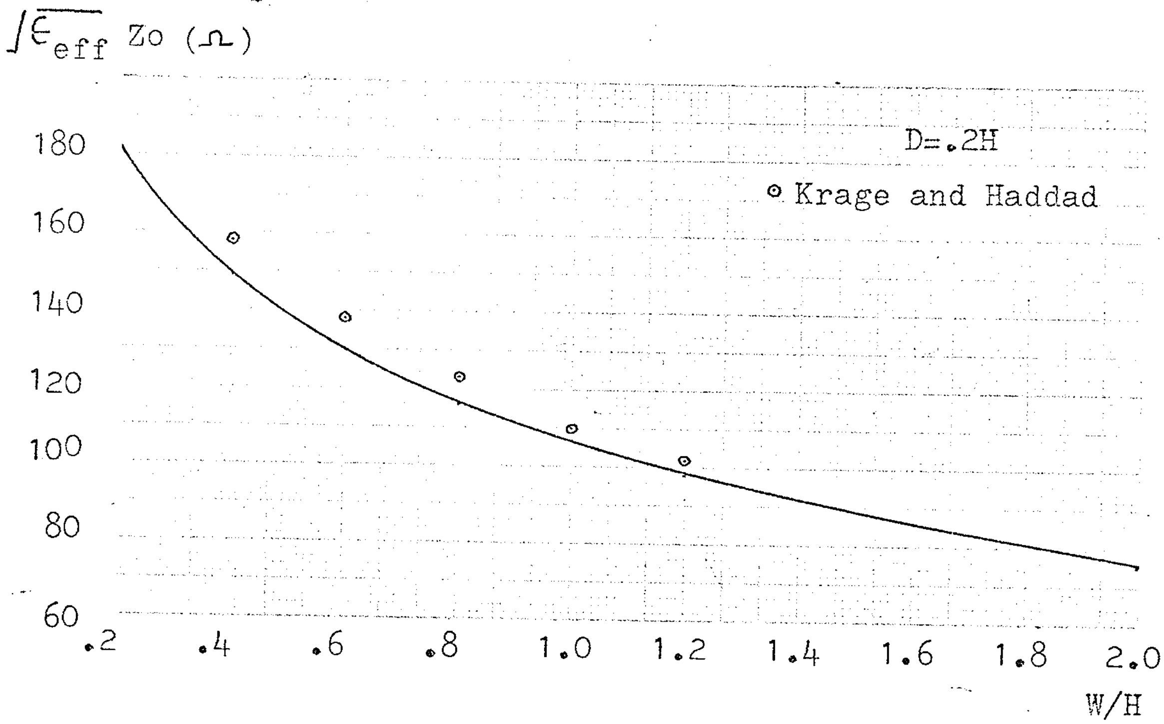

Fig.(4.7)

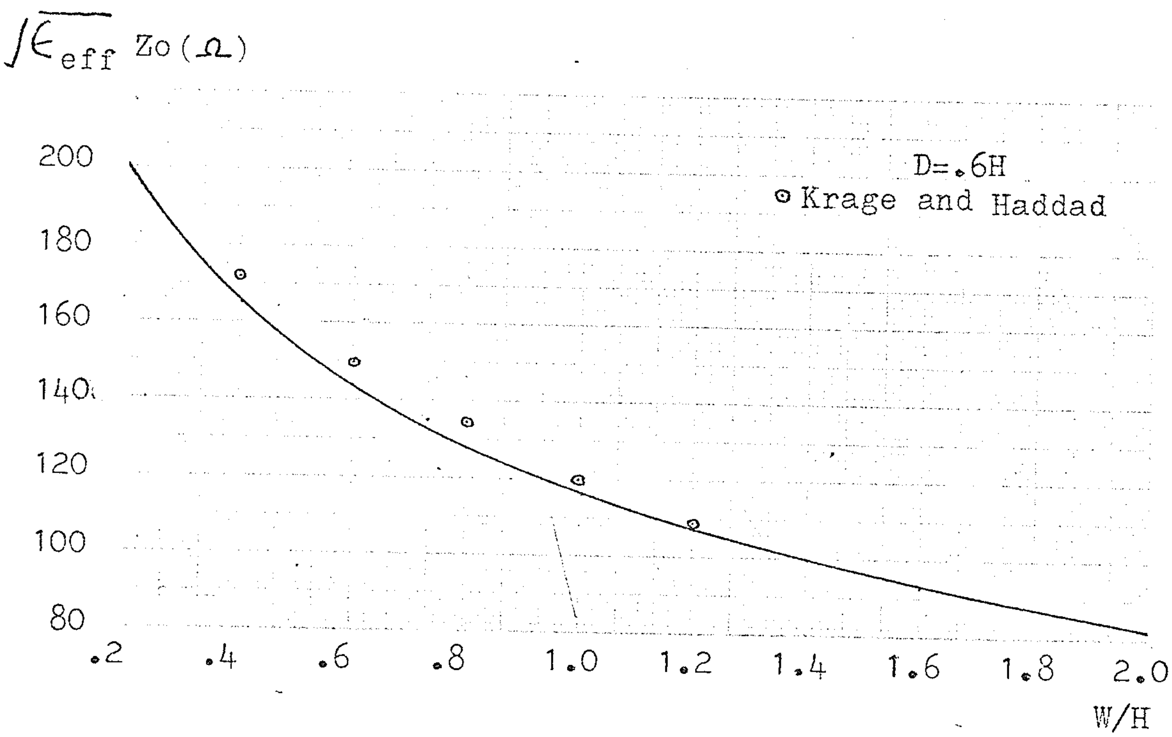

Fig.(4.8)

$\sqrt{\epsilon_{eff}}$ Zo versus W/H.

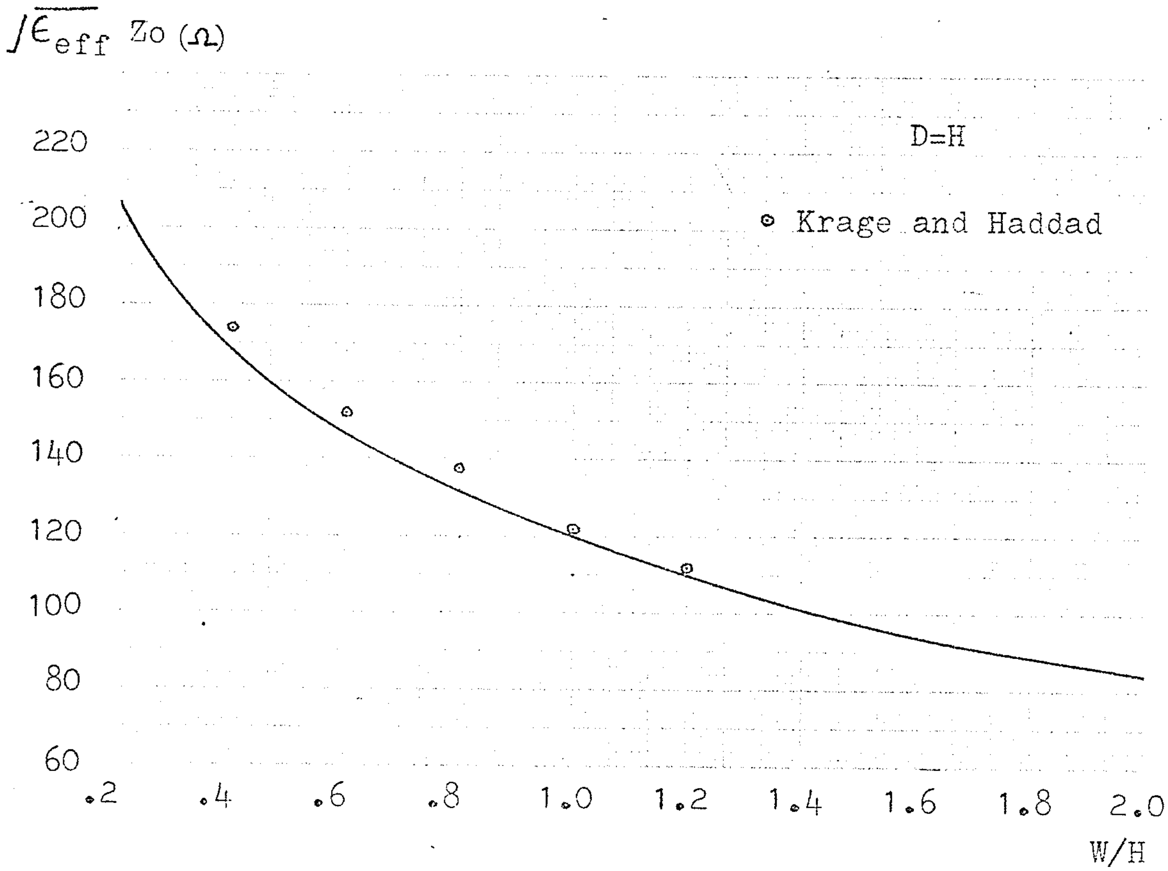

Fig.(4.9)

Effective dielectric constant versus W/H.

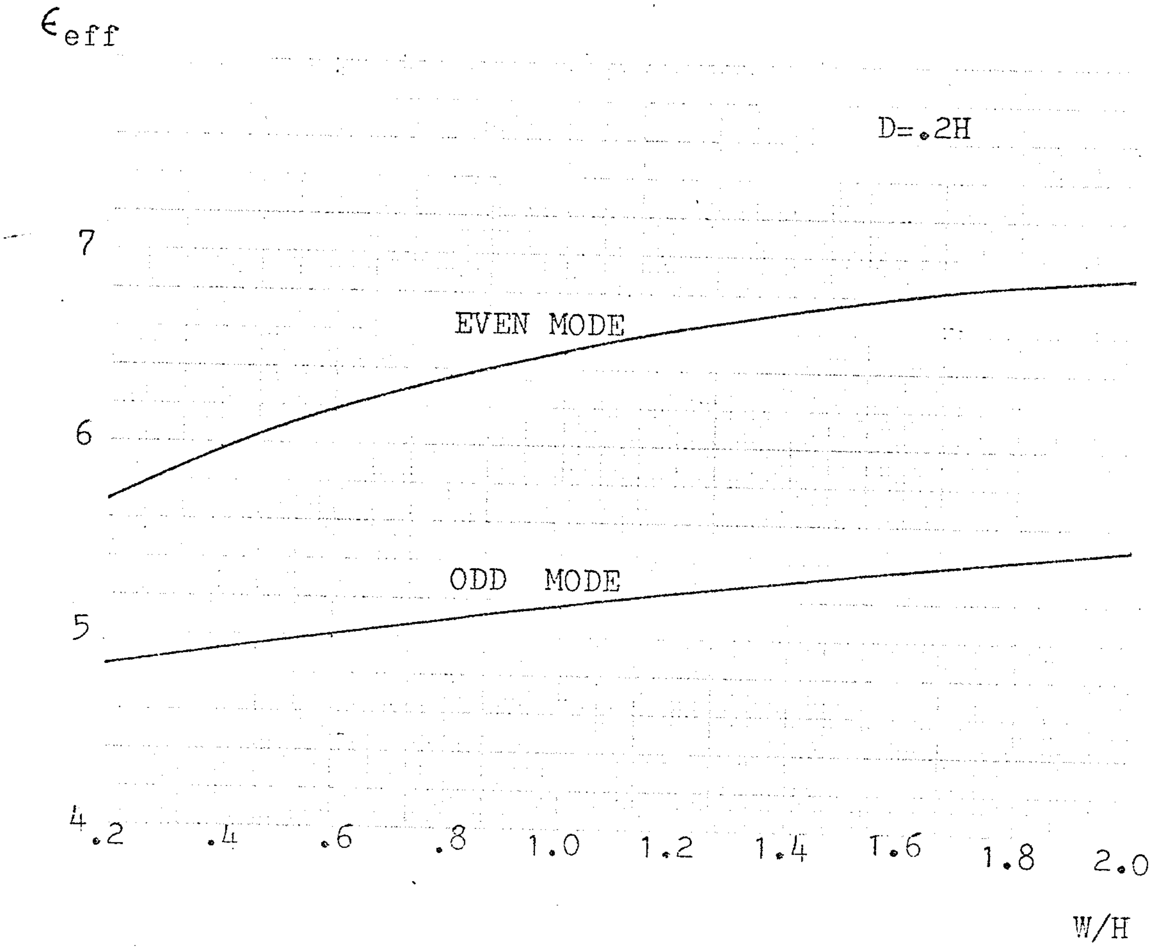

Fig.(4.10)

Effective dielectric constant versus W/H.

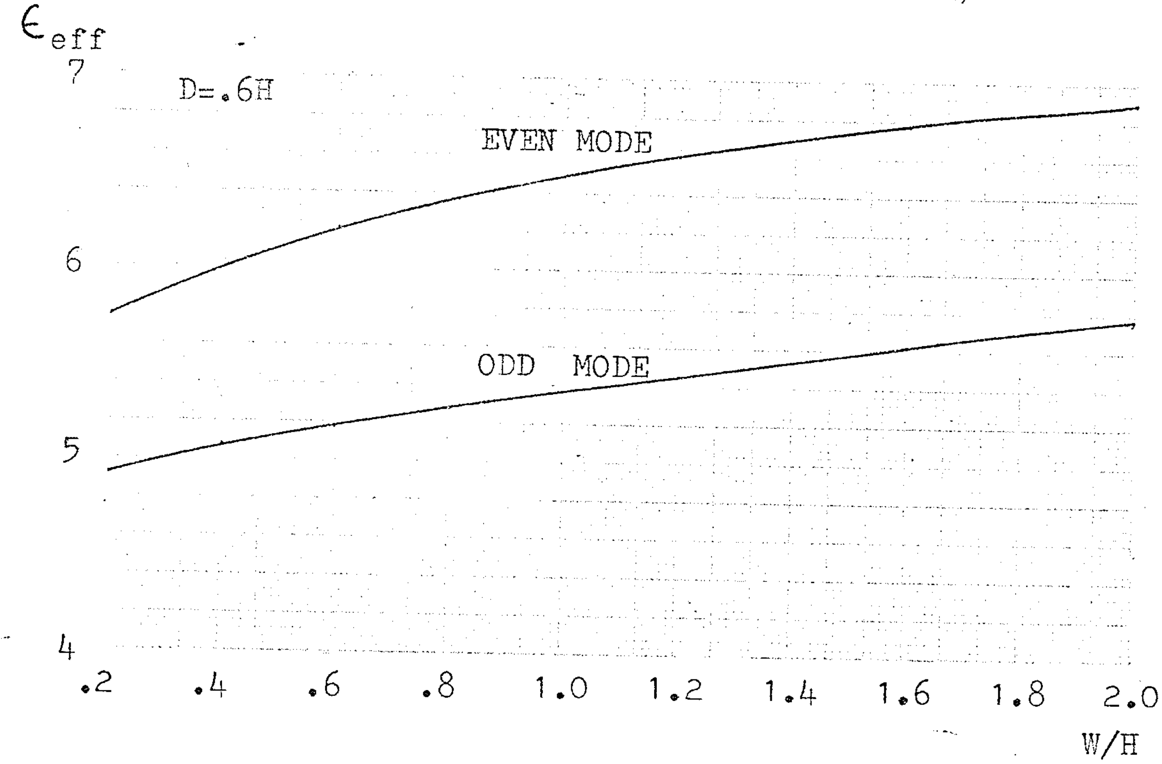

Fig.(4.11)

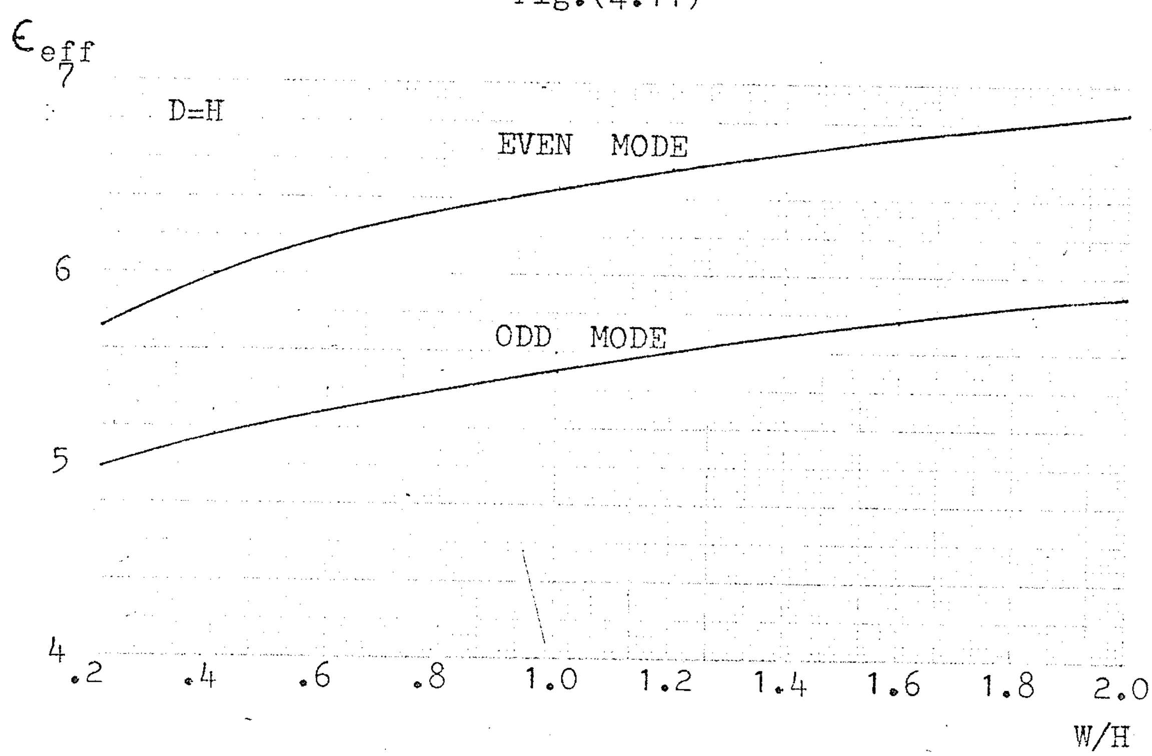

Fig.(4.12)

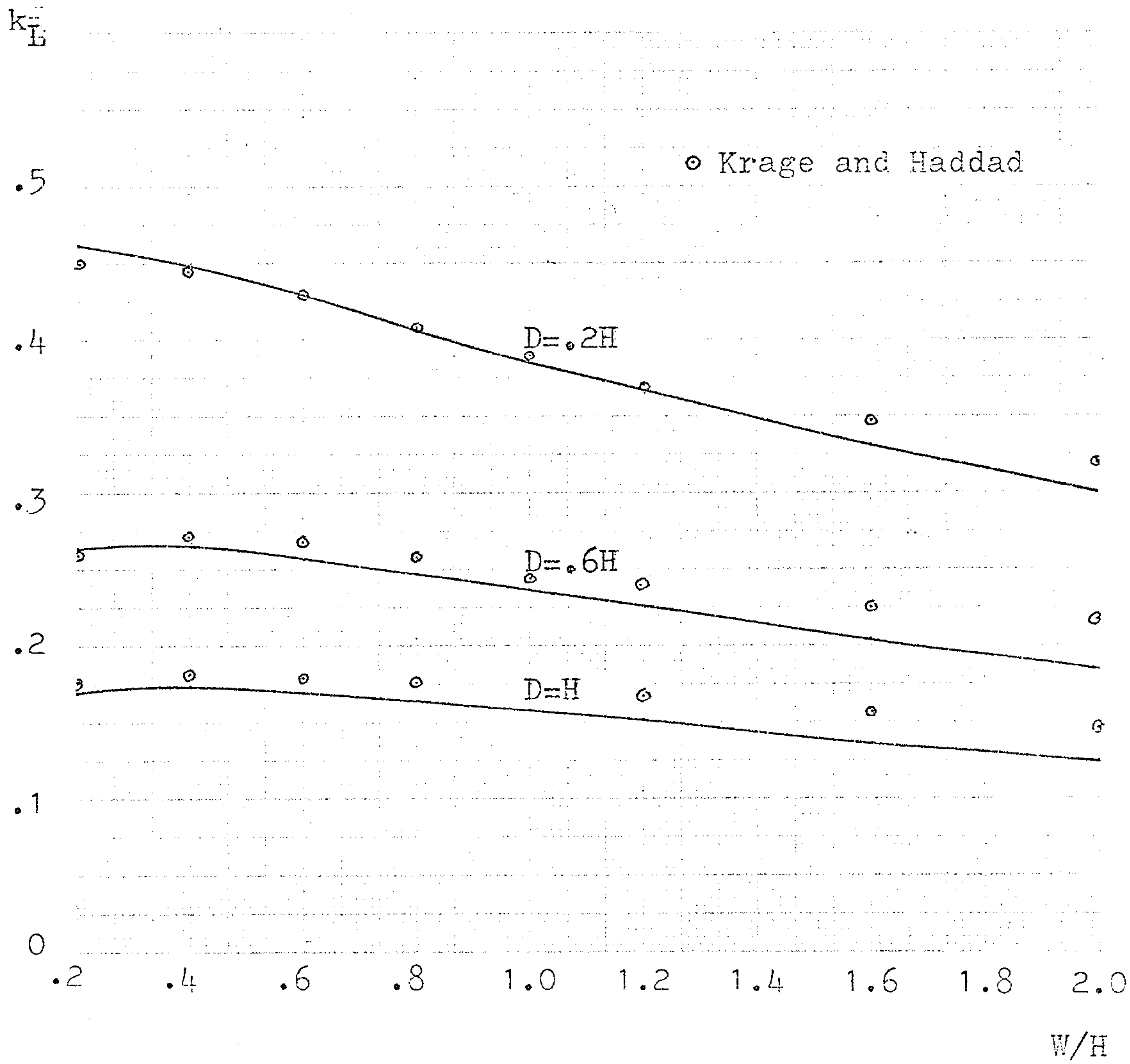

Fig.(4.13). Inductive coupling coefficient versus W/H.

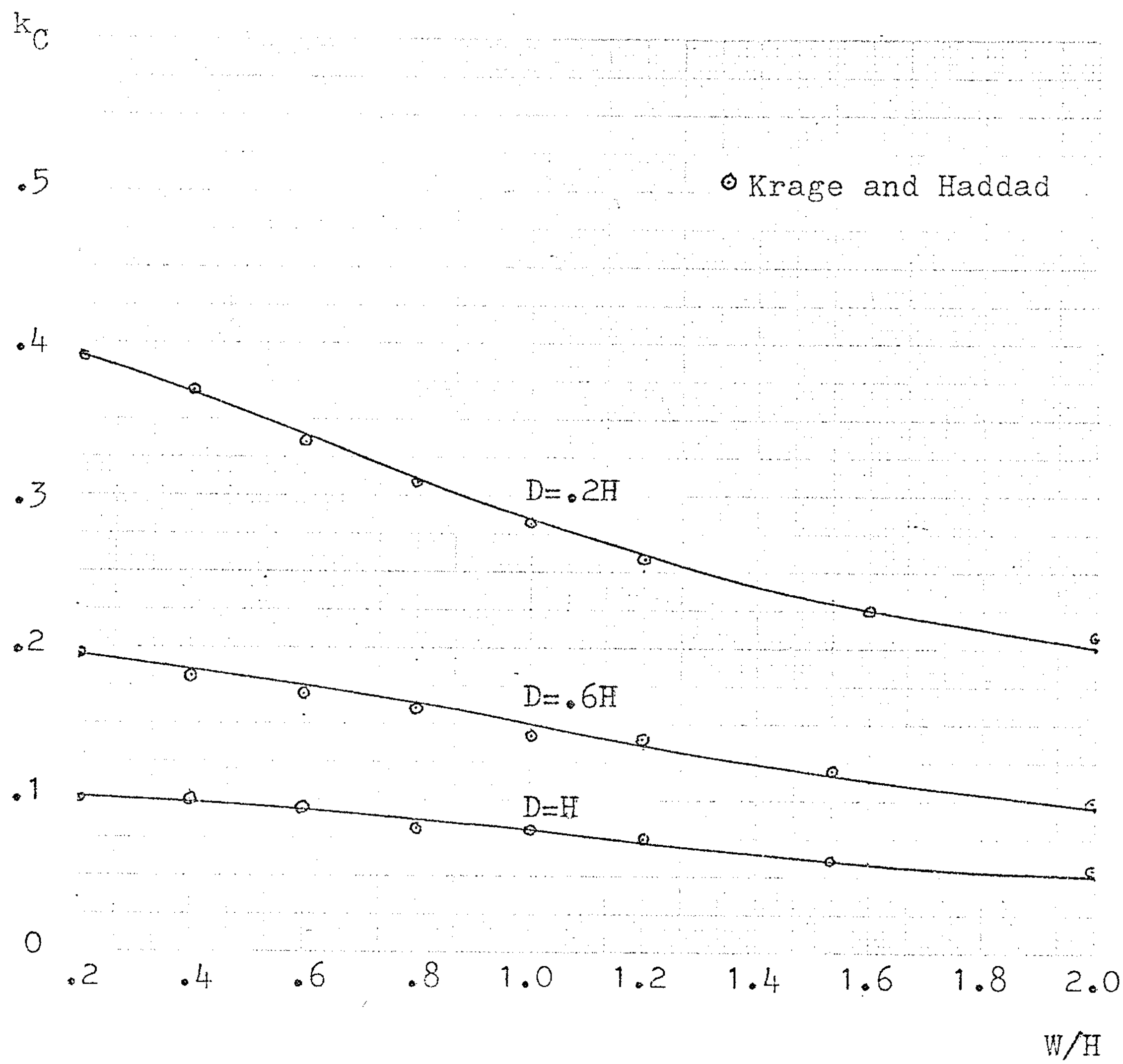

Fig.(4.14). Capacitive coupling coefficient versus W/H.

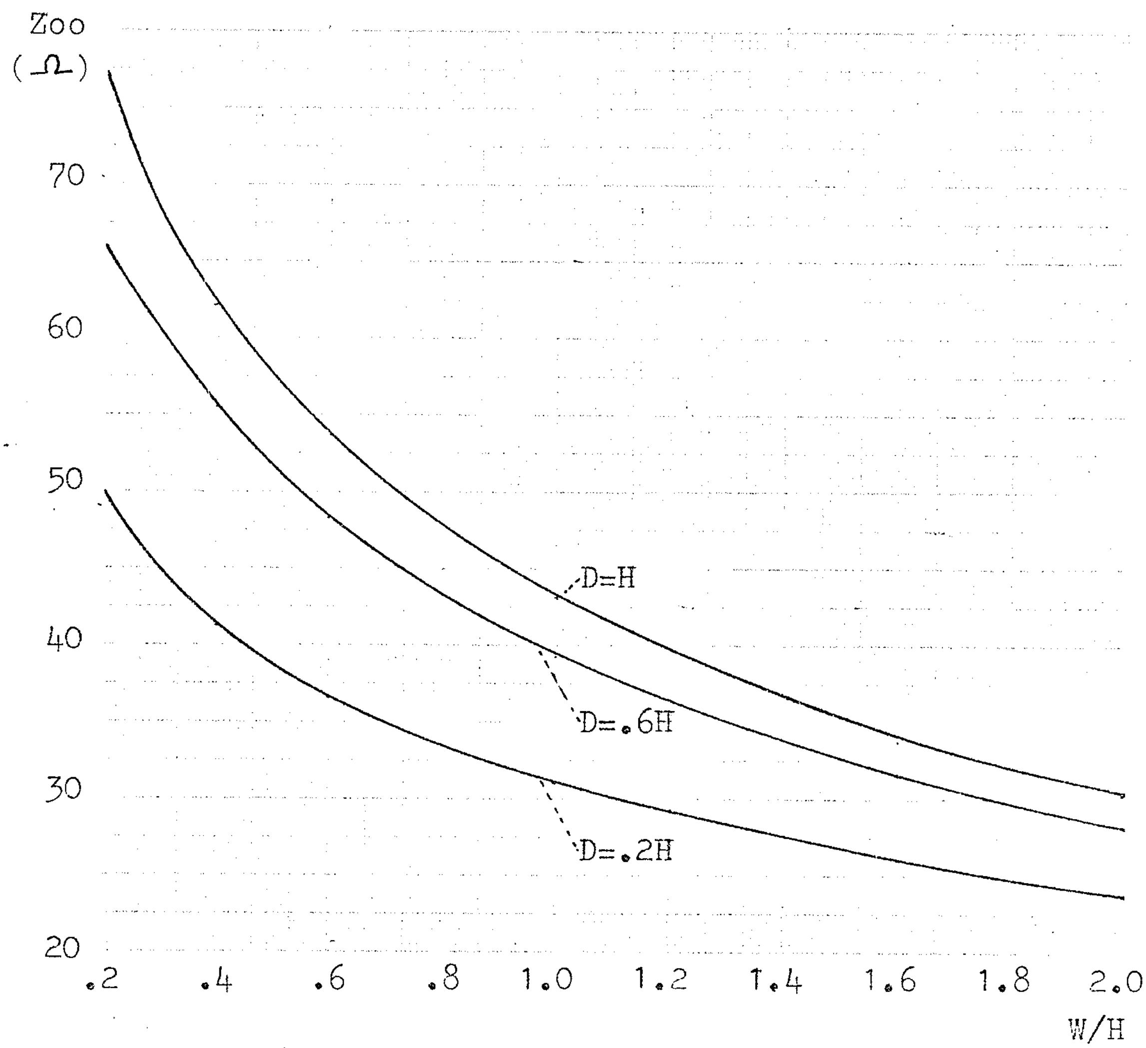

Fig.(4.15). Odd mode characteristic impedance versus W/H.

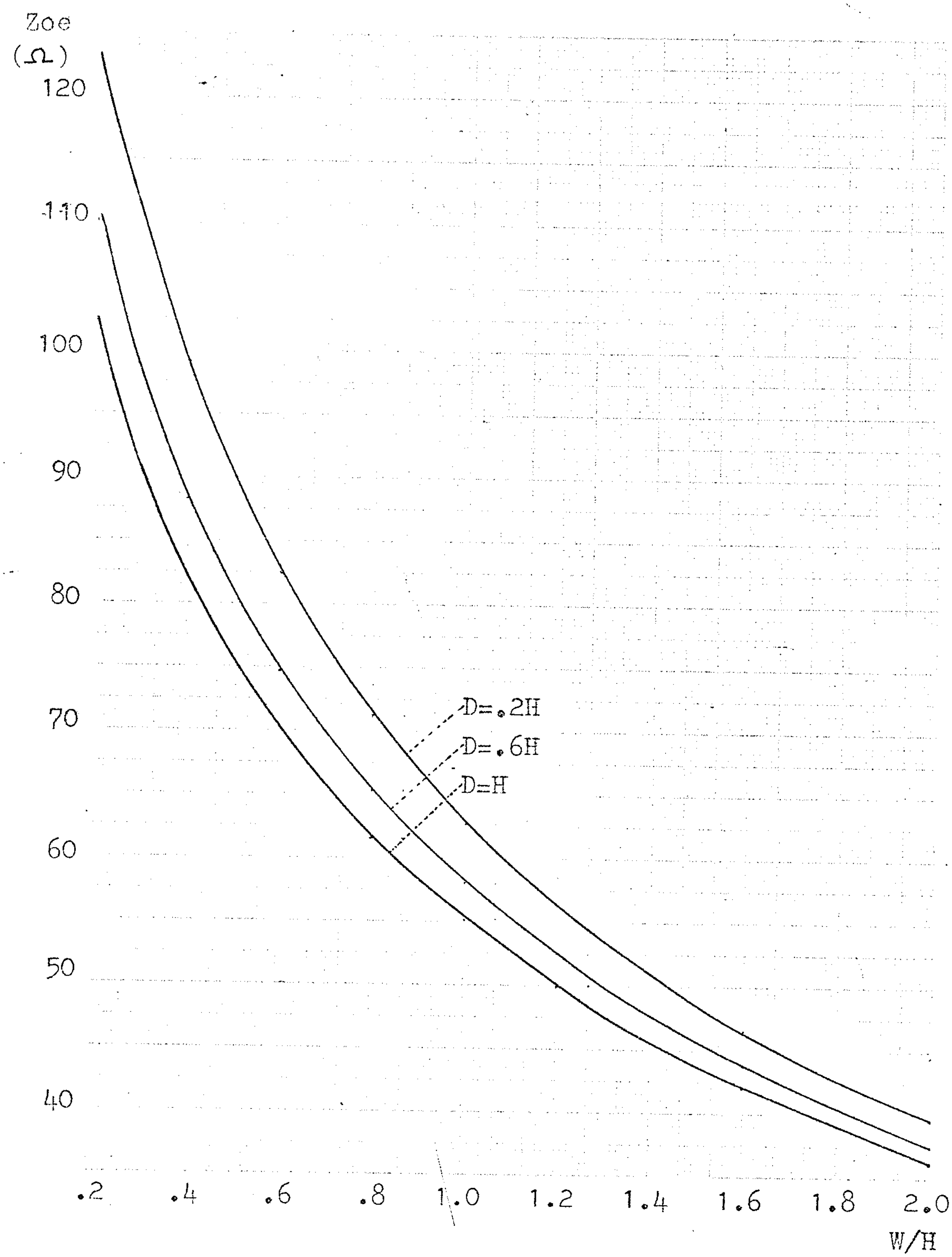

Fig.(4.16). Even mode characteristic impedance versus W/H.

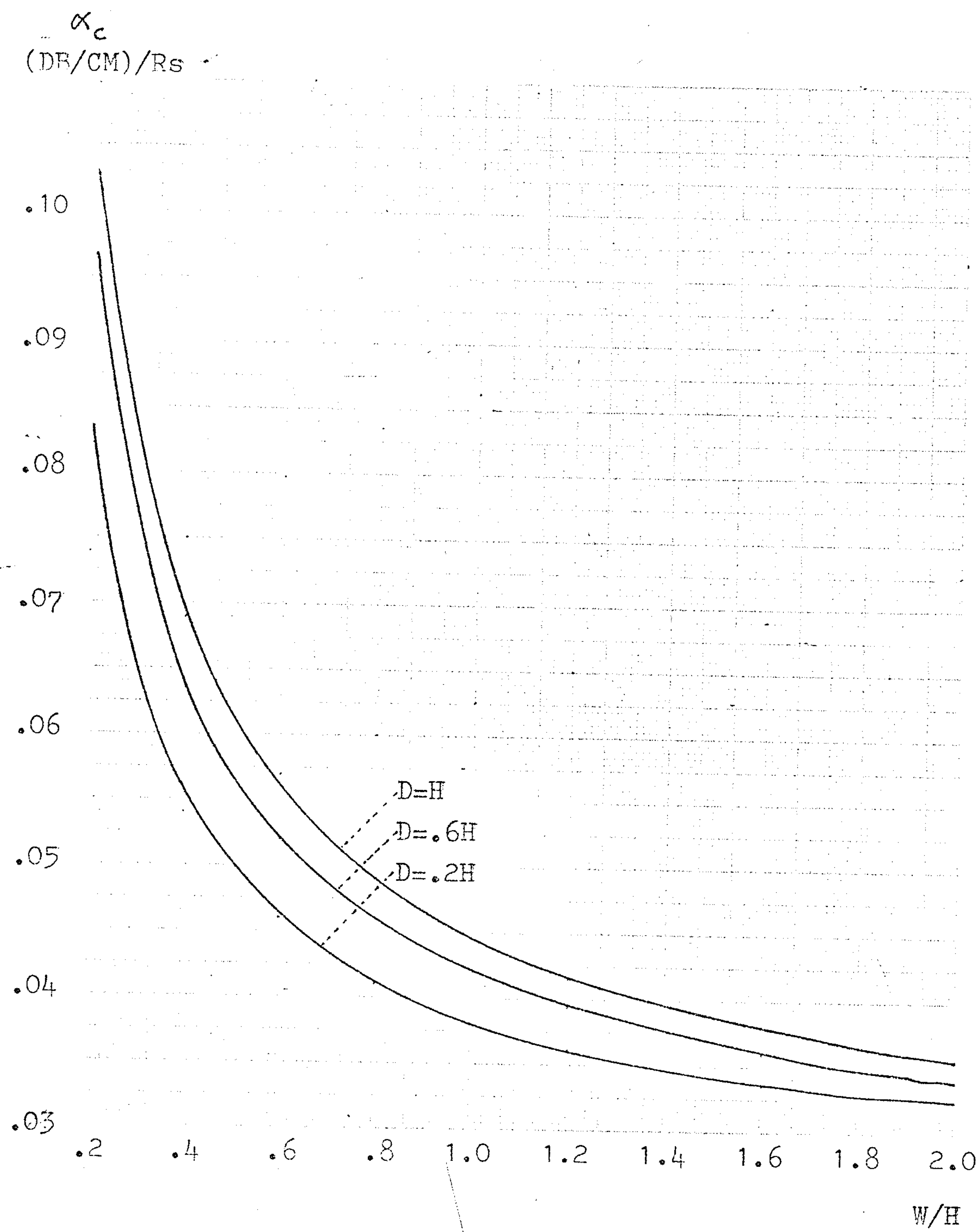

Fig.(4.17). Even mode attenuation constant versus W/H.

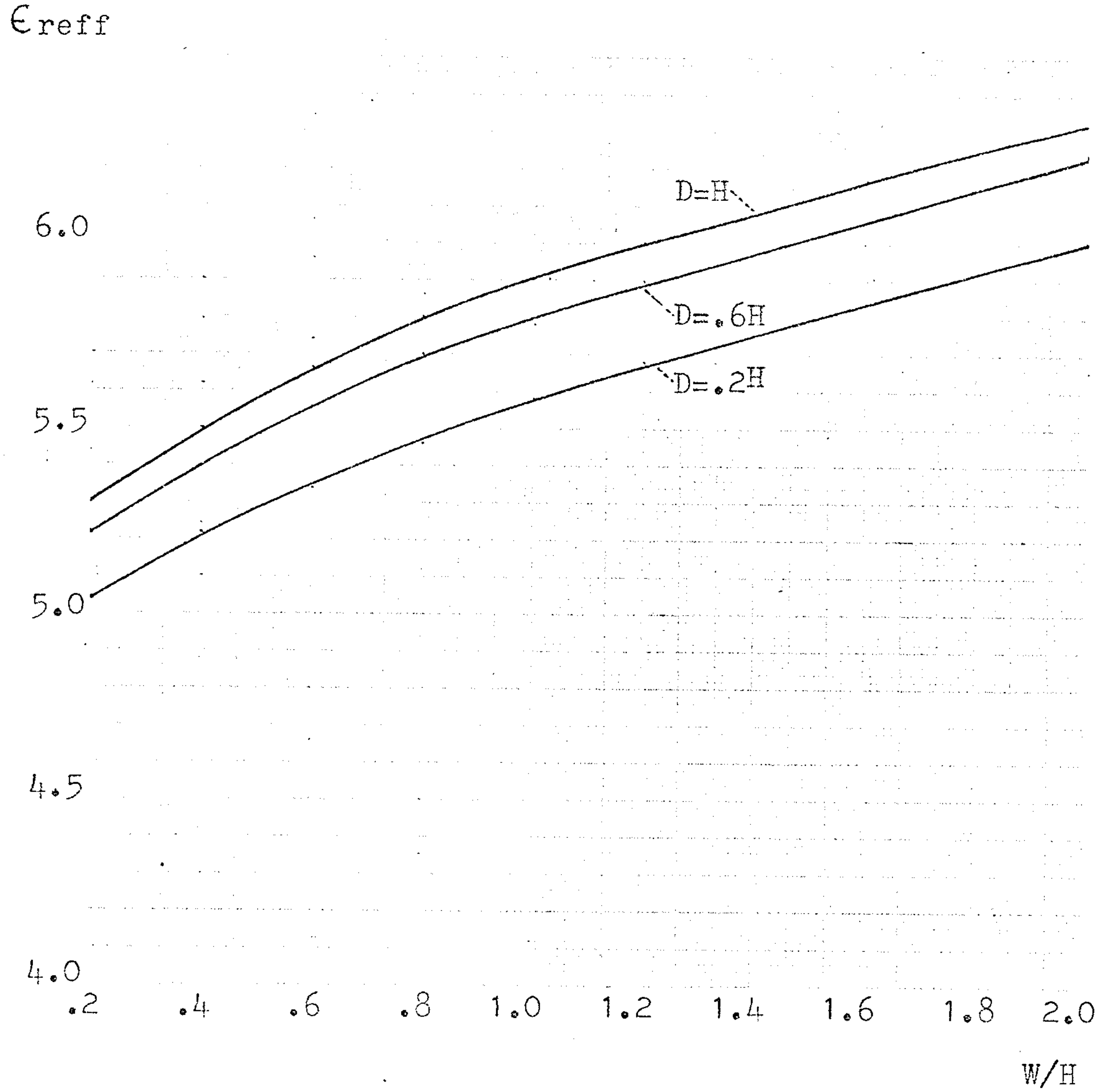

Fig.(4.18). Effective dielectric constant versus W/H.

TABLE (4.2)

COMPARISON OF CHARACTERISTIC IMPEDANCE OF THE COUPLED MICRO-STRIP CONFIGURATION OF FIG.(4.2), $\epsilon_r=9.60$.

Dimensions		Bryant and Weiss [12]		P.B. Johns et al. [13]		Judd et al [14]		This method	
D/H	W/H	Even	Odd	Even	Odd	Even	Odd	Even	Odd
0.2	1.0	64.5	31.6	63.4	33.1	63.0	31.5	62.8	31.2
0.2	2.0	41.0	27.4	40.7	25.1	40.1	23.0	39.6	23.7
1.0	1.0	56.5	43.2	56.2	44.3	55.0	42.3	55.1	43.4
1.0	2.0	37.6	30.1	37.6	31.2	36.7	29.7	36.4	30.3

Chapter 5

5.1 COUPLED SUSPENDED SUBSTRATE MICROSTRIP

The physical configuration of coupled suspended substrate microstrip that is considered in this chapter is shown in Fig. (5.1). Single layered coupled microstrip is a special case of this configuration when $h_1 = 0$ and this further reduces to the simple microstrip considered in Chapter 2 for $D/H = \infty$.

The quasistatic TEM mode of wave propagation is assumed and equation (2.1) must be satisfied by potential ϕ in every homogeneous sub-region of the coupled microstrip configuration. The two dimensional Laplace equation is solved satisfying appropriate boundary conditions.

As the microstrip structure of Fig. (5.1) is symmetrical about the y-axis only the right half region of the configuration is analysed as the field distribution is identical in the left half region.

If the boundary contours are numbered as shown in the Fig. (5.2), the boundary conditions to be satisfied follow:

(1) For the even-mode field

$$\phi = V1 \quad \text{on contours 1, 2 and 3,} \qquad (5.1)$$

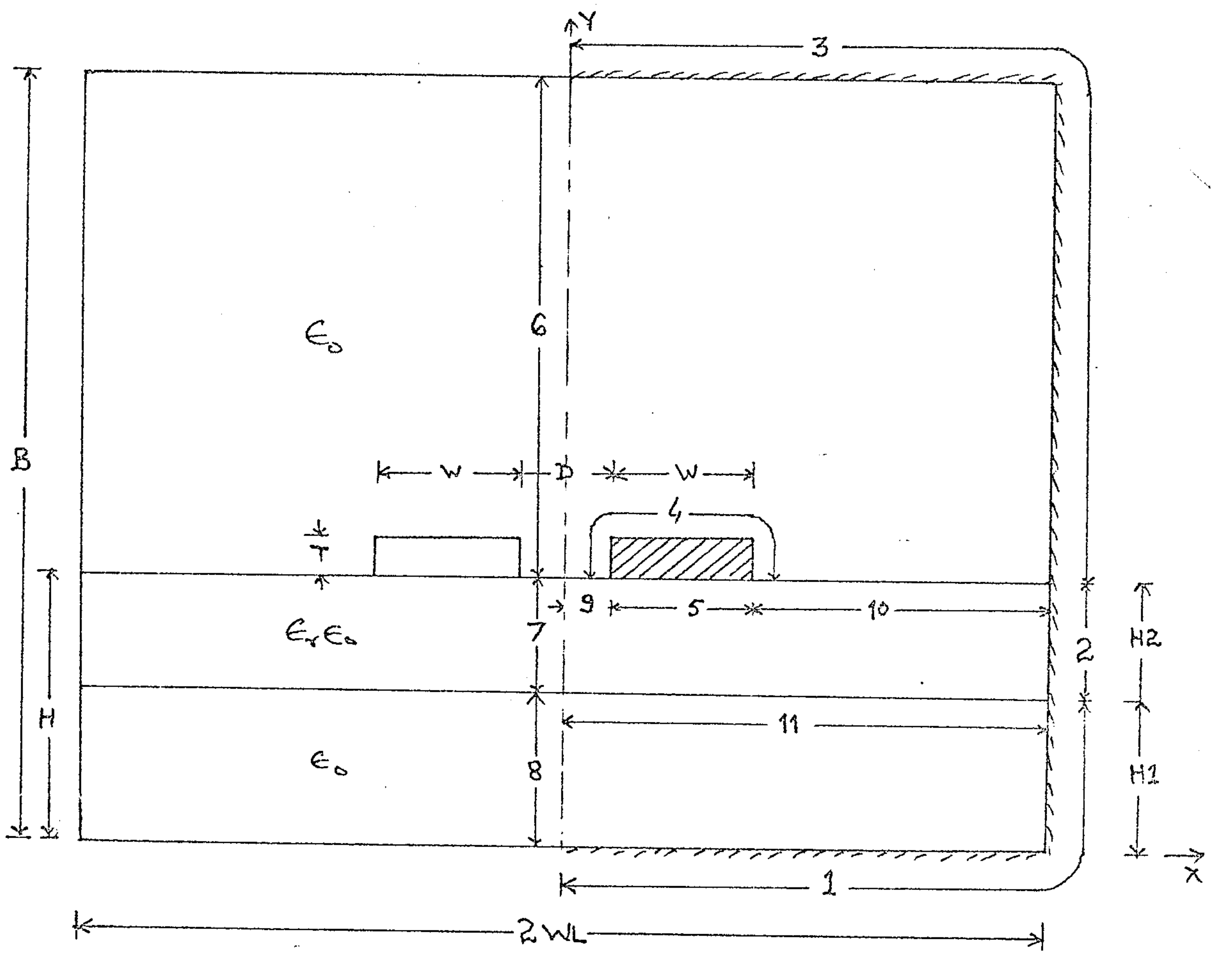
Y
3
6
ϵ_o
B
W
D
W
4
T
9
5
10
$\epsilon_r \epsilon_o$
7
2
H2
11
H
ϵ_o
8
H1
1
X
2WL

Fig.(5.1)

$$\phi = V2 \qquad \text{on contours 4 and 5,} \tag{5.2}$$

$$\frac{\partial \phi}{\partial n_1} = 0 \qquad \text{on contours 6, 7 and 8,} \tag{5.3}$$

$$\epsilon_{r2} \quad \frac{\partial \phi}{\partial n_1} + \frac{\partial \phi}{\partial n_2} = 0 \quad \text{on contour 9 and 10,} \tag{5.4}$$

$$\frac{\partial \phi}{\partial n_1} + \epsilon_{r2} \frac{\partial \phi}{\partial n_2} = 0 \quad \text{on contour 11.} \tag{5.5}$$

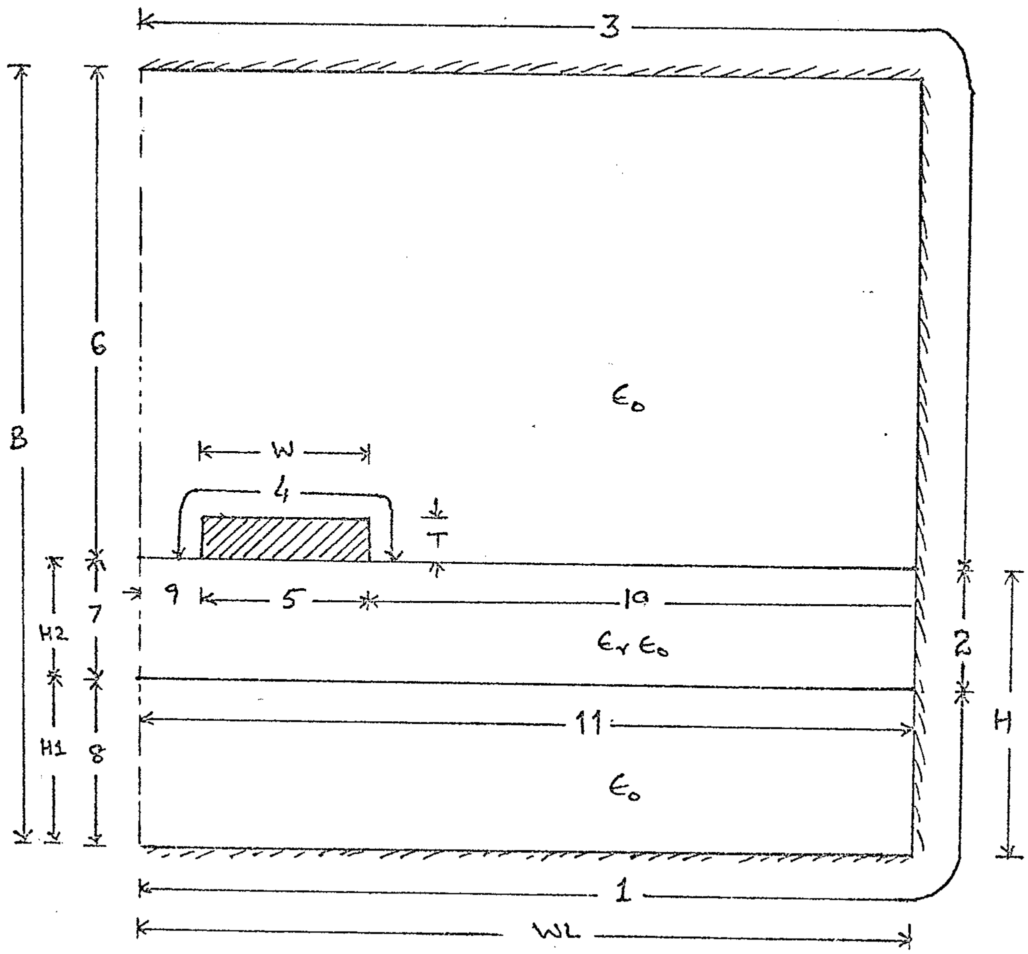

Fig. (5.2)

(2) For the odd-mode field all boundary conditions remain the same except (5.3) which is changed to

$$\emptyset = 0 \text{ on contours } 6, 7 \text{ and } 8. \qquad (5.6)$$

Here n_1, n_2, V1, V2, etc., have their usual meaning.

The analysis is again carried out for the dielectric empty and dielectric loaded cases. The capacitance per unit length of the line is determined for each case and parameters of the coupled line are obtained from relations (4.6) through to (4.21).

5.2 RESULTS AND DISCUSSION

Suspended substrate coupled microstrip configuration shown in Fig. (5.1), is analysed again using the computer program of Appendix E. Table (5.1) gives the number of segments taken on each contour.

Table (5.1)

Contour number	1	2	3	4	5	6	7	8	9	10	11
Number of segments	12	3	10	20	14	10	6	4	6	10	10
Total = 105											

The characteristic impedance, Figs. (5.7) and (5.12), relative velocity, Figs. (5.8) –– (5.9), effective dielectric constant, Figs. (5.5) –– (5.6), capacitive and inductive coupling coefficients, Figs. (5.3) –– (5.4) and attenuation, Fig. (5.10) is calculated with variation of strip width in the range $.2 \leq W/H \leq 1.4$. Substrate thickness ($H2 = .25H$), suspension height ($H1 = .75H$), enclosing box dimensions ($WL = 8.5H$, $B = 5H$) and strip thickness ($T = H/50$) were all kept constant. The dielectric constant of the substrate material was taken to be 10. Sets of results were obtained for strip separations ranging from $D = .2H$ to $D = .5H$.

The variation of suspended substrate coupled line parameters was next examined (Fig. (5.11) and Figs. (5.13) –– (5.22)) for different substrate thicknesses in the range $0.1H \leq H2 \leq 0.9H$ for constant strip width of $W = H$

and enclosing box dimensions of WL = 8.5H and B = 5H. For the attenuation calculation an H1 + H2 value of .025" was assumed.

Results for the capacitive coupling coefficient, Figs. (5.4) and (5.22), and for the effective dielectric constant, Figs. (5.13) and (5.14), show good agreement with corresponding results of Krage and Haddad [11]. Any non-agreement may partly be accounted for by the fact that the model considered was enclosed in a box and had a finite strip thickness whereas in [11] open coupled-strips are considered with zero strip thickness.

The configuration shown in Fig. (5.1) can be used to achieve equal inductive and capacitive coupling coefficients, i.e., $K_L = K_C$, which is useful for obtaining a high directivity and wide bandwidth at tight coupling. To accomplish this a region of air or some low dielectric constant material must separate the dielectric which supports the strips and the ground plane. For small values of H1/H the effect of the air gap is to reduce the even-mode effective dielectric constant more than the odd-mode value. Figs. (5.15) and (5.16) show values of odd-mode effective dielectric constant larger than even-mode effective dielectric constant and therefore a value of the K_C greater than K_L as seen from equations (4.18) and (4.20). The results in Fig. (5.3) and Fig. (5.4) indicate a value of $K_C > K_L$. So some value of H1 between $0 < H1 < .75$ will give a value of $K_C = K_L$.

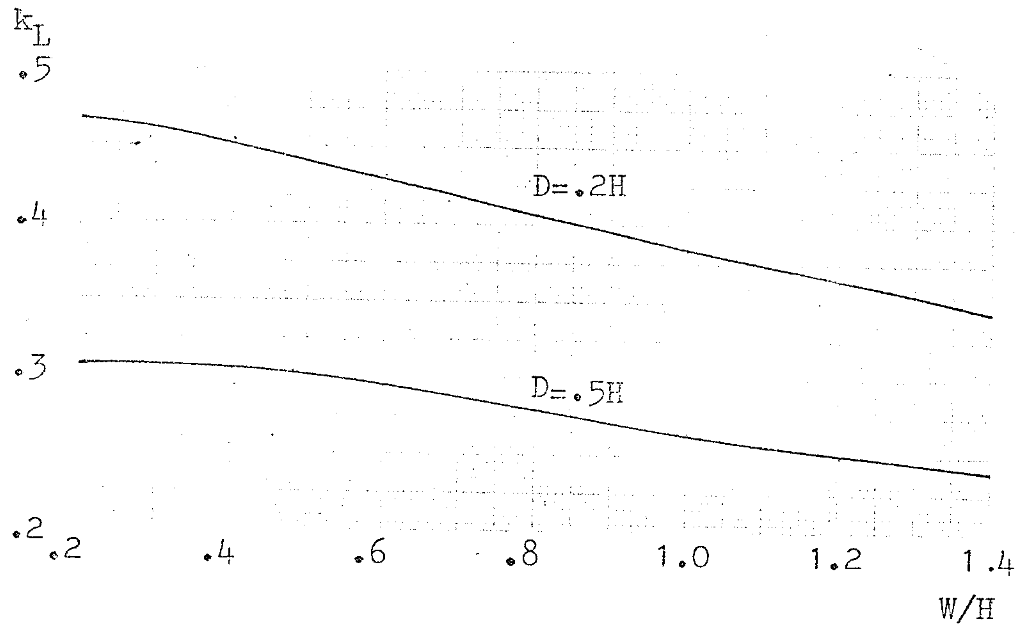

Fig.(5.3). Inductive coupling coefficient versus W/H.

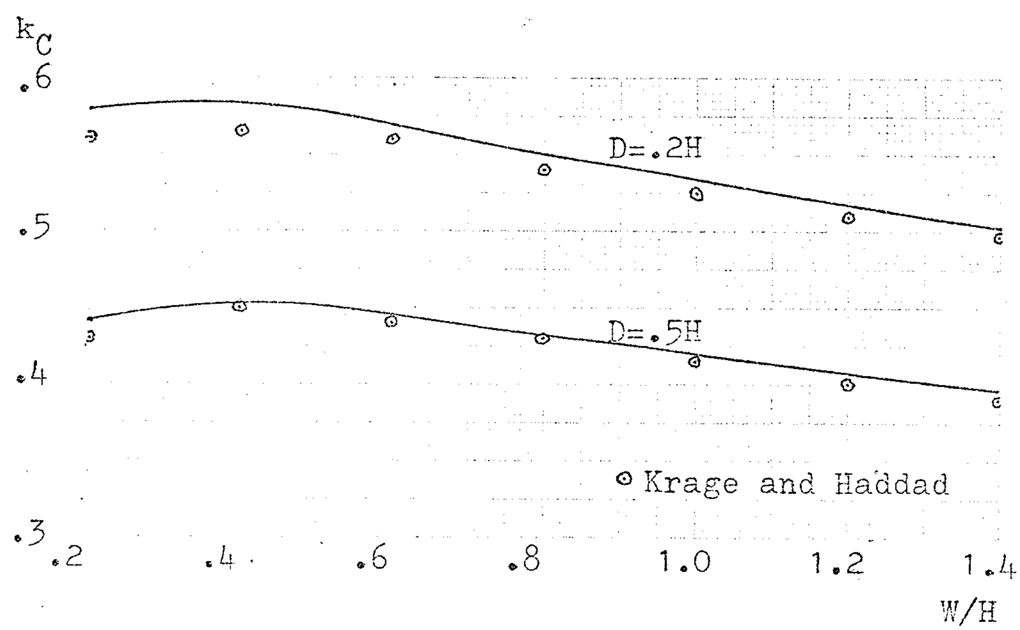

Fig.(5.4). Capacitive coupling coefficient versus W/H.

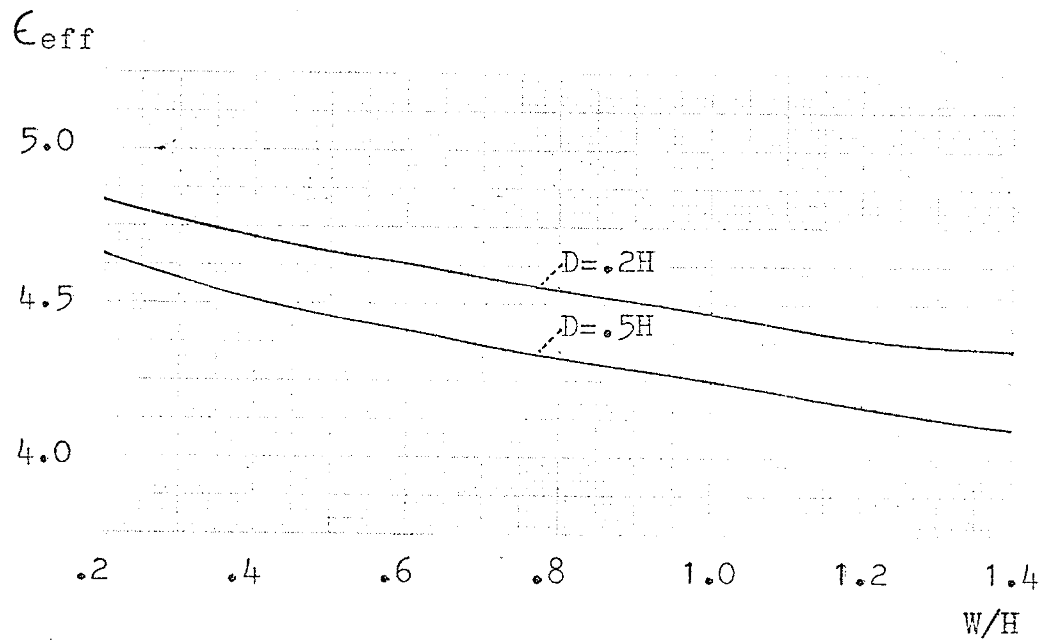

Fig.(5.5). Effective dielectric constant versus W/H.

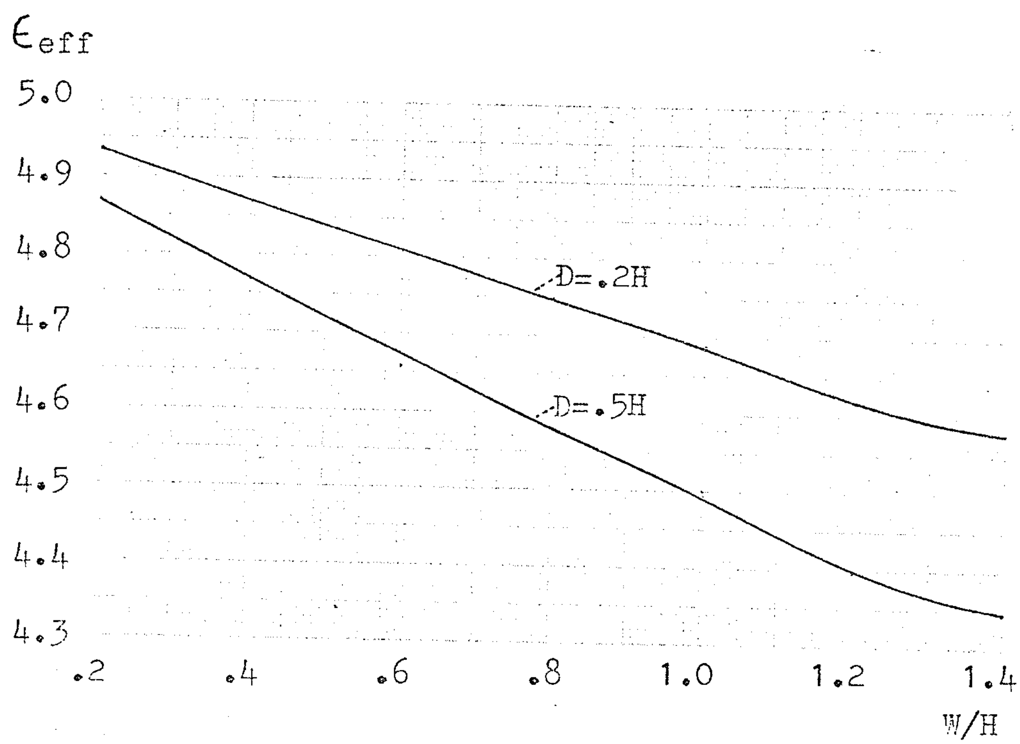

Fig.(5.6). Odd mode effective dielectric constant versus W/H.

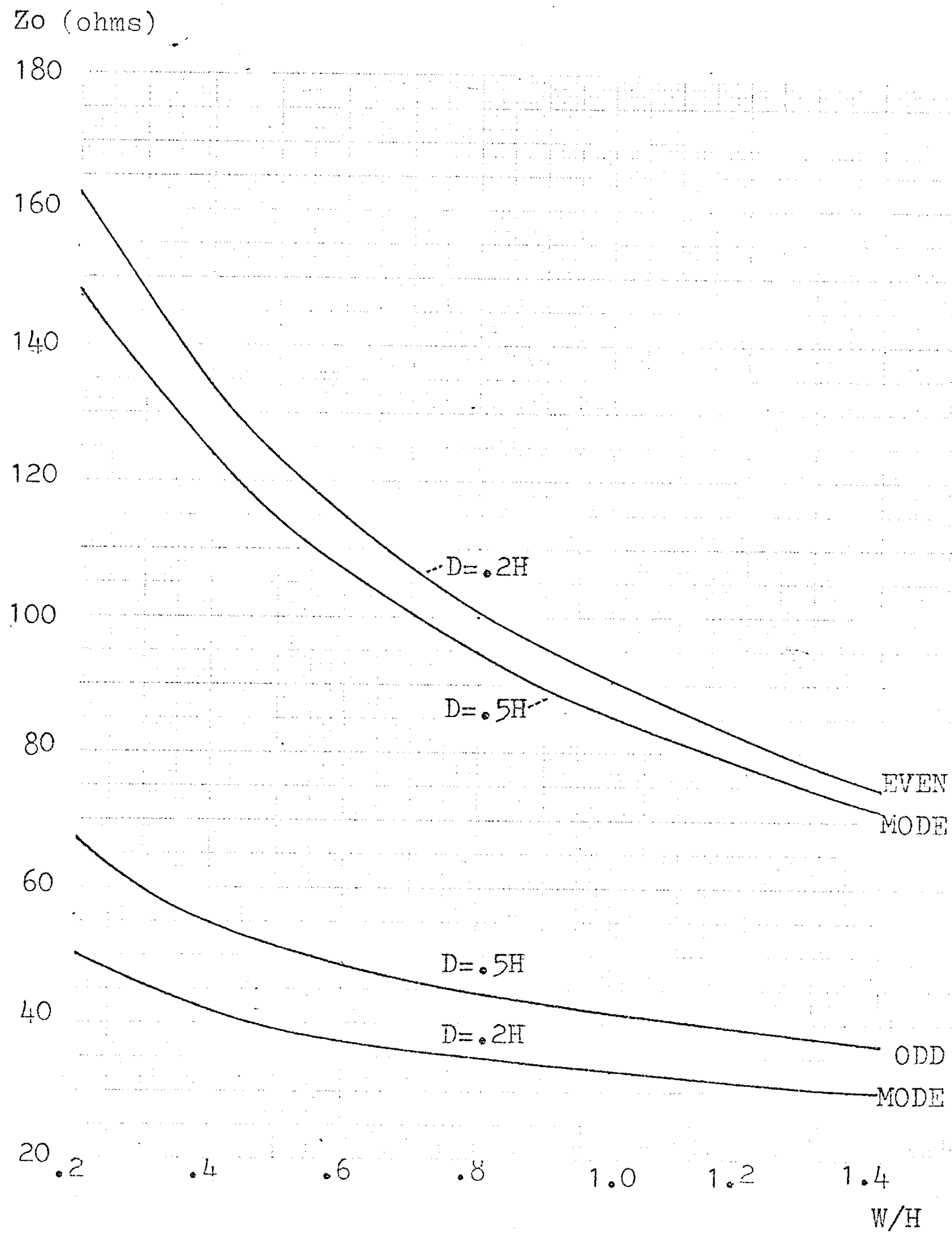

Fig.(5.7). Characteristic impedance versus W/H.

Relative velocity versus W/H.

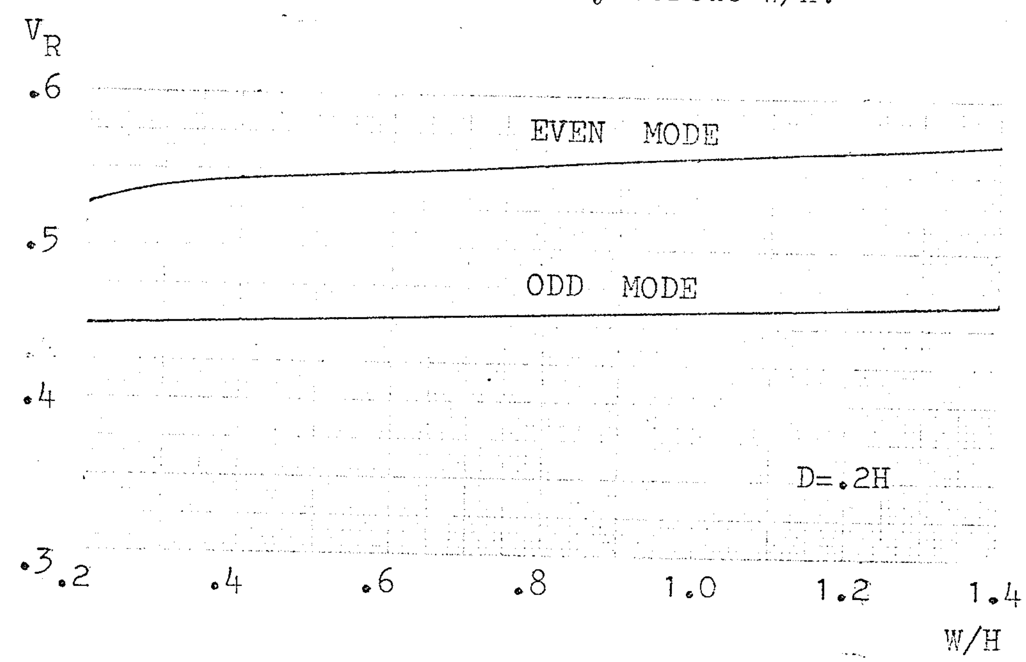

Fig.(5.8)

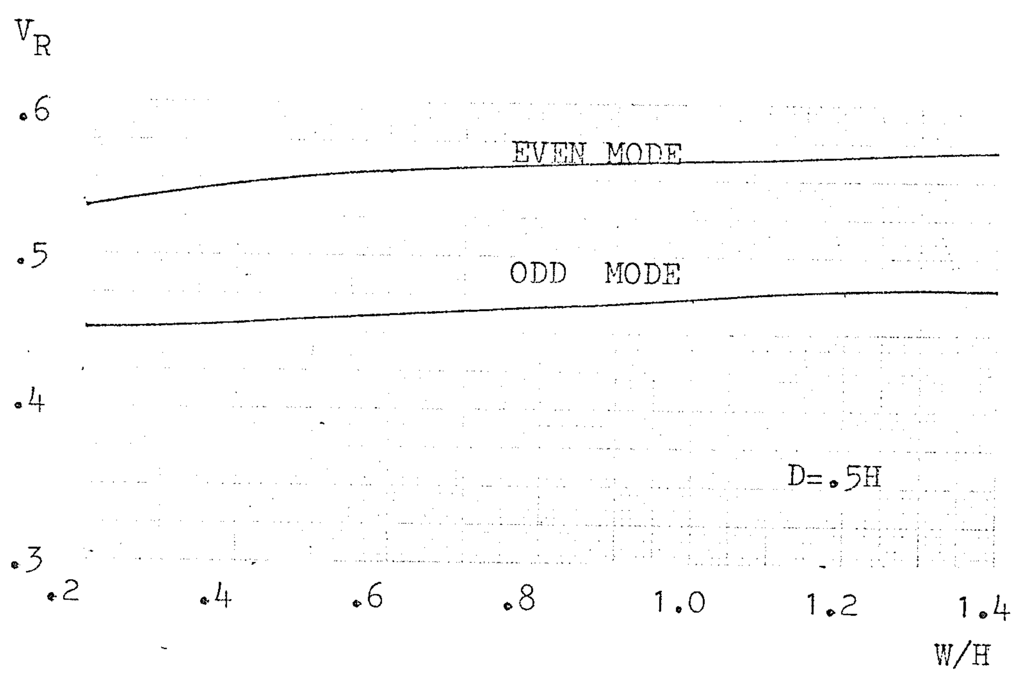

Fig.(5.9)

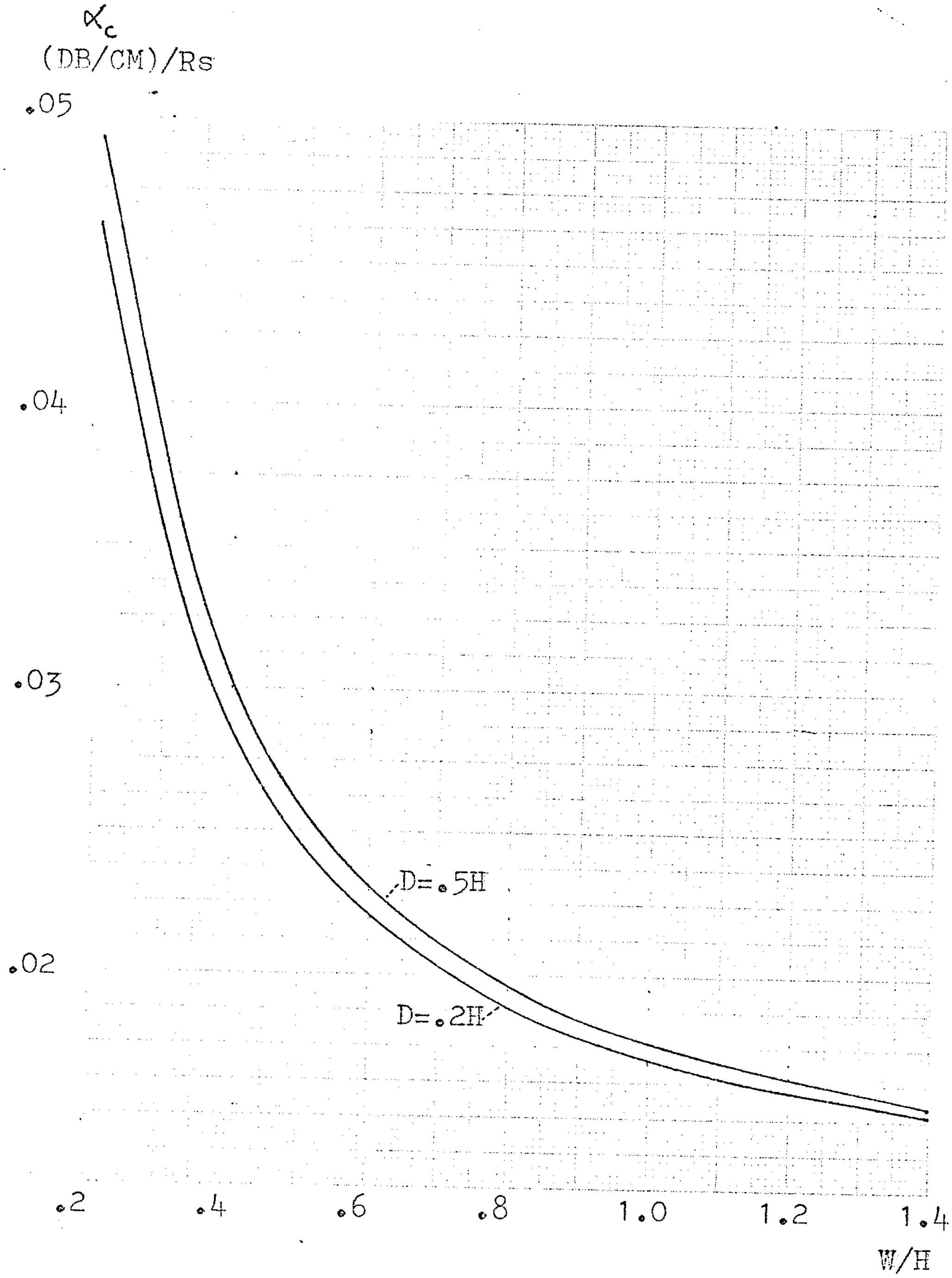

Fig.(5.10). Even mode attenuation constant versus W/H.

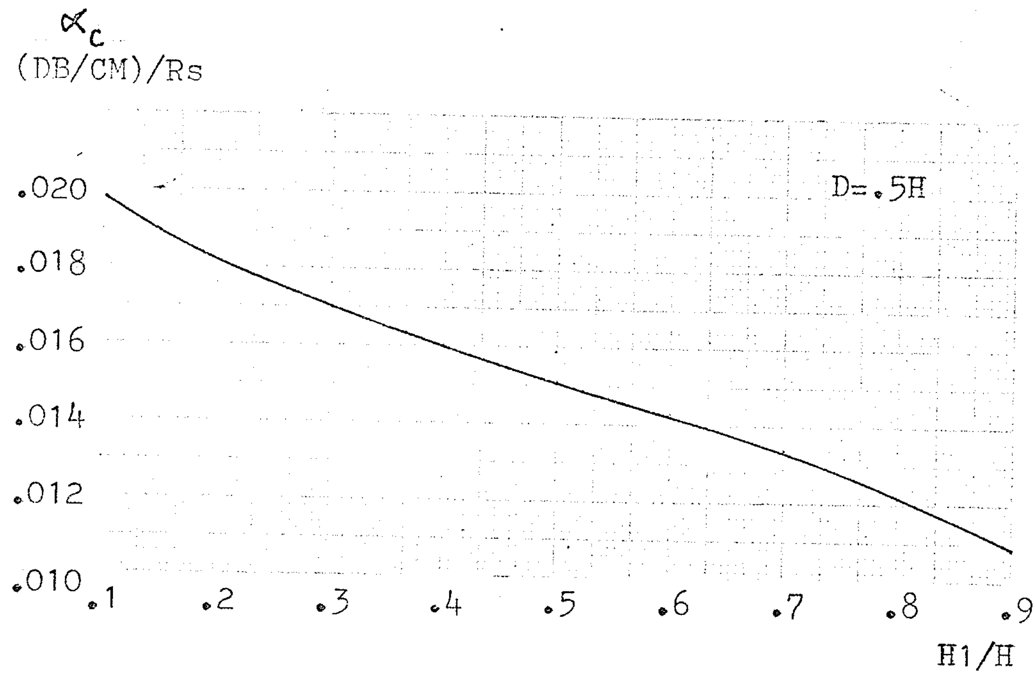

Fig.(5.11). Even mode attenuation constant versus H1/H.

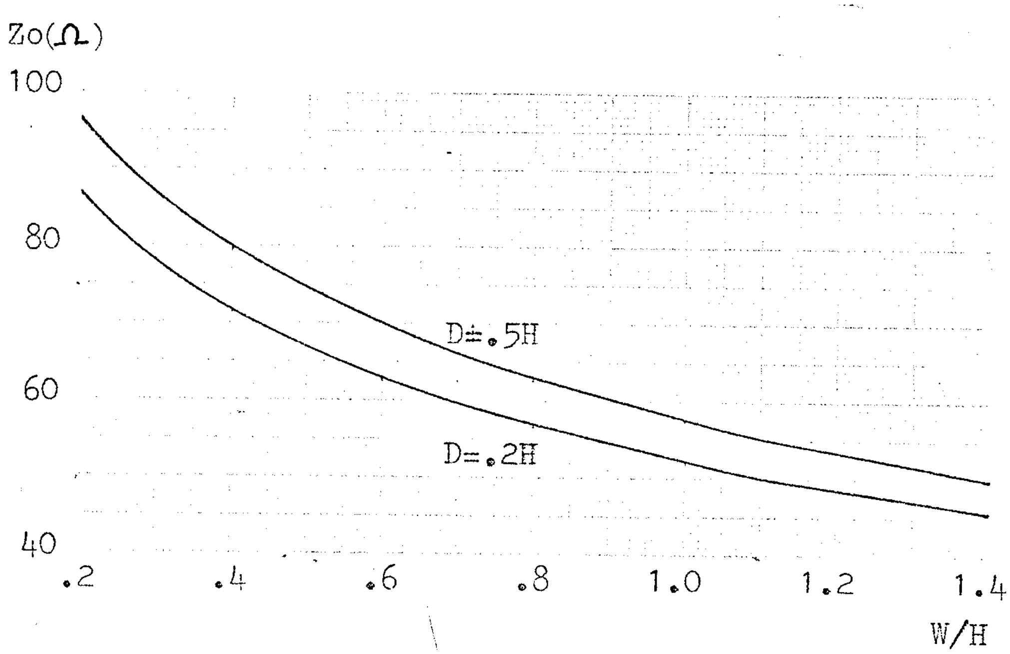

Fig.(5.12). Characteristic impedance of the coupled line versus W/H.

Effective dielectric constant versus H1/H.

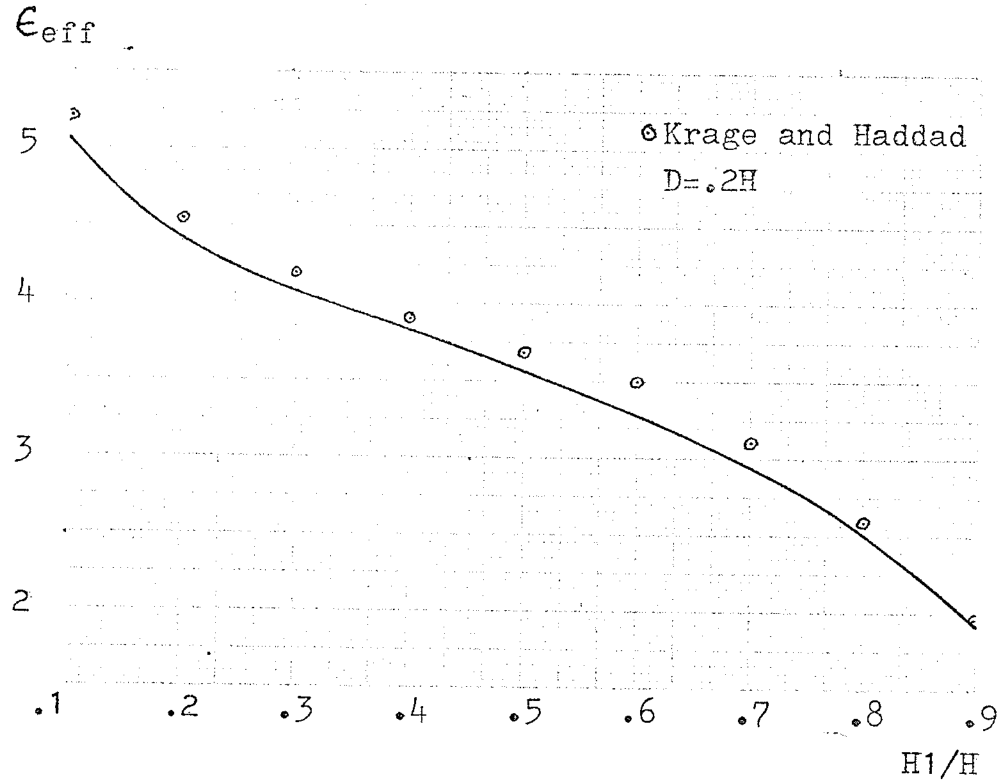

Fig.(5.13)

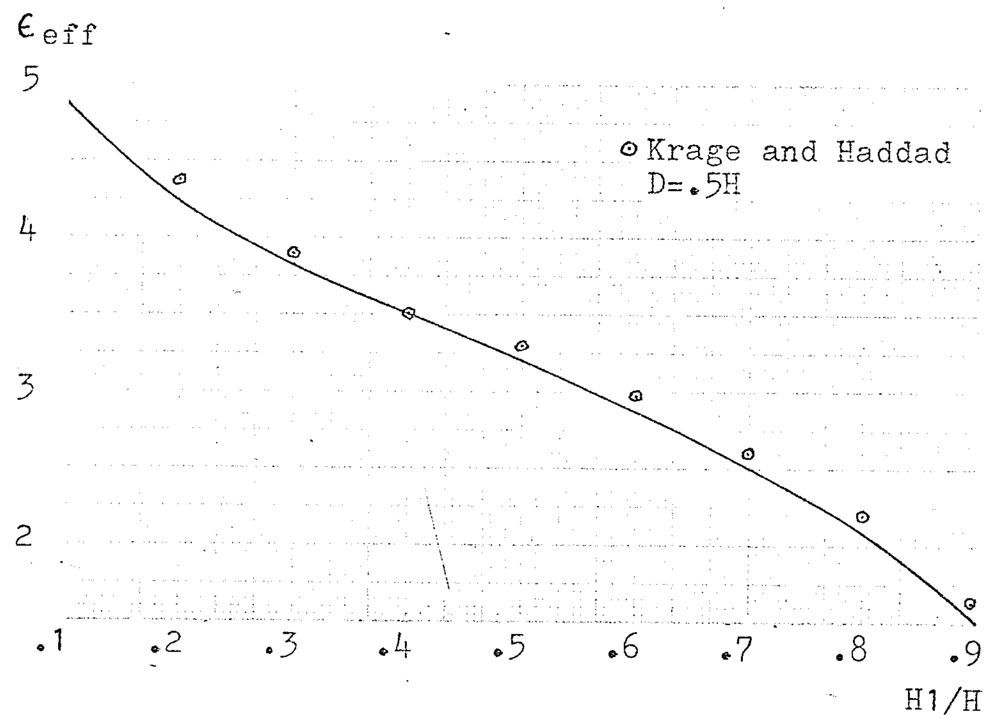

Fig.(5.14)

Effective dielectric constant versus H1/H.

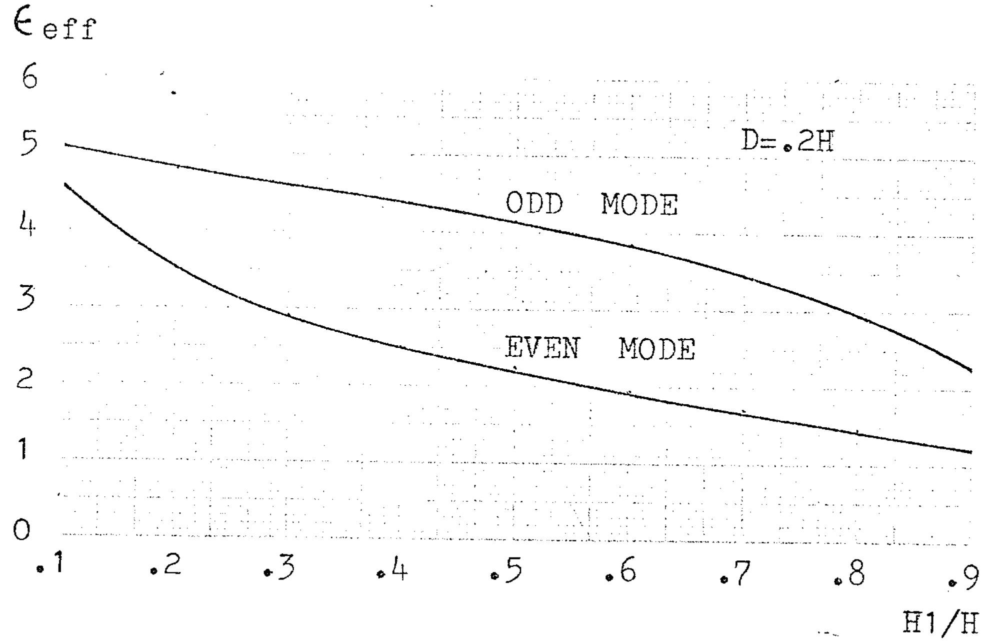

Fig.(5.15)

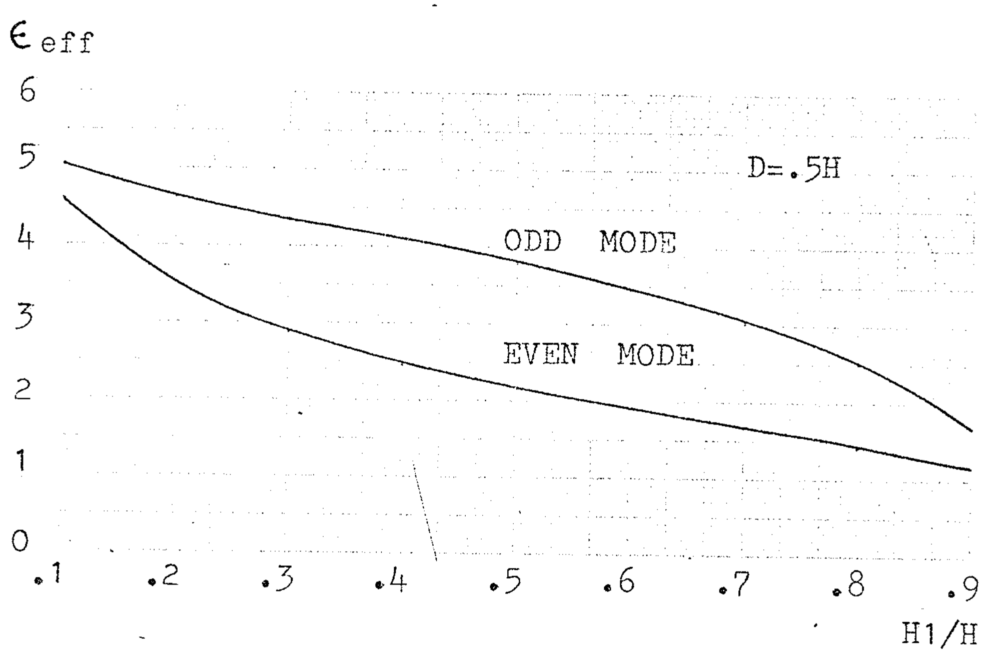

Fig.(5.16)

Relative velocity versus H1/H.

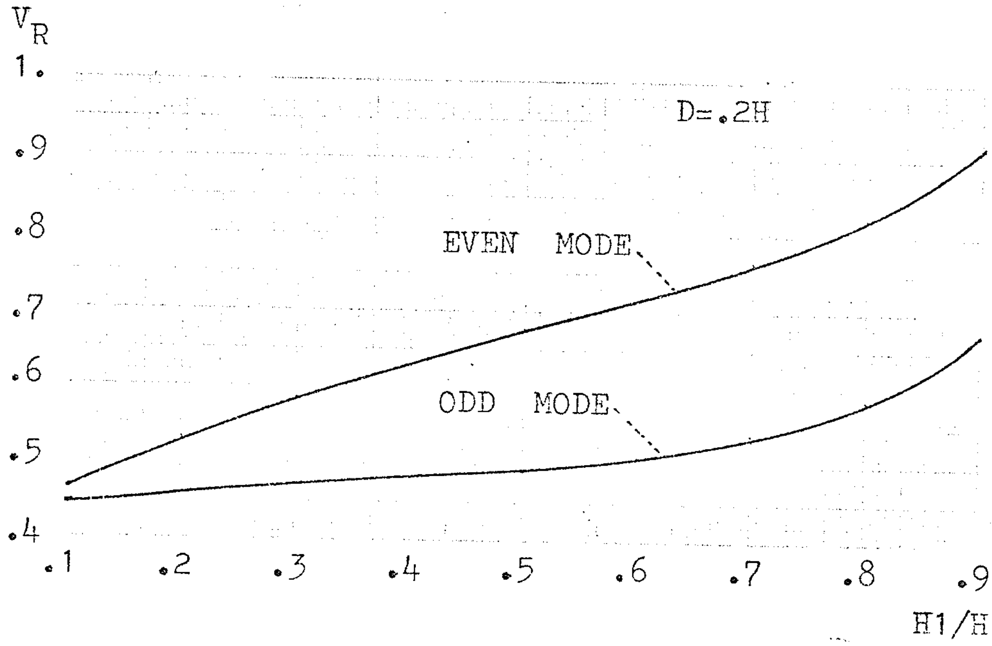

Fig.(5.17)

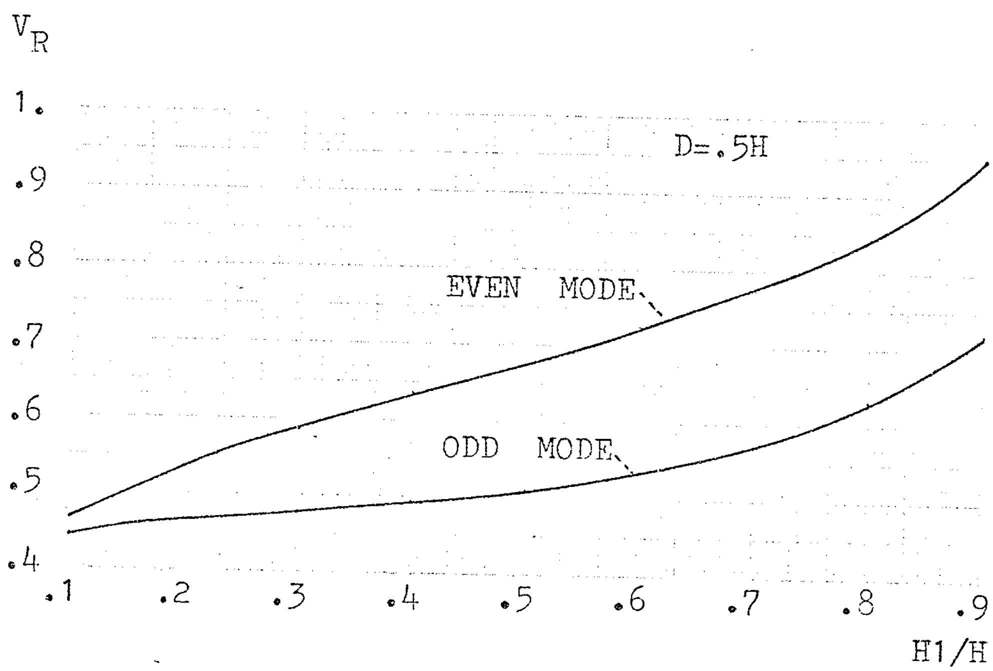

Fig.(5.18)

Characteristic impedance versus H1/H.

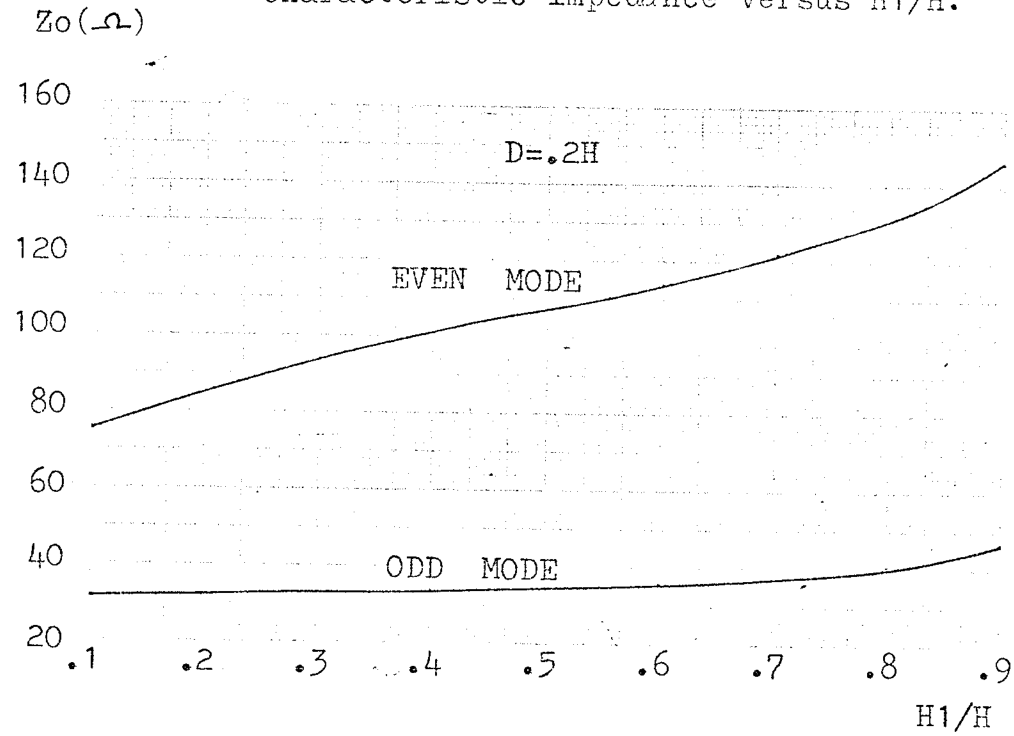

Fig.(5.19)

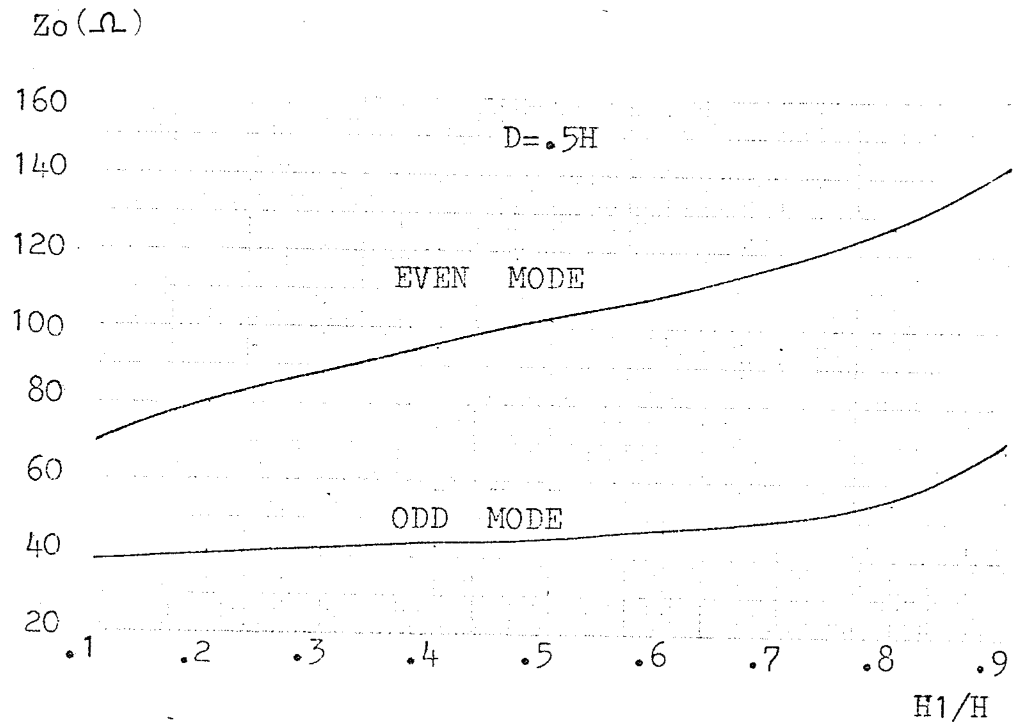

Fig.(5.20)

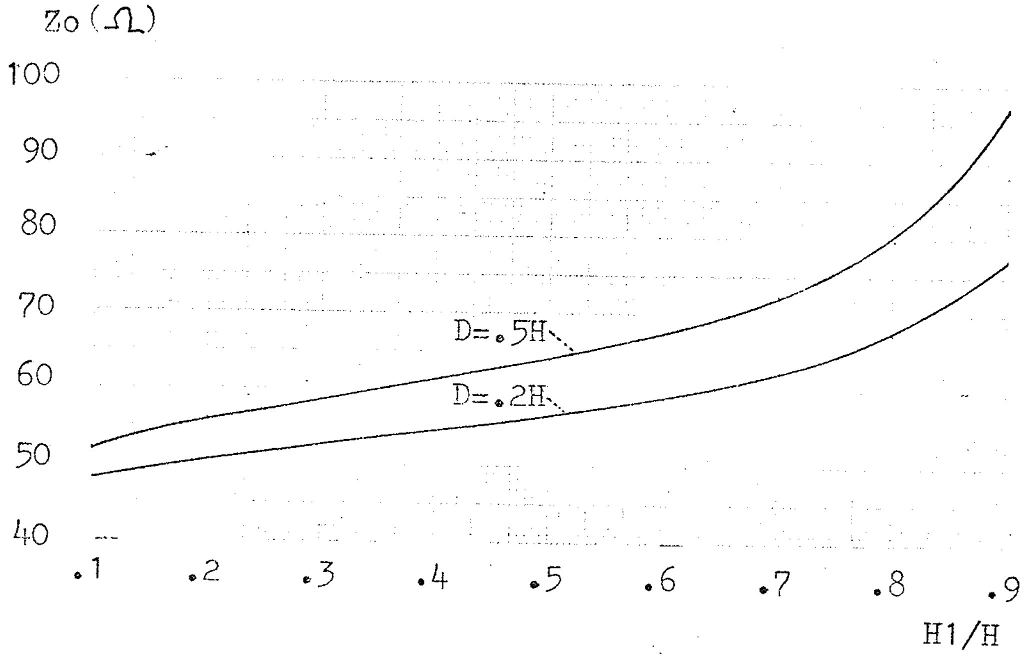

Fig.(5.21). Characteristic impedance of the coupled line versus H1/H.

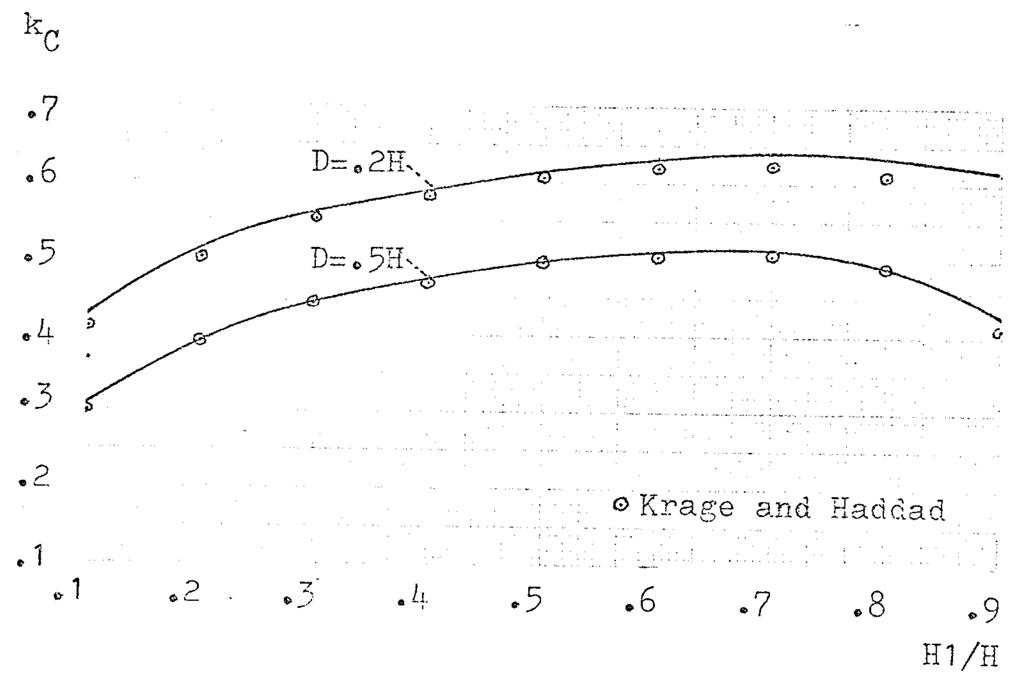

Fig.(5.22). Capacitive coupling coefficient versus H1/H.

CONCLUSION

This thesis describes a general method for analysing the characteristics of single and coupled microstrip transmission lines which have rectangular outer conductors and a multilayered dielectric. The method is numerical and is based on a TEM wave approximation and uses the equivalent source technique. The method is exact in the limit in that it includes no unavoidable approximations. The accuracy is limited by the available computer time and memory. The method involves reducing a functional equation to a matrix equation and then inverting the matrix to obtain a solution, which is particularly well suited to machine computation.

The method described is easily applied to boundaries of arbitrary shape. A major advantage is the ease with which arbitrary boundary conditions can be treated. Treatment of boundary conditions by the usual finite difference method is often complicated.

The equivalent source solution in this thesis has been extended to regions which contain two or more homogenious dielectrics. In this case additional surface sources on the boundary contours separating the two dielectric regions are needed. An advantage of this solution is that the strip thickness can be taken into account.

Both the finite difference and finite element solutions apply a differential operator in a two-dimensional region. This solution applies an integral operator to the one dimensional contour C. For given increments of contour segment length, better accuracy is expected for solutions presented since integral operators are better behaved than differential operators.

Other main features of this method are:

i) A non uniform mesh can be used to allow for the investigation of realistic structures and field distributions and to make optimum use of available computer capability.

ii) Microstrip contained within a conducting box can be easily considered to give information on the effect of the enclosure.

iii) It is possible to have enclosing conductor dimensions which are large compared with microstrip conductor width and substrate thickness.

iv) The method is sufficiently general to allow solutions to be obtained for single and coupled microstrip transmission lines and for related problems such as the slot line (static approximation only as the line is highly dispersive).

From the results obtained and their comparison with published theoretical and experimental results, it is seen that the method outlined is sufficiently accurate general and practicable to practical microstrip analysis and could serve as a great asset in the design of some microstrip components such as directional couplers, filters, delay lines and single to balanced strip line transformers.

APPENDIX A

THE EQUIVALENCE PRINCIPLE

There are many different source distributions outside a specified region of space which produce identical fields inside the region. Two sources producing the same field within a given region of space are said to be equivalent [3]. Thus we do not need to know the actual source distribution in order to find the field in the given region of space, an equivalent source distribution is sufficient to do this.

The equivalence principle can now be illustrated by a simple example. Let Fig. (A.1) represent a source internal to S with free space external to S.

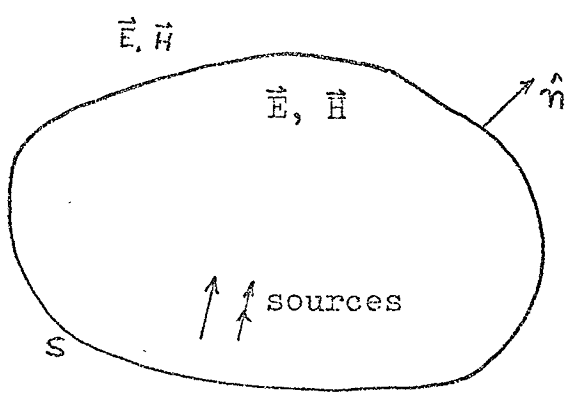

Fig. (A.1)

In order to set up an equivalent source system for the fields external to S let the original field exist external to S and a null field internal to S with free space everywhere as in Fig. (A.2).

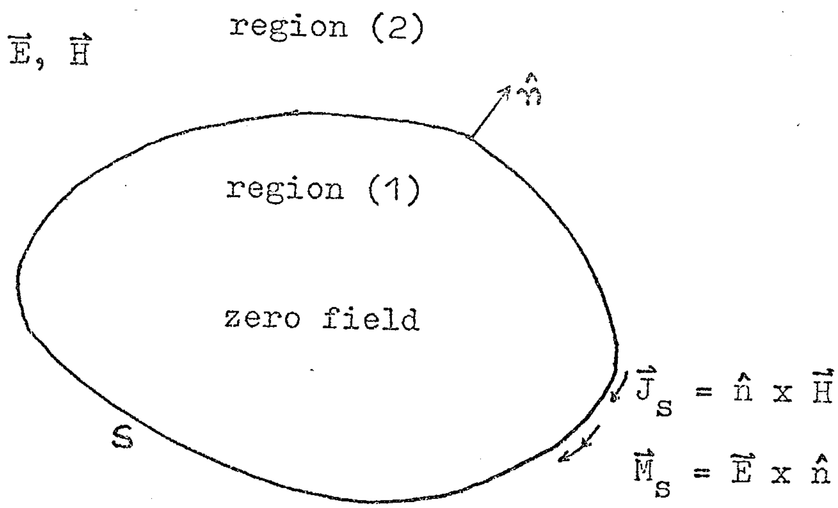

Fig. (A.2)

To support the external field there must exist on S electric and magnetic surface currents $\vec{J}_s$ and $\vec{M}_s$. If the regions are numbered as shown, the fields at S and surface currents are related by

$$\hat{n} \times \left[\vec{H}^{(2)} - \vec{H}^{(1)}\right] = \vec{J}_s \tag{A.1}$$

$$\left[\vec{E}^{(2)} - \vec{E}^{(1)}\right] \times \hat{n} = \vec{M}_s \tag{A.2}$$

As we have assumed zero field in region (1) we get

$$\vec{J}_s = \hat{n} \times \vec{H}, \tag{A.3}$$

$$\vec{M}_s = \vec{E} \times \hat{n} \tag{A.4}$$

Since $\vec{J}_s$ and $\vec{M}_s$ act in unbounded free space, the field values can be found from

$$\vec{E} = -\nabla \times \vec{F} + Y^{-1}(\nabla \times \nabla \times \vec{A} - \vec{J}) \tag{A.5}$$

$$\vec{H} = \nabla \times \vec{A} + Z^{-1}(\nabla \times \nabla \times \vec{F} - \vec{M}) \tag{A.6}$$

Where

$$Y = \sigma + jw\epsilon \tag{A.7}$$

$$Z = jw\mu \tag{A.8}$$

$$\vec{A}(r) = \frac{1}{4\pi} \iiint \frac{\vec{J}(r') \quad e^{-jk|r-r'|}}{|r-r'|} d\tau' \tag{A.9}$$

$$\vec{F}(r) = \frac{1}{4\pi} \iiint \frac{\vec{M}(r') \quad e^{-jk|r-r'|}}{|r-r'|} d\tau' \tag{A.10}$$

The sources are at r' and the field points are taken at r.

Use is next made of uniqueness theorem [3]. This theorem states that field in a lossy region is uniquely specified by the sources within that region plus the tangential component of $\vec{E}$ over the boundary or the tangential component of $\vec{H}$ over the boundary or the former over part of the boundary plus the latter over the rest of the boundary. It is known that the field so calculated will be the originally postulated field, i.e., $\vec{E}$ and $\vec{H}$ external to S and zero internal to S. The final result of this procedure gives a formula for $\vec{E}$ and $\vec{H}$ everywhere external to S in terms of the tangential components of $\vec{E}$ and $\vec{H}$ on S.

We do not have to specify a null field internal to S as previously considered. Any other field will serve equally as well giving infinitely many equivalent source currents as far as the external region is concerned. This is evident from (A.1) and (A.2).

It must be noted that equations (A.5) to (A.10) cannot be used to determine field values unless the equivalent source currents radiate into an unbounded homogeneous region.

We have used the tangential components of both $\vec{E}$ and $\vec{H}$ in setting up the equivalent source problem. From the uniqueness theorem we know that only the tangential component of $\vec{E}$ or $\vec{H}$ is needed to determine the field thus we will show how equivalent source problem can be set up in terms of only magnetic currents (tangential $\vec{E}$) or only electric currents (tangential $\vec{H}$).

Let us go back to the system shown in Fig. (A.1) where all sources lie within S and set up the equivalent source system shown in Fig. (A.3).

Over S we have placed a perfect electric conductor supporting a sheet of magnetic current $\vec{M}_s$. External to S the same field and medium as in the original system are specified. Since the tangential component of $\vec{E}$ is zero on the conductor (just behind $\vec{M}_s$) and equal to original field components in front of $\vec{M}_s$, we get, from (A.2)

$$\vec{M}_s = \vec{E} \times \hat{n}$$

We now have the same tangential component of $\vec{E}$ over S in Fig. (A.1) as in Fig. (A.3), so from uniqueness theorem the field outside S must be the same in each case.

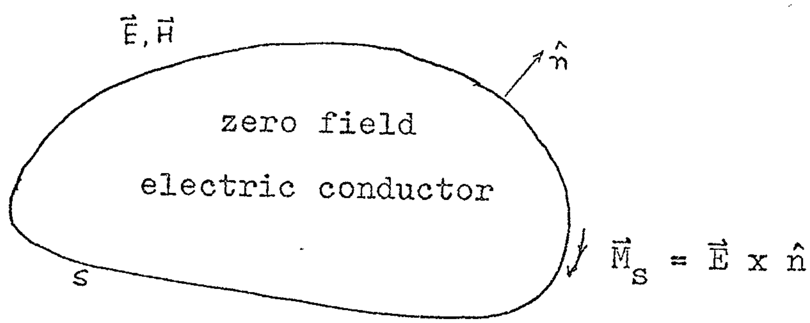

Fig. (A.3)

One can set up the equivalent source problem in terms of electric currents only in an analogous manner. In this case the electric current sheet, $\vec{J}_s = \hat{n} \times \vec{H}$, over a perfect magnetic conductor covering S (a boundary of zero tangential component of $\vec{H}$) produces the same field external to S as the original source system.

The equivalence principle is thus based on a one to one correspondence between fields and sources when the uniqueness conditions are met.

Consider now an analogous concept as applied in circuit theory to better understand the equivalence principle. Examine the situation of a source connected to a passive network, as shown in Fig. (A.4).

To set up an equivalent problem for the passive network, the original source is switched off but its source impedance is left connected.

A current source I, equal to the network terminal current of the original problem, is placed across the network terminals while a voltage source V, equal to the orig-

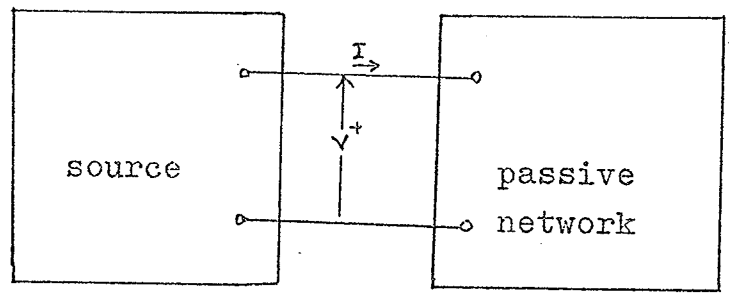

Fig. (A.4)

inal network terminal voltage is placed in series with the network terminals. This is shown in Fig. (A.5).

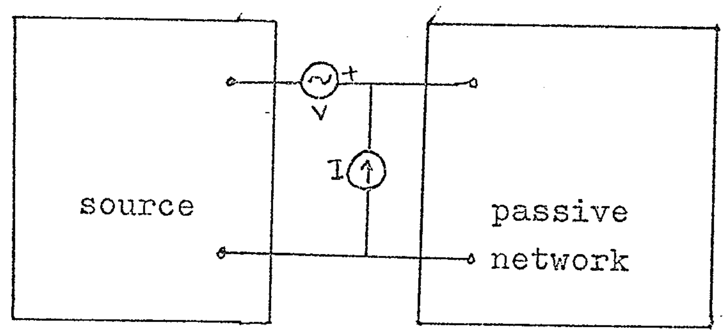

Fig. (A.5)

From basic circuit concepts we know that there is no excitation of the source impedance from the applied equivalent sources, whereas, the excitation of the passive network is unchanged. Thus the circuit of Fig. (A.5) is the circuit analogue of the field system in Fig. (A.2).

Since there is no excitation of the source impedance in the circuit in Fig. (A.5) we can replace the source impedance by any arbitrary impedance without affecting the excitation of the passive network. Replacing the source impedance by a short circuit, short circuits the current source, so that we are left with a voltage source alone and this is analogous to the problem depicted in Fig. (A.3). Similarly an infinite source impedance open circuits the voltage source leaving only a current source and this is analogous to the problem depicted in (A.3) with the electric conductor replaced by a magnetic conductor supporting an electric current sheet, $\vec{J}_S = \hat{n} \times \vec{H}$.

APPENDIX B

THE METHOD OF MOMENTS

The method of moments [2] is used for computing solutions to linear equations. The basic procedure involves reducing the functional equation to be solved to a matrix equation and then solving this matrix equation by known techniques such as a matrix inversion technique.

Let us consider an equation of the inhomogeneous type

$$L(f) = g \tag{B.1}$$

where L is an operator, g is the source or excitation and f is the required field or response function to be determined. Assume the solution to (B.1) to be deterministic, i.e., f is unique. We must identify the operator L, its domain (the function f on which it operates) and its range (the function g). Furthermore, we need an inner product $\langle f, g \rangle$ which is a scaler defined to satisfy

$$\langle f, g \rangle = \langle g, f \rangle \;, \tag{B.2}$$

$$\langle \alpha f + \beta g, h \rangle = \alpha \langle f, h \rangle + \beta \langle g, h \rangle, \tag{B.3}$$

$$\langle f^*, f \rangle > 0 \text{ if } f \neq 0, \tag{B.4}$$

$$\langle f^*, f \rangle = 0 \text{ if } f = 0 \tag{B.5}$$

where α, β are scalers and the asterisk (*) defines a complex conjugate.

We can now proceed to solve equation (B.1) where L is the linear operator, g is known and f is the function to be determined.

Let f be expanded in a series of functions f_1, f_2, f_3, ... f_n in the domain of f as

$$f = \sum_n \alpha_n \quad f_n \tag{B.6}$$

where α_n are constants and f_n are called expansion functions. For an exact solution (B.6) is usually an infinite summation whereas for an approximate solution it is a finite summation.

Substituting (B.6) into (B.1) and using the linearity property of L gives

$$\sum_n \alpha_n \; L(f_n) = g \tag{B.7}$$

If a suitable inner product $\langle f, g \rangle$ is available we can define a set of weighting functions w_1, w_2, w_3, ... w_m in the range of L. Taking the inner product of (B.7) with each w_m gives

$$\sum_n \alpha_n \langle w_m, L(f_n) \rangle = \langle w_m, g \rangle$$

$$\text{for} \quad m = 1, 2, 3 \ldots. \tag{B.8}$$

Writing (B.8) in matrix form, we get

$$\left[l_{mn} \right] \left[\alpha_n \right] = \left[g_m \right] \tag{B.9}$$

where

$$\left[l_{mn}\right] = \begin{bmatrix} w_1, L(f_1) & w_1, L(f_2) & \cdots\cdots \\ w_2, L(f_1) & w_2, L(f_2) & \cdots\cdots \\ \cdots\cdots & \cdots\cdots & \cdots\cdots \end{bmatrix},$$

$$\left[\alpha_n\right] = \begin{bmatrix} \alpha_1 \\ \alpha_2 \\ --- \\ --- \\ \alpha_n \end{bmatrix},$$

$$\left[g_m\right] = \begin{bmatrix} \langle w_1, g\rangle \\ \langle w_2, g\rangle \\ \cdots\cdots \\ \cdots\cdots \\ \langle w_m, g\rangle \end{bmatrix}.$$

If the matrix $[l]$ is non-singular, its inverse $[l]^{-1}$ exists and the α_n are then given by

$$\left[\alpha_n\right] = \left[l_{mn}\right]^{-1} \left[g_m\right] \qquad (B.10)$$

The solution for f is given by (B.6).

Define another matrix

$$\left[\tilde{f}_n\right] = \left[f_1 \;\; f_2 \;\; f_3 \cdots\cdots f_n\right] \qquad (B.11)$$

We may write (B.6) as

$$f = \left[\tilde{f}_n\right] \left[\alpha_n\right] \tag{B.12}$$

Substituting (B.10) in (B.12) we get

$$f = \left[f_n\right] \left[l_{mn}\right]^{-1} \left[g_m\right] \tag{B.13}$$

This solution can be exact or approximate depending upon the choice of f_n and w_m.

One of the main tasks in any particular problem is a suitable choice of f_n and w_m. The f_n should be linearily independent and chosen so that (B.6) can approximate f reasonably well. Additional factors which affect the choice of f_n and w_m are the accuracy of solution desired, the ease of evaluation of matrix elements, the size of the matrix that can be inverted and the realization of a well-conditioned matrix [1] .

APPENDIX C

THE VARIATIONAL METHOD

Fig. (C.1) shows a microstrip enclosed in a box with perfectly conducting walls.

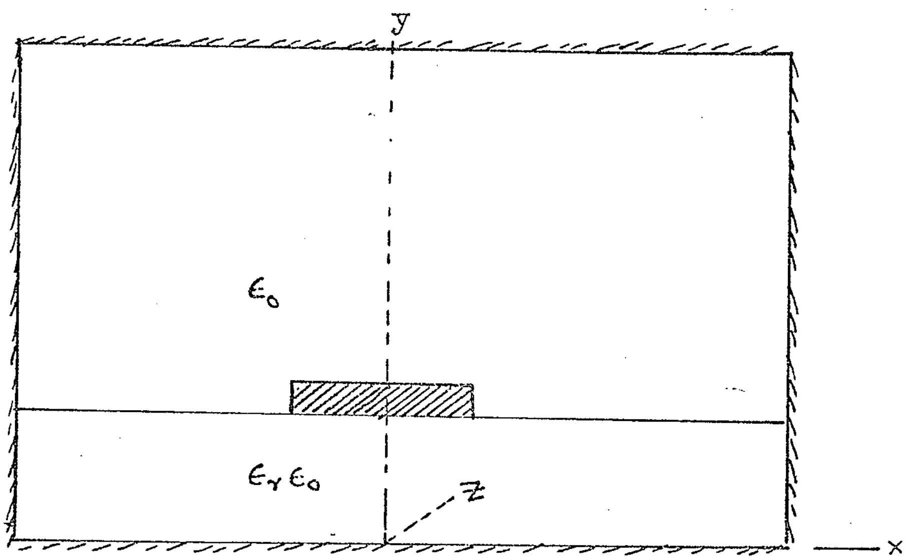

Fig. (C.1)

The box encloses inhomogeneous matter whose distribution may be a function of transverse co-ordinates but not of the co-ordinates along the direction of propagation. If Z is the direction of propagation as shown, the field vectors may be expressed as $\vec{E}(x, y)\, e^{-j\beta z}$ and $\vec{H}(x, y)\, e^{-j\beta z}$, where β is the propagation constant [6]. $\vec{E}$ and $\vec{H}$ are three dimensional vectors depending on x and y only.

Maxwell's equations are

$$\text{Curl } \vec{E} + jw\mu \vec{H} = 0, \tag{C.1}$$

$$\text{Curl } \vec{H} - jw\epsilon \vec{E} = 0, \tag{C.2}$$

Substituting for $\vec{E}$ and $\vec{H}$ into (C.1) and (C.2) yields

$$e^{-j\beta z} \text{ Curl } \vec{E}(x,y) + jw\mu\vec{H}(x,y)\, e^{-j\beta z}$$
$$= j\beta\, \vec{E}(x,y)\, e^{-j\beta z} (\hat{a}_y - \hat{a}_x), \tag{C.3}$$

$$e^{-j\beta z} \text{ Curl } \vec{H}(x,y) - jw\epsilon\, \vec{E}(x,y)\, e^{-j\beta z}$$
$$= j\beta\, \vec{H}(x,y)\, e^{-j\beta z} (\hat{a}_y - \hat{a}_x). \tag{C.4}$$

These two equations may be simplified to

$$\text{Curl } \vec{E} + jw\mu\vec{H} = j\beta\, \hat{a}_z \times \vec{E}, \tag{C.5}$$

$$\text{Curl } \vec{H} - jw\epsilon\vec{E} = j\beta\, \hat{a}_z \times \vec{H}. \tag{C.6}$$

Now by multiplying (C.5) scalerly by $\vec{H}$ and (C.6) scalerly by $\vec{E}$ and substracting the two resulting equations we get

$$\vec{H}\cdot\nabla\times\vec{E} + jw\mu\vec{H}\cdot\vec{H} - \vec{E}\cdot\nabla\times\vec{H} + jw\epsilon\,\vec{E}\cdot\vec{E}$$
$$= j\beta\,\vec{H}\cdot(\hat{a}_z\times\vec{E}) - j\beta\,\vec{E}\cdot(\hat{a}_z\times\vec{H}) \tag{C.7}$$

Rearranging (C.7) and combining the terms on the right hand side gives

$$\vec{H}\cdot\nabla\times\vec{E} - \vec{E}\cdot\nabla\times\vec{H} + jw\mu|H|^2 + jw\epsilon|E|^2$$
$$= 2\beta j\, \hat{a}_z\cdot(\vec{E}\times\vec{H}) \tag{C.8}$$

Integrating (C.8) over the cross-section of the microstrip and solving for β yields

$$\beta = \frac{w \iint_s (\epsilon |E|^2 + \mu |H|^2) \cdot ds + j \iint_s (\vec{E} \cdot \nabla \times \vec{H} - \vec{H} \cdot \nabla \times \vec{E}) ds}{2 \iint_s \hat{a}_z \cdot (\vec{E} \times \vec{H}) \cdot ds} \qquad (C.9)$$

If we specify $\vec{E}$ and $\vec{H}$ to be the gradients of scaler potentials ϕ and ψ , respectively, the second integral in the numerator vanishes as Curl (Gradient $\emptyset$) = 0 and Curl (Gradient ψ) = 0 (C.9) becomes

$$\beta = \frac{w \iint_s (\mu |H|^2 + \epsilon |E|^2) \cdot ds}{2 \iint_s \hat{a}_z \cdot (\vec{E} \times \vec{H}) \cdot ds} \qquad (C.10)$$

Equation (C.9) can easily be shown to be a variational expression of β . This is done by calculating the variation of β and observing that it vanishes provided $\vec{E}$ and $\vec{H}$ satisfy Maxwell's equations (C.5) and (C.6) and provided the tangential component of $\vec{E}$ vanishes over the walls of the microstrip. Thus trial fields $\vec{E}$ and $\vec{H}$ must be continous and must possess first order derivatives throughout the cross-section and at the boundary the tangential component of $\vec{E}$ must vanish.

Substituting $\vec{E} = \nabla \emptyset$ and $\vec{H} = \nabla \psi$ in (C.10) we get

$$\beta = \frac{w \iint_s [\mu (\nabla \psi \cdot \nabla \psi) + \epsilon (\nabla \phi \cdot \nabla \phi)] \cdot ds}{2 \iint_s (\nabla \phi \times \nabla \psi) \cdot \hat{a}_z \; ds} \qquad (C.11)$$

For ϕ and ψ satisfying Laplace's equation we have

$$\begin{aligned} \nabla\phi\cdot\nabla\phi &= \nabla\cdot(\phi\nabla\phi) \\ \nabla\psi\cdot\nabla\psi &= \nabla\cdot(\psi\nabla\psi) \end{aligned} \tag{C.12}$$

Substituting (C.12) into (C.11) and applying the divergence theorem we get

$$\beta = \frac{w\left[\oint_c \mu\psi \frac{\partial\psi}{\partial n}\,dl + \oint_c \epsilon\phi\frac{\partial\phi}{\partial n}\,dl\right]}{2\iint_S (\nabla\phi\times\nabla\psi)\cdot\hat{a}_3\,ds} \tag{C.13}$$

In the denominator of this equation substitute $\nabla\phi \times \nabla\psi = \nabla \times (\phi\nabla\psi)$ and change the surface integration to a line integration. This gives

$$\beta = \frac{w\left[\oint_c \mu\psi \frac{\partial\psi}{\partial n}\,dl + \oint_c \epsilon\phi\frac{\partial\phi}{\partial n}\,dl\right]}{2\oint_c \phi\,\nabla\psi\cdot dl} \tag{C.14}$$

Equation (C.14) can be written

$$\beta = \frac{W}{2}\left[\frac{A+B}{C}\right] \tag{C.15}$$

where

$$A = \oint_c \mu\psi\frac{\partial\psi}{\partial n}\,dl \tag{C.16}$$

$$B = \oint_c \epsilon\phi\frac{\partial\phi}{\partial n}\,dl \tag{C.17}$$

$$C = \oint_c \phi\,\nabla\psi\cdot dl \tag{C.18}$$

If a scaling is applied so that

$$\phi' = \eta \phi \tag{C.19}$$

then $\beta = \frac{W}{2} \frac{(A + \eta B)}{\eta C},$

$$= \frac{W}{2} \left(\frac{A}{\eta C} + \frac{\eta B}{C}\right). \tag{C.20}$$

For β to be stationary we need

$\frac{\partial \beta}{\partial \eta} = 0$, i.e.,

$$-\frac{1}{\eta^2} \frac{A}{C} + \frac{B}{C} = 0 \tag{C.21}$$

This gives $\eta^2 = \frac{A}{B}$ (C.22)

If (C.22) is substituted into (C.20) we get

$$\beta = \frac{W\sqrt{AB}}{C}$$

$$= \frac{W\sqrt{\left(\mu \oint_c \psi \frac{\partial \psi}{\partial n} \, dl\right)\left(\epsilon \oint_c \phi \frac{\partial \phi}{\partial n} \, dl\right)}}{\oint_c \phi \, \nabla\psi \cdot dl} .$$

APPENDIX D

GREEN'S FUNCTION AND IDENTITIES

To obtain the field caused by a distributed source we can proceed by calculating the effect of each elementary portion of source and then apply superposition to obtain the overall field. If $G(r/r_o)$ is the field at the observation point r caused by a unit point source at the source point r_o, then the field at r caused by a source distribution $\rho(r_o)$ is the integral of $G\rho$ over the whole range of r_o occupied by the source. The function G is called the Green's function 20 .

We will now derive Green's identities which are a mathematical statement of scaler reciprocity. The difference between Green's theorem and the reciprocity theorem is that no physical interpretation is given to the functions in the former.

The scaler Green's theorem is based on the following identity

$$\nabla \cdot (\psi \nabla \phi) = \psi \nabla^2 \phi + \nabla \psi \cdot \nabla \phi \qquad (D.1)$$

When (D.1) is integrated throughout a region and the divergence theorem is applied to the left hand term we obtain Green's first identity, which is

$$\oint\!\!\oint \psi \frac{\partial \phi}{\partial n} ds = \iint_R (\psi \nabla^2 \phi + \nabla\psi \cdot \nabla \phi)\, d\tau. \qquad (D.2)$$

Interchanging ψ and ϕ in this identity and substracting the original from the interchanged equation we obtain Green's second identity or Green's theorem

$$\oint_c \left(\phi \frac{\partial \psi}{\partial n} - \psi \frac{\partial \phi}{\partial n}\right) dc = \iint_R (\phi \nabla^2 \psi - \psi \nabla^2 \phi)\, d\tau \qquad (D.3)$$

The derivation of integral equations from Laplace's equation involves the application of (D.3) to the unknown field ϕ and to the Green's function

$$\psi(\rho, \rho') = \frac{1}{2\pi} \ln \frac{k}{|\rho - \rho'|} \qquad (D.4)$$

The Green's function is the potential of a point source, i.e., the solution to

$$\nabla^2 \psi = -\delta(\rho - \rho') \qquad (D.5)$$

where δ is the Dirac delta function and for reasons discussed in Chapter 1, k is selected such that

$$k > |\rho - \rho'|_{max}$$

Substituting equations (D.4) and (D.5) into (D.3) we get

$$\oint_c \left(\phi \frac{\partial \psi}{\partial n} - \psi \frac{\partial \phi}{\partial n}\right) dc' = \begin{cases} \phi(\rho) & \rho \text{ in } R \\ 0 & \rho \text{ in } R^1 \end{cases} \qquad (D.6)$$

where R is region internal to C and R^1 is region external to C.

To derive integral equation (1.3) we apply equation (D.6) twice, once for region R and once for R^1. Letting subscript i denote quantities in R (internal to C) and e quantities in R^1 (external to C) we have

$$\oint \left(\phi^i \frac{\partial \psi}{\partial n} - \psi \frac{\partial \phi^i}{\partial n}\right) dc' = \begin{cases} \phi^i & \rho \text{ in } R \\ 0 & \rho \text{ in } R^1 \end{cases} \qquad (D.7)$$

$$-\oint \left(\phi^e \frac{\partial \psi}{\partial n} - \psi \frac{\partial \phi^e}{\partial n}\right) dc' = \begin{cases} 0 & \rho \text{ in } R \\ \phi^e & \rho \text{ in } R^1 \end{cases} \qquad (D.8)$$

The reason for the minus sign in front of (D.8) is due to the direction of n which is kept fixed.

Adding (D.7) and (D.8) we get

$$\oint_c \left[(\phi^i - \phi^e)\frac{\partial \psi}{\partial n} - \left(\frac{\partial \phi^i}{\partial n} - \frac{\partial \phi^e}{\partial n}\right)\psi\right] dc' = \phi \qquad (D.9)$$

where $\phi = \phi^i$ in R

$\phi = \phi^e$ in R^1

Choosing $\phi^i = \phi^e$ on C, equation (D.9) can be rewritten as

$$\oint_c \left(\frac{\partial \phi^e}{\partial n} - \frac{\partial \phi^i}{\partial n} \right) \psi \, dc' = \phi \tag{D.10}$$

Letting $\sigma(c') = \frac{1}{2\pi} \left(\frac{\partial \phi^e}{\partial n} - \frac{\partial \phi^i}{\partial n} \right)$ (D.11)

We get equation (1.3), i.e.,

$$\begin{aligned} \phi &= 2\pi \oint \sigma(C') \psi \, dc' \\ &= \oint \sigma(C') \ln \frac{k}{|\rho - \rho'|} \, dc' \end{aligned}$$

The quantity $2\pi\epsilon\sigma$ can be thought of as the equivalent charge density on C which produces an electric potential ϕ.

APPENDIX E

THE COMPUTER PROGRAM

The program was coded in FORTRAN for operation on the IBM system 370 computer. Although lengthy, the program is rather simple with very little branching. Standard subroutine packages ARRAY and SIMQ are used for matrix inversion. All arithmetic is performed in single precision. The compile time for the program using the FORTRAN G level compiler was 18 seconds. Total execution time for one set of microstrip (described by a total of 70 segments) parameters, including a variational calculation, was 22 seconds.

A flow chart and a complete listing of the program follows:

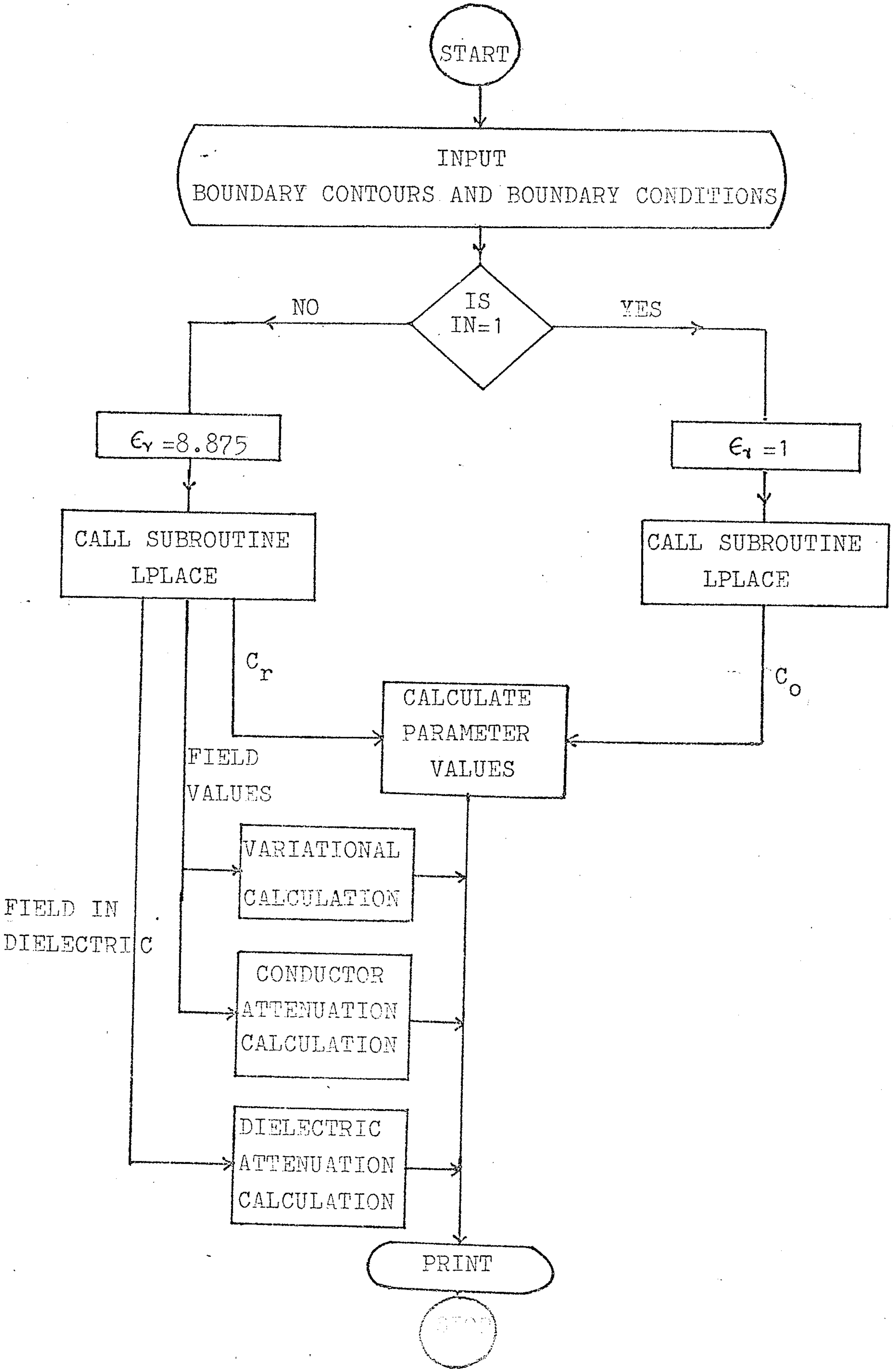
START
INPUT
BOUNDARY CONTOURS AND BOUNDARY CONDITIONS
IS IN=1
NO
YES
ϵ_r =8.875
ϵ_r =1
CALL SUBROUTINE LPLACE
CALL SUBROUTINE LPLACE
C_r
C_o
CALCULATE PARAMETER VALUES
FIELD VALUES
VARIATIONAL CALCULATION
FIELD IN DIELECTRIC
CONDUCTOR ATTENUATION CALCULATION
DIELECTRIC ATTENUATION CALCULATION
PRINT

Fig.(E.1)

```
$JOB WATFIV     B.AGGARWAL,NOEXT
C
C
C        SUBROUTINE LAPLACE
C
C       THIS PROGRAM IS A REVISION OF ONE DESCRIBED IN
C       K. FONTOPPIDAN,'EQUIVALENT SOURCE SOLUTIONS OF
C       ELECTROSTATIC AND MAGNETOSTATIC PROBLEMS' IEEE
C       INTERNATIONAL CONVENTION DIGEST,MARCH 1971.
C       THE METHOD USED IS GIVEN IN R.F.HARRINGTON,
C       K.FONTOPPIDAN,P.ABRAHAMSEN AND N.C.ALBERTSEN, COMPUTATION
C       OF LAPLACIAN POTENTIALS BYBAN EQUIVALENT SOURCE METHOD,
C       PROC IEE,VOL 116, NO 10,OCTOBER 1969,PP 1715-1720.
C
C    THIS SUBROUTINE SOLVES THE LAPLACE EQUATION IN TWO
C    DIMENSIONS.THE BOUNDARY CONDITIONS ARE GIVEN ALONG AN
C    ARBITRARY NUMBER OF OPEN OR CLOSED CURVES IN THE X-Y PLANE.
C    IF F=F(X,Y) IS THE SOLUTION, THE BOUNDARY CONDITIONS
C    MUST BE EXPRESSED IN THE FORM-
C
C    FOR THE ELECTROSTATIC PROBLEM
C
C    ALFE(I,L)*F+BT1E(I,L)*(DF/DN1)+BT2E(I,L)*(DF/DN2)=GAME(I,L)
C
C    FOR THE MAGNETOSTATIC PROBLEM
C
C    ALFM(I,L)*F+BT1M(I,L)*(DF/DN1)+BT2M(I,L)*(DF/DN2)=GAMM(I,L)
C
C    WHERE ALF, BT1, BT2 AND GAM ARE GIVEN FUNCTIONS ALONG THE
C    BOUNDARY CURVES.DF/DN1 AND DF/DN2 ARE THE NORMAL
C    DERIVATIVES ON EACH SIDE OF A BOUNDARY.
C
C    DESCRIPTION OF PARAMETERS
C
C    NO      IS THE NUMBER OF CURVES ALONG WHICH DISTINCT BOUNDARY
C            CONDITIONS ARE TO BE SATISFIED.
C
C    N(L) IS THE NUMBER OF CONTOUR POINTS USED TO APPROXIMATE
C    BOUNDARY CURVE L.
C
C    X(I,L),
C    Y(I,L)   ARE THE X-Y COORDINATETS TO THE I TH POINT ON
C    BOUNDARY CURVE L.
C
C    R       IS A CONSTANT CHOSEN TO BE GREATER  THAN THE DISTANCE
C            BETWEEN ANY TWO BOUNDARY POINTS.
C
C    NDIM     IS EQUAL TO THE TOTAL NUMBER OF BOUNDARY SEGMENTS.
C
C    ALFE(I,L),
C    BT1E(I,L),
C    BT2E(I,L),
C    GAME(I,L)   ARE THE ELECTROSTATIC BOUNDARY VALUES FOR THE
C        BOUNDARY SEGMENT BETWEEN POINTS I AND I+1 ON CURVE L.
C
C    ALFM(I,L),
C    BT1M(I,L),
C    BT2M(I,L),
C    GAMM(I,L) ARE THE MAGNETOSTATIC BOUNDARY VALUES FOR THE
C        BOUNDARY SEGMENT BETWEEN POINTS I AND I+1 ON CURVE  L.
C
C    PTE(I,L),
C    PTM(I,L) ARE RESPECTIVELY THE ELECTROSTATIC AND
C        MAGNETOSTATIC POTENTIAL AT BOUNDARY SEGMENT I ON
C        CURVE L.
C
```

```
C     GRDNE(I,L),
C     GRDNM(I,L)   ARE RESPECTIVELY THE ELECTROSTATIC AND
C          MAGNETOSTATIC POTENTIAL NORMAL DERIVATIVES AT BOUNDARY
C          SEGMENT I ON CURVE L.
C
C     GRDTE(I,L),
C     GRDTM(I,L)ARE RESPECTIVELY THE ELECTROSTATIC AND
C          MAGNETOSTATIC TANGENT POTENTIAL DERIVATIVES AT
C          BOUNDARY SEGMENT I ON CURVE L.
C
C     TSCD(I,L,4)   IS AN ARRAY USED FOR STORING THE SEGMENT
C     LENGTH AND DIRECTION INFORMATION.
C
C     XMIN,
C     XMAX,
C     YMIN,
C     YMAX-DEFINE A RECTANGULAR REGION IN X-Y PLANE FROM XMIN TO
C          XMAX IN THE X-DIRECTION AND FROM YMIN TO YMAX IN THE
C          Y-DIRECTION.
C
C     NX,NY ARE THE NUMBER OF MESH POINTS IN THE X AND
C     Y-DIRECTION RESPECTIVELY.
C
C     SUBROUTINES REQUIRED - ARRAY AND SIMQ(STANDARD SCIENTIFIC
C                             PACKAGES).
C
C
      SUBROUTINE LPLACE(NC,N,X,Y,R,NDIM,ALFE,BT1E,BT2E,GAME,
     *ALFM,BT1M,BT2M,GAMM,NCC,PTE,PTM,GRDNE,GRDNM,GRDTM,
     *TSCD,SCH,NX,NY,XMIN,XMAX,YMIN,YMAX,PLTD,EP,GRDTE)
C
      DIMENSION X(13,7),Y(13,7),N(7),ALFE(12,7),BT1E(12,7),
     *BT2E(12,7),GAME(12,7),GRDNE(12,7),TSCD(12,7,4),
     *GRDNM(12,7),GRDTM(12,7),GF1(70,70),GF3(70,70),AM(70,70),
     *ALFM(12,7),BT1M(12,7),BT2M(12,7),GAMM(12,7),PTE(12,7),
     *AC(10,10),BC(10,10),CC(10,10),EP(2),BES(70),PTM(12,7),
     *XMIN(5),XMAX(5),YMIN(5),YMAX(5),NX(5),NY(5),DX(5),DY(5),
     *BM(70),BMS(70),BMT(70),CHM(12,7),BET(70),GRDTE(12,7),
     *GF2(70,70),AE(70,70),BE(70),CHE(12,7),SCH(4),PLTD(5)
      PI=3.1415926
      RR=R**2
C
C     CALCULATE DIRECTION AND LENGTH OF SEGMENTS.
C
      DO 1 L=1,NC
      NN=N(L)-1
      DO 1  I=1,NN
      XI=X(I+1,L)-X(I,L)
      YI=Y(I+1,L)-Y(I,L)
      TSCD(I,L,1)=ATAN2(YI,XI)
      TSCD(I,L,2)=SIN(TSCD(I,L,1))
      TSCD(I,L,3)=COS(TSCD(I,L,1))
    1 TSCD(I,L,4)=SQRT(XI**2+YI**2)
C
C     GENERATE THE ELECTROSTATIC(AE) AND MAGNETOSTATIC(AM)
C     COEFFICIENT MATRICES.
C
      JJJ=0
      DO 4 LJ=1,NC
      NJ=N(LJ)-1
      JAJ=JJJ
      JJJ=JJJ+NJ
      DO 4  J=1,NJ
      JJ=JAJ+J
      XJ=(X(J,LJ)+X(J+1,LJ))/2.
      YJ=(Y(J,LJ)+Y(J+1,LJ))/2.
```

```
      III=0
      DO 4 LI=1,NO
      NI=N(LI)-1
      III=III+NI
      IAI=III-NI
      DO 4 I=1,NI
      II=IAI+I
      IF(II.EQ.JJ) GO TO 3
      X1=XJ-X(I,LI)
      X2=XJ-X(I+1,LI)
      Y1=YJ-Y(I,LI)
      Y2=YJ-Y(I+1,LI)
      R1=X1**2+Y1**2
      R2=X2**2+Y2**2
      S1=0.
      S2=0.
      YT=X1*Y2-X2*Y1
      XT=X1*X2+Y1*Y2
      TETA=ATAN2(YT,XT)
C
C     GREEN FUNCTION EVALUATION.
C
      S1=TSCD(I,LI,4)*(1.-0.5*ALOG(R2/RR))
     $+0.5*ALOG(R2/R1)*(X1*TSCD(I,LI,3)
     $+Y1*TSCD(I,LI,2))+TETA*(X1*TSCD(I,LI,2)
     $-Y1*TSCD(I,LI,3))
      TETA1=TSCD(J,LJ,1)-TSCD(I,LI,1)
      S2=0.5*SIN(TETA1)*ALOG(R2/R1)
     $+COS(TETA1)*TETA
      S3=-S2
      S2P=0.5*COS(TETA1)*ALOG(R2/R1)-SIN(TETA1)*TETA
      GF1(JJ,II)=S1
      GF2(JJ,II)=S2
      GF3(JJ,II)=S2P
      GO TO 2
 3    S1=TSCD(I,LI,4)*(1.-
     $ALOG(TSCD(I,LI,4)/2./R))
      S2=PI
      S2P=0.
      S3=PI
      GF1(JJ,II)=S1
      GF2(JJ,II)=S2
      GF3(JJ,II)=S2P
 2    AE(JJ,II)=ALFE(J,LJ)*S1+BT1E(J,LJ)*S2+BT2E(J,LJ)*S3
 4    AM(JJ,II)=ALFM(J,LJ)*S1+BT1M(J,LJ)*S2+BT2M(J,LJ)*S3
C
C     CALCULATETHE TOTAL NUMBER OF SEGMENTS
C
      M=0
      DO 5 L=1,NO
 5    M=M+N(L)-1
C
C     GENERATE THE ELECTROSTATIC (BE) AND MAGNETOSTATIC (BM)
C     RIGHT HAND SIDE COLUMN MATRICES.
C
      JJJ=0
      DO 6 L=1,NO
      NN=N(L)-1
      JAJ=JJJ
      JJJ=JJJ+NN
      DO 6 J=1,NN
      JJ=JAJ+J
      BE(JJ)=GAME(J,L)
 6    BM(JJ)=GAMM(J,L)
C
C
```

```
C       SOLVE THE ELECTROSTATIC EQUATION SYSTEM.
C
        CALL ARRAY (2,M,M,NDIM,NDIM,AE,AE)
        CALL SIMQ (AE,BE,M,KS)
        IF(KS.NE.0) WRITE (6,100)
  100   FORMAT  (1H0,33H ELECTROSTATIC SYSTEM IS SINGULAR)
        IF    (KS.NE.0) GO TO 17
C
C       SOLVE THE MAGNETOSTATIC EQUATION SYSTEM.
C
        CALL ARRAY(2,M,M,NDIM,NDIM,AM,AM)
        CALL SIMQ(AM,BM,M,KS)
        IF(KS.NE.0) WRITE(6,101)
  101   FORMAT(1H0,33H MAGNETOSTATIC SYSTEM IS SINGULAR)
        IF(KS.NE.0) GO TO 17
C
C       PLACE THE ELECTROSTATIC AND MAGNETOSTATIC EQUIVALENT
C       SOURCE SOLUTIONS IN RESPECTIVELY CHE AND CHM.
C
        JJJ=0
        DO 7 L=1,NO
        NN=N(L)-1
        JAJ=JJJ
        JJJ=JJJ+NN
        DO 7 J=1,NN
        JJ=JAJ+J
        CHE(J,L)=BE(JJ)
    7   CHM(J,L)=BM(JJ)
C
C       CALCULATE FOR EACH BOUNDARY SEGMENT THE ELECTROSTATIC
C       POTENTIAL(PTE) AND NORMAL(GRDNE) AND TANGENT(GRDTE)
C       FIELD MAGNITUDE,MAGNETOSTATIC POTENTIAL(PTM), AND
C       NORMAL(GRDNM) AND TANGENT(GRDTM) FIELD MAGNITUDES.
C
        JJJ=0.
        DO 80 LJ=1,NO
        NJ=N(LJ)-1
        JAJ=JJJ
        JJJ=JJJ+NJ
        DO 80 J=1,NJ
        JJ=JAJ+J
        BE(JJ)=0.
        BES(JJ)=0.
        BET(JJ)=0.
        BM(JJ)=0.
        BMS(JJ)=0.
        BMT(JJ)=0.
        III=0.
        DO 80 LI=1,NO
        NI=N(LI)-1
        III=III+NI
        IAI=III-NI
        DO 80 I=1,NI
        II=IAI+I
        BE(JJ)=BE(JJ)+GE1(JJ,II)*CHE(I,LI)
        BES(JJ)=BES(JJ)+GE2(JJ,II)*CHE(I,LI)
        BET(JJ)=BET(JJ)+GE3(JJ,II)*CHE(I,LI)
        BM(JJ)=BM(JJ)+GE1(JJ,II)*CHM(I,LI)
        BMT(JJ)=BMT(JJ)+GE3(JJ,II)*CHM(I,LI)
   80   BMS(JJ)=BMS(JJ)+GE2(JJ,II)*CHM(I,LI)
        JJJ=0.
        DO 81 L=1,NN
        NN=N(L)-1
        JAJ=JJJ
        JJJ=JJJ+NN
        DO 81 J=1,NN
```

```
      JJ=JAJ+J
      PTE(J,L)=BF(JJ)
      GRDNE(J,L)=BES(JJ)
      GRDTE(J,L)=BET(JJ)
      PTM(J,L)=BM(JJ)
      GRDTM(J,L)=BMT(JJ)
   81 GRDNM(J,L)=BMS(JJ)
C
C     PRINT FIELD VALUES.
C
      WRITE(6,83)
   83 FORMAT(31H0ELECTROSTATIC CURVE POTENTIALS)
      WRITE(6,88) PTE
       WRITE (6,84)
   84  FORMAT (33H0ELECTROSTATIC CURVE NORMAL FIELD)
       WRITE (6,88) GRDNE
      WRITE(6,89)
   89 FORMAT(34H0ELECTROSTATIC CURVE TANGENT FIELD)
      WRITE(6,88)GRDTE
      WRITE(6,85)
   85 FORMAT(31H0MAGNETOSTATIC CURVE POTENTIALS)
      WRITE(6,88) PTM
      WRITE(6,86)
   86 FORMAT(33H0MAGNETOSTATIC CURVE NORMAL FIELD)
      WRITE(6,88) GRDNM
      WRITE(6,87)
   87 FORMAT(34H0MAGNETOSTATIC CURVE TANGENT FIELD)
      WRITE(6,88) GRDTM
   88   FORMAT(1H0,7F15.4)
C
C     CALCULATE FIELD VALUES IN A RECTANGULAR NET.
C
      IF(EP(1).EQ.1.) GO TO 19
      DO 20 L=1,5
      PLTD(L)=0.
      IF(NX(L)-1)17,9,10
    9 DX(L)=0.
      GO TO 11
   10 DX(L)=(XMAX(L)-XMIN(L))/FLOAT(NX(L)-1)
   11 IF(NY(L)-1)17,12,13
   12 DY(L)=0.
      GO TO 14
   13 DY(L)=(YMAX(L)-YMIN(L))/FLOAT(NY(L)-1)
   14 NXX=NX(L)
      DO 199 II=1,NXX
      XJ=XMIN(L)+FLOAT(II-1)*DX(L)
      NYY=NY(L)
      DO 199 JJ=1,NYY
      YJ=YMIN(L)+FLOAT(JJ-1)*DY(L)
      AC(II,JJ)=0.
      BC(II,JJ)=0.
      CC(II,JJ)=0.
      DO 18 LI=1,NO
      NN=N(LI)-1
      DO 18 I=1,NN
      X1=XJ-X(I,LI)
      X2=XJ-X(I+1,LI)
      Y1=YJ-Y(I,LI)
      Y2=YJ-Y(I+1,LI)
      R1=X1**2+Y1**2
      R2=X2**2+Y2**2
      YT=X1*Y2-X2*Y1
      XT=X1*X2+Y1*Y2
      TETA=ATAN2(YT,XT)
      KST=0
      IF((R1.EQ.0.).OR.(R2.EQ.0.))KST=1
```

```
      IF(KST.EQ.1) S2=PI
      IF(KST.EQ.1) S2P=0.
      IF(KST.NE.1) S2=0.5*TSCD(I,LI,2)*ALCG(R2/R1)
     *+TSCD(I,LI,3)*TETA
      IF(KST.NE.1) S2P=0.5*TSCD(I,LI,3)*ALCG(R2/R1)
     *-TSCD(I,LI,2)*TETA
      AC(II,JJ)=AC(II,JJ)+S2*CHE(I,LI)
      BC(II,JJ)=BC(II,JJ)+S2P*CHE(I,LI)
18    CC(II,JJ)=SQRT(AC(II,JJ)**2+BC(II,JJ)**2)
199   PLTD(L)=PLTD(L)+(CC(II,JJ)**2)*CX(L)*CY(L)
20    CONTINUE
19    DO 191 L=1,NOC
      NN=N(L)-1
      SCH(L)=0.
      DO 191 I=1,NN
      SCH(L)=SCH(L)+GRDNE(I,L)*TSCD(I,L,4)
191   CONTINUE
17    RETURN
      END
C
      SUBROUTINE ARRAY(MODE,I,J,N,M,S,D)
C
      DIMENSION S(4900),D(4900)
      NI=N-I
      IF(MODE-1) 100,100,120
100   IJ=I*J+1
      NM=N*J+1
      DO 110 K=1,J
      NM=NM-NI
      DO 110 L=1,I
      IJ=IJ-1
      NM=NM-1
110   D(NM)=S(IJ)
      GO TO 140
120   IJ=0
      NM=0
      DO 130 K=1,J
      DO 125 L=1,I
      IJ=IJ+1
      NM=NM+1
125   S(IJ)=D(NM)
130   NM=NM+NI
140   RETURN
      END
C
      SUBROUTINE SIMQ(A,B,N,KS)
C
      DIMENSION A(4900),B(70)
      TOL=0.0
      KS=0
      JJ=-N
      DO 65 J=1,N
      JY=J+1
      JJ=JJ+N+1
      BIGA=0
      IT=JJ-J
      DO 30 I=J,N
      IJ=IT+I
      IF(ABS(BIGA)-ABS(A(IJ))) 20,30,30
20    BIGA=A(IJ)
      IMAX=I
30    CONTINUE
      IF(ABS(BIGA)-TOL) 35,35,40
35    KS=1
```

```
      RETURN
   40 I1=J+N*(J-2)
      IT=IMAX-J
      DO 50 K=J,N
      I1=I1+N
      I2=I1+IT
      SAVE=A(I1)
      A(I1)=A(I2)
      A(I2)=SAVE
   50 A(I1)=A(I1)/BIGA
      SAVE=B(IMAX)
      B(IMAX)=B(J)
      B(J)=SAVE/BIGA
      IF(J-N) 55,70,55
   55 IQS=N*(J-1)
      DO 65 IX=JY,N
      IXJ=IQS+IX
      IT=J-IX
      DO 60 JX=JY,N
      IXJX=N*(JX-1)+IX
      JJX=IXJX+IT
   60 A(IXJX)=A(IXJX)-(A(IXJ)*A(JJX))
   65 B(IX)=B(IX)-(B(J)*A(IXJ))
   70 NY=N-1
      IT=N*N
      DO 80 J=1,NY
      IA=IT-J
      IB=N-J
      IC=N
      DO 80 K=1,J
      B(IB)=B(IB)-A(IA)*B(IC)
      IA=IA-N
   80 IC=IC-1
      RETURN
      END
C
C     SINGLE MICROSTRIP-PARAMETER CALCULATION.
C

      DIMENSION X(13,7),Y(13,7),N(7),ALFE(12,7),BT1E(12,7),
     *BT2E(12,7),GAME(12,7),GRDNE(12,7),TSCD(12,7,4),
     *ALFM(12,7),BT1M(12,7),BT2M(12,7),GAMM(12,7),PTE(12,7),
     *GRDNM(12,7),GRDTM(12,7),GRDTE(12,7),PTM(12,7),
     *XMIN(5),XMAX(5),YMIN(5),YMAX(5),NX(5),NY(5),DX(5),DY(5),
     *PTR(2),ATTC(2),ATCD(2),ATDD(2),ATTD(2),W1(7),PLTD(5),
     *RHO(12,4),CRTD(12,4),SIS(12,4),PL(12,4),PLT(12,4),
     *EP(2),Q1(2),Q2(2),CAP1(2),CAP2(2),SCH(4),SIST(2),PLTS(2)
C
C     READ IN CONSTANTS.
C

      R=100.
      PI=3.1415926
      EMO=PI*4.E-7
      UO=2.997925E+8
      EPO=1./(EMO*UO**2)
      SIGMA=5.8E+7
      FREQ=1.E+9
      EP(2)=1.
      EP2=EP(2)*EPO
      V1=0.
      V2=100.
      NO=7
      NOC=4
C
C
C
```

```
C      NUMBER OF SEGMENTS ON EACH CONTOUR.
C
       N(1)=13
       N(2)=9
       N(3)=13
       N(4)=11
       N(5)=12
       N(6)=7
       N(7)=12
       NDIM=70
       DO 1 L=1,5
       NX(L)=10
 1     NY(L)=10
       W1(1)=0.5
       W1(2)=0.7
       W1(3)=1.0
       W1(4)=1.5
       W1(5)=2.0
       W1(6)=3.0
       W1(7)=4.0
       H=1.
       B=15.*H
       WL=12.5*H
       T=H/8.
       DO 300 M=1,7
       EP(1)=1.
       EP1=EP(1)*EPO
       W=W1(M)
       W2=W/2.
C
C      RECTANGULAR MESH IN THE DIELECTRIC REGION.
C
       XMIN(1)=.5*(W2-.2*W2)/10.
       XMIN(2)=.5*.2*W2/10.+W2-.2*W2
       XMIN(3)=0.5*.2*W2/10.+W2
       XMIN(4)=0.5*.4*W2/10.+W2-.2*W2
       XMIN(5)=0.5*(WL-W2-.2*W2)/10.+W2+.2*W2
       XMAX(1)=9.5*(W2-.2*W2)/10.
       XMAX(2)=9.5*.2*W2/10.+W2-.2*W2
       XMAX(3)=9.5*.2*W2/10.+W2
       XMAX(4)=9.5*.4*W2/10.+W2-.2*W2
       XMAX(5)=9.5*(WL-W2-.2*W2)/10.+W2+.2*W2
       YMIN(1)=.5*H/10.
       YMIN(2)=0.5*.2*H/10.+.8*H
       YMIN(3)=0.5*.2*H/10.+.8*H
       YMIN(4)=0.5*.8*H/10.
       YMIN(5)=.5*H/10.
       YMAX(1)=9.5*H/10.
       YMAX(2)=9.5*.2*H/10.+.8*H
       YMAX(3)=9.5*.2*H/10.+.8*H
       YMAX(4)=9.5*.8*H/10.
       YMAX(5)=9.5*H/10.
C
C      BOUNDARY CONTOURS.
C
       L=1
       DA1=H/5.
       DA2=5.*H/4.
       DA3=(WL-6.*H)/2.
       DO 11 I=1,6
       X(I,L)=DA1*FLOAT(I-1)
 11    Y(I,L)=0.
       DO 12 I=7,10
       X(I,L)=H+DA2*FLOAT(I-6)
 12    Y(I,L)=0.
       DO 13 I=11,12
```

```
      X(I,L)=6.*H+DA3*FLOAT(I-10)
13    Y(I,L)=0.
      I=13
      X(I,L)=WL
      Y(I,L)=H
      L=2
      DA1=(B-H)/2.
      DA2=(WL-4.*H)/2.
      DA3=4.*H/4.
      DO 21 I=1,3
      X(I,L)=WL
21    Y(I,L)=H+DA1*FLOAT(I-1)
      DO 22 I=4,5
      X(I,L)=WL-DA2*FLOAT(I-3)
22    Y(I,L)=B
      DO 23 I=6,9
      X(I,L)=4.*H-DA3*FLOAT(I-5)
23    Y(I,L)=B
      L=3
      DA1=.02*W/2.
      DA2=.46*W/4.
      DA3=.02*W/2.
      DA4=T/4.
      DO 31 I=1,3
      X(I,L)=DA1*FLOAT(I-1)
31    Y(I,L)=H+T
      DO 32 I=4,7
      X(I,L)=.02*W+DA2*FLOAT(I-3)
32    Y(I,L)=H+T
      DO 33 I=8,9
      X(I,L)=.48*W+DA3*FLOAT(I-7)
33    Y(I,L)=H+T
      DO 34 I=10,13
      X(I,L)=W2
34    Y(I,L)=H+T-DA4*FLOAT(I-9)
      L=4
      DA1=.02*W/2.
      DA2=.46*W/6.
      DA3=.02*W/2.
      DO 41 I=1,3
      X(I,L)=W2-DA1*FLOAT(I-1)
41    Y(I,L)=H
      DO 42 I=4,9
      X(I,L)=.48*W-DA2*FLOAT(I-3)
42    Y(I,L)=H
      DO 43 I=10,11
      X(I,L)=.02*W-DA3*FLOAT(I-9)
43    Y(I,L)=H
      L=5
      DA1=(B-H-T-6.*H)/2.
      DA2=5.*H/4.
      DA3=H/5.
      DO 51 I=1,3
      X(I,L)=0.
51    Y(I,L)=B-DA1*FLOAT(I-1)
      DO 52 I=4,7
      X(I,L)=0.
52    Y(I,L)=H+T+6.*H-DA2*FLOAT(I-3)
      DO 53 I=8,12
      X(I,L)=0.
53    Y(I,L)=H+T+H-DA3*FLOAT(I-7)
      L=6
      DA1=H/6.
      DO 61 I=1,7
      X(I,L)=0.
61    Y(I,L)=H-DA1*FLOAT(I-1)
```

```
      L=7
      DA1=(WL-W2-2.*T-H)/4.
      DA2=H/5.
      DA3=2.*T/2.
      DO 71 I=1,5
      X(I,L)=WL-DA1*FLOAT(I-1)
   71 Y(I,L)=H
      DO 72 I=6,10
      X(I,L)=W2+2.*T+H-DA2*FLOAT(I-5)
   72 Y(I,L)=H
      DO 73 I=11,12
      X(I,L)=W2+2.*T-DA3*FLOAT(I-10)
   73 Y(I,L)=H
C
C     BOUNDARY CONDITIONS.
C
      DO 15 L=1,2
      NN=N(L)-1
      DO 15 I=1,NN
      ALFE(I,L)=1.
      BT1E(I,L)=0.
      BT2E(I,L)=0.
      GAME(I,L)=V1
      ALFM(I,L)=0.
      BT1M(I,L)=1.
      BT2M(I,L)=0.
   15 GAMM(I,L)=0.
      DO 16 L=3,4
      NN=N(L)-1
      DO 16 I=1,NN
      ALFE(I,L)=1.
      BT1E(I,L)=0.
      BT2E(I,L)=0.
      GAME(I,L)=V2
      ALFM(I,L)=0.
      BT1M(I,L)=1.
      BT2M(I,L)=0.
   16 GAMM(I,L)=0.
      DO 17 L=5,6
      NN=N(L)-1
      DO 17 I=1,NN
      ALFE(I,L)=0.
      BT1E(I,L)=1.
      BT2E(I,L)=0.
      GAME(I,L)=0.
      ALFM(I,L)=1.
      BT1M(I,L)=0.
      BT2M(I,L)=0.
   17 GAMM(I,L)=V2*FLOAT(6-L)
C
C     CALCULATE PARAMETERS BY CAPACITANCE METHOD.
C
      DO 70 IN=1,2
      IF(IN.EQ.1) GO TO 75
      EP(1)=8.875
      EP1=EP(1)*EP0
   75 CONTINUE
      L=7
      NN=N(L)-1
      DO 18 I=1,NN
      ALFE(I,L)=0.
      BT1E(I,L)=EP(1)
      BT2E(I,L)=EP(2)
      GAME(I,L)=0.
      ALFM(I,L)=0.
      BT1M(I,L)=1.
```

```
      BT2M(I,L)=1.
   18 GAMM(I,L)=0.
      CALL LPLACE(NO,N,X,Y,R,NDIM,ALFE,BT1E,BT2E,GAME,ALFM,
     *BT1M,BT2M,GAMM,NOC,FTE,FTM,GRDNE,GRDNM,GRDTM,TSCD,SCH,
     *NX,NY,XMIN,XMAX,YMIN,YMAX,PLTD,EP,GRDTE)
      Q1(IN)=SCH(1)*EP1+SCH(2)*EP2
      Q2(IN)=SCH(3)*EP2+SCH(4)*EP1
      CAP1(IN)=ABS(Q1(IN)/V2)
      CAP2(IN)=ABS(Q2(IN)/V2)
   70 CONTINUE
      U1=U0*SQRT(CAP1(1)/CAP1(2))
      U2=U0*SQRT(CAP2(1)/CAP2(2))
      Z01=0.5/(U1*CAP1(2))
      Z02=0.5/(U2*CAP2(2))
      UR1=U1/U0
      UR2=U2/U0
      EPS1=1./UR1**2
      EPS2=1./UR2**2
      AMBDA1=U0/U1
      AMBDA2=U0/U2
C
C     ATTENUATION CALCULATION.
C
      WIDTH=.508E-3
C
C     CALCULATE SURFACE CHARGE DENSITY.
C
      DO 131 L=1,4,3
      NN=N(L)-1
      DO 131 I=1,NN
  131 RHO(I,L)=GRDNE(I,L)*EP1/WIDTH
      DO 132 L=2,3
      NN=N(L)-1
      DO 132 I=1,NN
  132 RHO(I,L)=GRDNE(I,L)*EP2/WIDTH
C
C     CALCULATE ATTENUATION FOR FREQUENCIES OF 1-5 GHZ.
C
      DO 140 K=1,5
      FREQ1=FLOAT(K)*1.E+9
      FREQ=FREQ1
C
C     CALCULATE SURFACE RESISTENCE.
C
      SKN=SQRT(2./(2.*PI*EMO*SIGMA*FREQ))
      RS=1./(SKN*SIGMA)
      SIGMA1=2.1E-4*2.*PI*FREQ*EP1
C
C     CALCULATE CURRENT DENSITY AND POWER LOSS IN EACH SEGMENT.
C
      DO 133 L=1,4
      NN=N(L)-1
      DO 133 I=1,NN
      CRTD(I,L)=RHO(I,L)*U1
      SIS(I,L)=CRTD(I,L)*TSCD(I,L,4)*WIDTH
      PL(I,L)=RS*CRTD(I,L)**2
  133 PLT(I,L)=PL(I,L)*TSCD(I,L,4)*WIDTH
C
C     CALCULATE TOTAL CURRENT THROUGH THE SHIELD.
C
      SIST(1)=0.
      DO 134 L=1,2
      NN=N(L)-1
      DO 134 I=1,NN
  134 SIST(1)=SIST(1)+ABS(SIS(I,L))
C
```

```
C         CALCULATE TOTAL CURRENT THROUGH THE STRIP.
C
          SIST(2)=0.
          DO 135 L=3,4
          NN=N(L)-1
          DO 135 I=1,NN
  135     SIST(2)=SIST(2)+ABS(SIS(I,L))
C
C         CALCULATE TOTAL POWER LOSS IN THE SHIELD.
C
          PLTS(1)=0.
          DO 136 L=1,2
          NN=N(L)-1
          DO 136 I=1,NN
  136     PLTS(1)=PLTS(1)+ABS(PLT(I,L))
C
C         CALCULATE TOTAL POWER LOSS IN THE STRIP.
C
          PLTS(2)=0.
          DO 137 L=3,4
          NN=N(L)-1
          DO 137 I=1,NN
  137     PLTS(2)=PLTS(2)+ABS(PLT(I,L))
C
C         TOTAL POWER LOSS IN THE DIELECTRIC.
C
          PLTDT=0.
          DO 138 L=1,5
          PLTDT=PLTDT+PLTD(L)*SIGMA1
  138     CONTINUE
          DO 139 I=1,2
          PTR(I)=V2*SIST(I)
          ATTC(I)=PLTS(I)/(2.*PTR(I))
          ATTD(I)=PLTDT/(2.*PTR(I))
          ATDD(I)=ATTD(I)*8.6858/100.
  139     ATCD(I)=ATTC(I)*8.6858/100.
          WRITE(6,107)
  107     FORMAT(35H0ATTENUATION CONSTANT FOR CONDUCTOR)
          WRITE(6,109) ATCD
          WRITE(6,108)
  108     FORMAT(36H0ATTENUATION CONSTANT FOR DIELECTRIC)
          WRITE(6,109) ATDD
  109     FORMAT(6H0SHLD=,F12.7,6H DB/CM,5X,6H STRP=,F12.7,
         *6H DB/CM)
  140     CONTINUE
C
C         VARIATIONAL CALCULATION.
C
C
C         EVALUATE 'A' INTEGRAL.
C
          AA=0.
          L=5
          NN=N(L)-1
          DO 201 I=1,NN
  201     AA=AA+GRDNM(I,L)*TSCD(I,L,4)
          AA=AA*2.*V2*EMO
C
C         EVALUATE 'B' INTEGRAL.
C
          BB1=0.
          L=4
          NN=N(L)-1
          DO 202 I=1,NN
  202     BB1=BB1+PTE(I,L)*GRDNE(I,L)*TSCD(I,L,4)
          BB1=BB1*2.*EP1
```

```
      BB2=0.
      L=7
      NN=N(L)-1
      DO 203 I=1,NN
  203 BB2=BB2+PTE(I,L)*GRDNE(I,L)*TSCD(I,L,4)
      BB2=BB2*2.*(EP1-EP2)
      BB3=0.
      L=3
      NN=N(L)-1
      DO 204 I=1,NN
  204 BB3=BB3+PTE(I,L)*GRDNE(I,L)*TSCD(I,L,4)
      BB3=BB3*2.*EP2
      BB=BB1+BB2+BB3
C
C     EVALUATE 'C' INTEGRAL.
C
      CC=0.
      DO 205 L=3,4
      NN=N(L)-1
      DO 205 I=1,NN
  205 CC=CC+TSCD(I,L,4)*ABS(GRDTM(I,L))
      CC=CC*2.*V2
C
C     CALCULATE VARIATIONAL PARAMETERS.
C
      EFFK=1./RVEL**2
      VEL=ABS(CC/SQRT(AA*BB))
      RVEL=VEL/U0
C
      WRITE(6,101)
  101 FORMAT(14H0TOTAL CURRENT)
      WRITE(6,106) SIST
      WRITE(6,102) CAP1,UR1,ZC1
  102 FORMAT(14H0C(SHLD HMGS)=,E12.4,5X,16H C(SHLD INHMGS)=,
     *E12.4,5X,12H VELR(SHLD)=,F10.4,5X,10H ZC(SHLD)=,F12.4)
      WRITE(6,103) CAP2,UR2,ZC2
  103 FORMAT(14H0C(STRP HMGS)=,E12.4,5X,16H C(STRP INHMGS)=,
     *E12.4,5X,12H VELR(STRP)=,F10.4,5X,10H ZC(STRP)=,F12.4)
      WRITE(6,104)
  104 FORMAT(20H0RELATIVE WAVELENGTH)
      WRITE(6,106) AMBDA1,AMBDA2
      WRITE(6,105)
  105 FORMAT(39H0RELATIVE EFFECTIVE DIELECTRIC CONSTANT)
      WRITE(6,106) EPS1,EPS2
  106 FORMAT(6H0SHLD=,F12.7,10X,6H STRP=,F12.7)
      WRITE(6,110)
  110 FORMAT(24H0VARIATIONAL CALCULATION)
      WRITE(6,111)VEL,RVEL,EFFK
  111 FORMAT(10H0VELOCITY=,E12.4,5X,19H RELATIVE VELOCITY=,
     *F12.4,5X,40H RELATIVE EFFECTIVE DIELECTRIC CONSTANT=,
     *F12.4)
  300 CONTINUE
      WRITE(6,112)
  112 FORMAT(9H0X VALUES)
      WRITE(6,114) X
      WRITE(6,113)
  113 FORMAT(9H0Y VALUES)
      WRITE(6,114) Y
  114 FORMAT(1H0,10F10.4)
      WRITE(6,115) U0,EM0,EP0
  115 FORMAT(5H0 U0=,E15.4,10X,5H EM0=,E15.4,10X,5H EP0=,
     *E15.4)
      STOP
      END
$ENTRY
```

BIBLIOGRAPHY

[1] R. F. Harrington, K. Pontoppidan, P. Abrahamsen, and N. C. Albertsen, "Computation of Laplacian potentials by an equivalent source method," Proc. IEE, vol. 116, pp. 1715-1720, Oct. 1969.

[2] R. F. Harrington, FIELD COMPUTATION BY MOMENT METHODS. New York: Macmillan, 1968.

[3] R. F. Harrington, TIME HARMONIC ELECTROMAGNETIC FIELDS. New York: McGraw Hill, 1961.

[4] Eikichi Yamishta and Kazuhiko Atsuki, "Strip line with rectangular outer conductor and three dielectric layers," IEEE Trans. Microwave Theory Tech., vol. MTT-8, pp. 238-244, May 1970.

[5] Eikichi Yamishta, "Variational method for the analysis of microstrip-like transmission lines," IEEE Trans. Microwave Theory Tech., vol. MTT-16, pp. 529-535, Aug. 1968.

[6] A. D. Berk, "Variational principles for electromagnetic resonators and waveguides," IRE Trans. antennas Propagat., vol. AP-4, pp. 104-110, Apr. 1956.

[7] R. A. Pucel, D. J. Masse, and C. P. Hartwig, "Losses in microstrip," IEEE Trans. Microwave Theory Tech., vol. MTT-16, pp. 342-350, June 1968.

[8] H. A. Wheeler, "Transmission line properties of parallel wide strips by a conformal-mapping approximation," IEEE Trans. Microwave Theory Tech., vol. MTT-12, pp.280-289, May 1964.

[9] I. J. Albrey and M. W. Gunn, "Reduction of the attenuation constant of microstrip," IEEE Trans. Microwave Theory Tech., vol. MTT-22, pp. 739-742, July 1974.

[10] M. K. Krage and G. I. Haddad, "Frequency dependent characteristics of microstrip transmission lines," IEEE Trans. Microwave Theory Tech., vol. MTT-20, pp. 678-688, Oct. 1972.

[11] M. K. Krage and G. I. Haddad, "Characteristics of coupled microstrip transmission lines-II: Evaluation of coupled line parameters," IEEE Trans. Microwave Theory Tech., vol. MTT-18, pp. 222-228, Apr. 1970.

[12] T. G. Bryant and J. A. Weiss, "Parameters of microstrip transmission lines and of coupled pairsof microstrip lines," IEEE Trans. Microwave Theory Tech., vol. MTT-16, pp. 1021-1027, Dec. 1968.

[13] S. Akhtarzad, T. R. Rowbotham, and P. B. Johns, "The design of coupled microstrip lines," IEEE Trans. Microwave Theory Tech., vol. MTT-23, pp. 486-492, June 1975.

[14] S. V. Judd, I. WHITELEY, R. J. Clowes, and D. C. Rickard, "An analytic method for calculating microstrip line parameters," IEEE Trans. Microwave Theory Tech., vol. MTT-18, pp. 78-87, Feb. 1970.

[15] H. E. Stinehelfer, "An accurate calculation of uniform microstrip transmission lines," IEEE Trans. Microwave Theory Tech., vol. MTT-16, pp.439-444, July 1968.

[16] P. Silvester, "TEM wave properties of microstrip transmission lines," Proc. IEE, vol. 115, pp. 43-48, Jan. 1968.

[17] H. Guckel, "Characteristic impedance of generalised rectangular transmission lines," IEEE Trans. Microwave Theory Tech., vol. MTT-13, pp. 270-274, May 1965.

[18] M. V. Schneider, "Computation of impedance and attenuation of TEM-Lines by finite difference methods," IEEE Trans. Microwave Theory Tech., vol. MTT-13, pp. 793-800, Nov. 1965.

[19] R. Mittra and T. Itoh, "Theory of shielded microstrip lines," Proc. European Microwave Conference, pp. 14-17, Sept. 1969.

[20] P. M. Morse and H. Feshbach, METHODS OF THEORETICAL PHYSICS, VOL. 1. New York: McGraw Hill, 1953.